Review of Results and Recommendations from the GCMRC 2000-2003 Remote- Sensing Initiative for Monitoring Environmental Resources within the Colorado River Ecosystem

REVIEW COPY

Philip A. Davis[2], Remote Sensing Coordinator

Contributors (alphabetical order):
Michael J. Breedlove[2]
Pat S. Chavez[2]
Donna M. Galuszka[2]
F. Mark Gonzales[2]
Joseph E. Hazel[1]
Jeffrey R. Johnson[2]
Matthew A. Kaplinski[1]
Michael J. C. Kearsley[1]
Keith A. Kohl[2]
Michael J. Liszewski[2]
William W. MacFarlane[3]
Christopher S. Magirl[2]
Mark F. Manone[1]
Theodore S. Melis[2]
Steven N. Mietz[2]
Joel L. Pederson[3]
Paul A. Petersen[3]
Jeffrey B. Plescia[2]
Barbara E. Ralston[2]
Mark R. Roseik[2]
John C. Schmidt[3]
Matthew I. Staid[2]
William S. Vernieu[2]

[1]Northern Arizona University
Flagstaff, Arizona 86001

[2]U.S. Geological Survey
Flagstaff and Tucson, Arizona 86001

[3]Utah State University
Logan, Utah 84322

September 17, 2003

Executive Summary

In mid-2000, the Grand Canyon Monitoring and Research Center (GCMRC) began a remote-sensing initiative to evaluate all remote-sensing technologies and methods that had potential for providing improved data (capability) for its various programs that monitor the Colorado River ecosystem (CRE). The primary objective of the initiative was to determine the most cost-effective data collection protocols for GCMRC programs that (1) provide the accuracies required for currently measured parameters, (2) provide additional parameters for ecological monitoring, (3) reduce environmental impact by being less invasive than current methods, and (4) expand geographic extent of current ground approaches. The initial phase of the remote-sensing initiative determined the types of sampling parameters and their required accuracies for monitoring. This information was used to determine the most appropriate sensors for evaluation. The initiative evaluated 25 different data collections over a three-year period; many more remote-sensing instruments were considered, but were not evaluated because they could not meet the basic requirements on spatial resolution, wavelength, positional accuracy, or elevation accuracy. It was hoped that the evaluations would lead to a minimum set of technologies that would satisfy many program requirements. The results from all of our evaluations are reviewed in this report and are briefly summarized in the following paragraphs.

Of the three research and monitoring programs within GCMRC, the cultural resources program presented the most difficult set of requirements on remote-sensing data due to the small size and obscuration of its resources. For example, very small, individual ethnobotanical stands require very high resolution imagery for monitoring, which is extremely expensive to acquire. Also, mineral resources within rock walls are obscured from aerial view and therefore cannot be approached using airborne remote-sensing data. Cultural resources that were evaluated with remote-sensing technologies consisted of: (1) camping sites and beaches; (2) archaeological structures, (3) natural springs, and (4) arroyos and their effects of check dams and archaeological structures. Of these resources remote-sensing approaches proved useful for mapping camping sites and beaches. The composite/beach map produced in this evaluation includes more sediment sites than can reasonably be mapped by ground surveys, is a more rapid and more accurate product for change detection, and was produced at a fraction of the time and expense of the traditional ground surveys. Our evaluations for archeological structures and natural springs showed that (1) daytime thermal infrared (TIR) and 6-11 cm resolution visible imagery do not provide sufficient resolution or thermal differences to unambiguously identify or determine changes of the resources, and (2) although imagery at 3-cm resolution could only produce elevation accuracies near 20 cm, which is below the accuracies required to detect small changes in arroyos, the data do provide catchment-scale topography that allows geomorphic modeling of the potential effects of rainfall on arroyo development and on down-slope structure modification. With respect to the detection of archaeological structures and natural springs, previous TIR data collected just after dawn and after sunset were capable of mapping natural springs and should also detect archaeological structures. However, such data would require a separate data

collection for just these two resources and not all parts of the corridor would be illuminated during early morning collections.

Remote-sensing technologies were evaluated for two important terrestrial aspects of the physical resource program: (1) mapping the distribution of sediment deposits and (2) mapping the topography and volumes of fine- and coarse-grained sediment deposits. We found remote-sensing technologies to be very useful for both of these aspects. Our evaluations showed that (1) digital CIR image data are more accurate than digital or film natural-color and panchromatic imagery for mapping terrestrial sediment deposits; (2) digital CIR image data provide a relatively rapid and accurate means for this mapping; and (3) these deposits can be accurately mapped using 22–44 cm resolution data. Our evaluations of different airborne approaches for monitoring terrestrial sediment volumes showed that (1) low-resolution LIDAR (one point every four to six meters) produced 26-103 cm vertical accuracies on bare ground, whereas moderate-resolution LIDAR (one point every one to two meters) produced 9-26 cm vertical accuracies; (2) although the moderate-resolution LIDAR did provide acceptable elevation accuracies on bare ground, these data were only acceptable after correction for a vertical offset that varied with river reach; (3) the accuracies at both LIDAR resolutions decreased (average 1.5-m error) in vegetated terrain; (4) the accuracy and precision of high-resolution LIDAR data (10 points every meter) is 8 cm and 3 cm, respectively, with essentially no vertical offsets. Although the cost for the high-resolution LIDAR data is high ($6,200 per river km), it has wide applicability across many GCMRC programs for detailed, site-specific monitoring requirements; and (5) photogrammetric methods using 1:4,000 scale aerial photography provide acceptable elevation data on bare and vegetated ground (28-cm accuracy), but the cost for analysis is about $2,000 per river mile and the analysis requires control panels within the study sites and its accuracy is lower in winter months due to shadows.

Remote-sensing technologies were evaluated for two major components of the terrestrial biologic resources: (1) estimating canopy volumes and (2) inventorying the vegetation. Remote sensing technologies were found to be useful for both program components with some qualifications. Manual photogrammetric methods using 1:4,000-scale aerial photography provided about 85% accuracy in canopy height compared to ground surveys. However, manual photogrammetry requires the placement of ground panels and is both invasive and expensive. Automated photogrametric methods and very high resolution LIDAR data sets (15–30 points per square meter), which do not require ground control panels, are currently being evaluated and may provide similar accuracies to that provided by manual photogrammetry in a less invasive manner and at a lower cost. In terms of vegetation inventories, our evaluations showed that calibrated, digital four-band data with 30-cm resolution provide acceptable spectral and textural discrimination of CRE vegetation *communities* for developing inventory maps. However, certain vegetation *species* were not effectively discriminated, due to either (1) miscalibration of one of the sensor's detectors, such that the two or three of the highest reflectance species appear similar in the data, or (2) the inherent inability of the four wavelength bands to distinguish these species. It may be that more spectral information at lower spatial resolution (without texture) might provide better *species* separation, or that correctly

calibrated four-band image data can provide adequate vegetation mapping. This issue needs to be resolved by an additional evaluation of existing or new airborne data that examines vegetation species instead of vegetation communities.

Remote-sensing technologies were evaluated for several *physical* characteristics of the aquatic environment: (1) chlorophyll, (2) total suspended sediment, (3) turbidity, (4) warm backwater areas amenable to fish habitats, (5) sediment storage, and (6) substrate grain-size distribution. Remote-sensing technologies were found useful in mapping all of these characteristics. Digital (12-bit), high-gain CIR image data and thermal-infrared image data can provide large-area maps of chlorophyll, total suspended sediment, turbidity, warm backwater areas amenable to fish habitats, sediment storage, and substrate grain-size distribution. All of these characteristics can be mapped with airborne sensor having a few visible/near-infrared bands and a thermal-infrared band. However, the cost for this data in orthorectified form is about $850 per river mile. Thus, these remote sensing data cannot economically provide high-frequency data that are currently obtained by ground collection, but ground collection cannot achieve the rapid, wide-area coverage provided by the airborne data. For mapping channel substrate geomorphology, airborne technology easily surpasses side-scan sonar surveys in all aspects, but the water needs to be relatively clear for the airborne approach to work well and its depth of penetration in clear water is limited to about 20 m. An unanticipated result of our evaluations of low-resolution LIDAR elevation data was that the data actually mapped the elevation of the water's surface over the main stem, which compared with historical elevation profiles of the main stem indicated changes in submerged cobble bars since the historical measurements. Remote sensing data are generally not useful for monitoring the chemical characteristics of running water because chemical concentrations are too low.

Overall, the remote-sensing initiative has resulted in establishing the basic requirements on remote-sensing data and the technologies that can meet these requirements and has produced the most functional data sets to date. As a result, program scientists are making more and better use of these data each month, which has increased productivity and monitoring accuracy, made monitoring less invasive, and opened new avenues for improved ecological studies. Additional positive outcomes of this initiative are listed at the end of this report. Remote-sensing technology continually advances and improves in terms of capability and cost. CRE monitoring can benefit even more in the future from these improvements, but the technologies need to be thoroughly understood and evaluated for their potential benefits and against GCMRC monitoring requirements.

1.0 Introduction

For the past two decades, monitoring and research teams in the physical, biological, and cultural resource programs within the Glen Canyon Environmental Studies (GCES), and now the Grand Canyon Monitoring and Research Center (GCMRC), have been monitoring and modeling the effects of the Glen Canyon dam flows on various ecological resources within the Colorado River ecosystem (CRE). The overall objective of these programs is to determine flow regimes that maintain the resources at recent levels, and possibly restore the resources to pre-dam conditions. The research and monitoring has been performed mostly by *in-situ* measurements, supplemented by annual airborne image data provided by the information technology (IT) program. The image data that were acquired generally consisted of analog, stereo black-and-white photography (color-infrared or CIR photography in particular locations) at 11-cm spatial resolution. These data were point-perspective (unrectified) without pointing or camera information necessary to rectify (georeference) the data to make accurate maps or to perform photogrammetry to derive accurate topography. Correct use of these image data by scientists required a complex process to transform the distorted, point-perspective analog data into an undistorted (rectified), map-projected digital form so that accurate information could be obtained for any particular area. The complexity of the process did not encourage many scientists to use the image data to its fullest potential or accuracy. Therefore, the approaches that were used by GCMRC cooperators before the year 2000 were similar to approaches used by image scientists in the early 1970's.

The GCMRC monitoring and research programs (i.e., physical, biological, and cultural) were reviewed by external protocol evaluation panels (PEP) within the past few years (Wohl et al., 1999; Doelle et al., 2000; Urquhart et al., 2000; Anders et al., 2001; Jones et al., 2001). In general, these panels recommended that these programs conduct more integrated, corridor-wide monitoring in order to more accurately determine the effects of dam flow on ecosystem resources. In addition, the Remote Sensing PEP for the IT Program (Berlin et al., 1998) recommended that more modern, advanced remote-sensing technologies be examined to provide better data to the research programs. These two factors prompted GCMRC to establish a remote-sensing initiative whose purpose was to determine the most appropriate remote sensing technologies and approaches that could increase the capabilities and efficiencies of the research scientists in order to help them perform more integrated, less-invasive, corridor-wide studies. The first step in that initiative, which started in the fall of 2000, was a review of the types of ecological parameters being monitored, the collection methods being used, the precision required for each parameter, and alternative remote-sensing and GIS approaches for such monitoring. The latter aspect involved a review of published literature to determine technologies and approaches that produced useful results for problems analogous to those faced by GCMRC. The useful approaches were reviewed in Davis (2002a), which also includes a table of over 100 operational airborne and spaceborne sensor systems that lists relevant characteristics of the sensors. The sensor table was used to select appropriate sensors for consideration and possible evaluation, based on their capabilities for meeting the requirements for a particular program parameter. Although the review found that many resource parameters that are currently monitored could not be adequately approached using airborne remote-sensing technology, these being mostly chemical characteristics of water, the review also found an equal number of parameters that might be approached, if data of the correct type and format were collected and provided to the scientists. During this initial fact-finding process, we found that the level of detail recorded by previous airborne data collections was not being used during scientific analysis, despite initial claims by scientists that they needed the high resolution provided by historical data. This initial review also produced a table of CRE resource categories whose monitoring might be enhanced by remote

sensing, along with the types of remote-sensing data that might satisfy required measurement accuracies; the types of data subject to investigation are listed in Table 1 in order of increasing complexity and generally increasing cost. Personnel involved in the remote-sensing initiative collected and analyzed remote-sensing data listed in the table, starting with the least complex and proceeding to the most complex data, until a particular data set was found to provide acceptable accuracies for a particular resource parameter. This approach was followed because cost of data is an issue.

The remote-sensing initiative was supervised by Mike Liszewski (IT program manager) and coordinated by Philip Davis (research scientist at the U.S. Geological Survey). The initiative involved all of the IT personnel and many scientists from different disciplines, whose expertise was required for evaluation of specific remote-sensing technologies, data-provider performance, data-analysis methods, and resulting accuracies. This process is now near completion. This report reviews the GCMRC program objectives and measured parameters and the results from our remote-sensing investigations on those parameters that might benefit from improved data acquisition and/or analysis. The resources are discussed in order of the increasing capabilities found by remote-sensing approaches. Thus, the order of our discussions proceeds from the cultural resource program to the biologic resource program and then the physical resource program.

Remote sensing of radiation on Earth is limited to the wavelength region from the visible to microwave energies and it is this broad energy region that we have investigated for monitoring applications within the CRE. The different types of remote-sensing data sets that were collected and investigated for the different environmental parameters are listed in Table 2. Radar data were not included in this evaluation because the aircraft used for radar data collections are large, impossible to maneuver in the canyon, and provide too low spatial resolutions (about 5 m) when flown above the canyon rim. In addition, the walls of the canyon can produce secondary radar reflections that interfere with the primary reflections and make the image data unintelligible.

The collection of numerous wavelength bands by multi- and hyperspectral sensors limits the spatial resolution that can be achieved by such sensors because of data-rate limitations of current storage devices. Spectral resolution refers to the wavelength band width for a particular image, whereas spatial resolution refers to the surface dimension of a single picture element within that image. For example, multispectral sensors that record 12 wavelength bands with 50 nm spectral resolution can obtain image data at a 1-m ground resolution, while hyperspectral sensors that record up to 220 wavelength bands with 10 nm spectral resolution can only obtain data at a 2-4 m ground resolution. The cost for image data (listed in Table 1) increases with the number of wavelength bands collected, which effects the benefit/cost ratio and makes use of more sophisticated data difficult to justify, unless these data provide information that cannot be obtained by more simple, less expensive data. Therefore, our evaluations proceeded from the simpler to the more complex data sets, until a viable data set was found for a particular resource parameter. The final section presents the team's recommendations for future remote-sensing monitoring activities based on all of our investigations.

2.0 Cultural/Socio-Economic Resources

The primary goal of the cultural/socio-economic resource program is to monitor cultural and socio-economic resources with respect to Glen Canyon dam operations, so that ultimately a model can be constructed and used to predict and possibly mitigate the effects of dam operations on these resources. The primary resources for monitoring consist of camping beaches, prehistoric and historic sites, and traditional tribal resources, such as ethnobotanical, faunal and physical

(springs, sediment deposits, and mineral deposits) resources. Four specific program objectives are: (1) to conserve downstream resources, (2) to design mitigation procedures where necessary, (3) to maintain physical access to cultural resources, and (4) to provide quality recreational resources that do not adversely affect natural/cultural resources. There are other socio-economic objectives associated with hydropower supply and water resources, but these are outside the realm of remote sensing.

Many of the traditional tribal resources (such as ethnobotanical stands) are very small (< 1 m) and difficult to discriminate from similar, surrounding materials using airborne approaches. Some other resources (such as mineral occurrences within wall adits) are obstructed from aerial view. Resource monitoring that might benefit from a remote-sensing approach include: (1) detecting of natural springs, (2) monitoring beach and camp-site changes through time associated with different flow regimes, (3) detecting and monitoring of archaeological structures (including those that are partly buried), and (4) evaluating the effectiveness of vegetation and earth check dams in mitigating erosion and degradation of historic and prehistoric resources.

2.1 Natural springs

The most identifiable characteristic of spring water in remote-sensing data is their colder temperature relative to the surrounding geologic materials or vegetation. This characteristic is best detected using thermal-infrared (TIR) image data. Thus, our investigation of natural springs centered on the ability of TIR imagery to detect the occurrence of small, less obvious springs. Thermal imagery used in this evaluation was collected at a spatial resolution of 1 meter in mid-afternoon. A multispectral instrument was used to collect 12 different wavelength bands, two of which were TIR bands. These data were collected for our evaluations of a number of GCMRC parameters, which included (1) mapping terrestrial vegetation, (2) mapping warm-water eddies and backwaters, (3) detection and monitoring of partly buried or degraded archaeological structures, and (4) detection of natural springs. The mid-afternoon collection time for these data was dictated by the period of maximum solar heating for quiescent water in order to detect warm backwaters and by full illumination of vegetation in order to map vegetation, but this was not the optimal time for data acquisition for detecting natural springs.

Our analysis of the TIR data showed that the thermal contrast between the spring water and surrounding ground was too small during our daylight acquisition time to distinguish small springs from the surrounding geology on the walls of the canyon (Davis, 2002b). Only the larger springs (such as Vaseys Paradise) were detected. Previous TIR investigations using data collected just after sunset or just after sunrise seemed to be more successful at detecting warm springs along the Little Colorado River (Holroyd, 1995a, b) because thermal conductivity and emissivity differences between surface materials are most pronounced during these two time periods. However, these "detections" could not be confirmed by ground studies due to poor aircraft positional information. If springs are to be mapped within the canyon, it would require a separate, georeferenced TIR survey during post-sunrise hours; a post-sunset flight within the canyon would be unsafe.

2.2 Archaeological structures

One of the priorities of the cultural resource program is monitoring historic and pre-historic structures and check dams at certain structures to determine (1) the degradation of these structures and (2) the effectiveness of the check dams in mitigating the effects of arroyo erosion and river flow stage. Thermal infrared is very sensitive to subtle differences (or changes) in density and grain size (Hussein, 1982; Johnson et al., 1998). Thus, minor disruptions of the

surface will change the surface's density and/or grain size, which may be detected in TIR imagery (Johnson et al., 1998). Thermal-infrared images can also distinguish a degraded, buried ruin from its surrounding alluvium, as long as the ruin and the alluvium have different compositions or densities (Berlin et al., 1977; Nash, 1985; Berlin et al., 1990). Thus, we investigated the use of TIR data, as well as visible and near-infrared (NIR) imagery of different spatial resolutions, for detection and mapping archaeological structures at Unkar Delta (Davis, 2002b). Our results showed that spatial resolution was the key factor in mapping these structures for data acquired during the middle of a day. We could not unambiguously identify the structures at Unkar Delta using the daytime TIR data at 1-m resolution or using any of the ten reflectance wavelength band images that were acquired at 1-m resolution with the TIR data (Figures 1 and 2). The ambient air temperature in the canyon during our mid-day July data acquisition was close to 38 ºC. TIR sensors require liquid nitrogen cooling systems to maintain the sensor near absolute zero degrees, but the cooling system could not compensate for this high air temperature. Thus, the sensitivity of the TIR data was only 0.3 degrees, whereas a sensitivity of 0.1 degrees is required to detect thermal anomalies associated with geologic materials (such as the archaeological structure relative to its alluvial surroundings; Nash, 1985). Panchromatic (black-and-white) imagery at 18-cm resolution was also found to be much less useful in uniquely identifying the structures than CIR (green, red, and NIR composite) imagery at 11-cm resolution, which is attributed to the lack of contrast between the alluvial and archaeological materials in black-and-white imagery. We found that the most unambiguous detection of these structures requires CIR or natural-color imagery with resolutions near 11 cm. The incipient stage of arroyo development may manifest itself more as subtle changes in surface materials due to recent exposure or transport than as changes in surface topography. However, the CIR imagery do not provide good discrimination of alluvial geologic materials that may indicate mass movement and arroyo development. In order to detect subtle changes in alluvial surface materials it would be better to acquire multispectral data that include at least one short-wave infrared wavelength band, where more distinctive energy absorptions occur for geologic minerals. Such systems cannot obtain spatial resolutions better than 0.5 m. Although this resolution will not detect morphometric changes in structures, the data could better map changes in surface materials that may indicate mass movement.

For the detection of morphometric (dimensional) changes in archaeological structures and in the arroyos that affect these structures, even higher resolution imagery (2-3 cm or 1:1,600-scale photography) is required (MacFarlane et al., 2002; Petersen et al., 2002), especially for monitoring the very fine-scale (centimeter) changes in arroyos that could indicate potential impacts on such structures. Photogrammetric analyses of such extremely high-resolution image data, which were acquired within the remote-sensing initiative, produced an elevation accuracy of 6-10 cm; the average vertical error at the 95% confidence level (for normally distributed errors) of 18 cm. These data could resolve sub-meter-scale changes, but the vertical error exceeds the change-detection threshold for the smaller, cm-scale gullies (MacFarlane et al., 2002). Field studies at four selected sites by Petersen et al. (2002) indicated that vegetation cover, soil permeability, and soil shear strength to be inversely related to gully erosion activity. These observed trends, plus the fact that gully head locations can be predicted by slope and drainage area relations derived from the photogrammetric data, suggest that up-catchment control of gully initiation and knick-point retreat are more critical factors in structural degradation than is base-level changes related to Colorado River stage or Glen Canyon Dam operations (Petersen et al., 2002). The stereo-image data that were collected did however provide a catchment DEM that allows geopmorphic modeling of potential impacts of rainfall on arroyo development and, in turn, of potential impacts of arroyo development on down-slope archaeological structures. One of the major drawbacks to this approach for long-term monitoring of archaeological site degradation is the large expense for collection of the very high-resolution imagery required to detect the fine-scale changes; image acquisition costs for just four 100-m-wide archaeological sites was $20,000.

In addition, collection of such data requires a very low (240 m AGL) helicopter flight, which may become a noise issue within the Park.

We have found photogrammetric elevation data produced from 1:4,000-scale photography to yield vertical RMSE values of 28 cm (Davis et al., 2002b) and average elevation errors of 34 cm (at the 95% confidence level) at a cost of about $3,000 per river km. Stereo image data at this scale may be obtained annually for the entire river corridor for only $180 per river km to support other GCMRC monitoring protocols. Although such data may be acquired for other resource needs, only a small fraction (35 km) of the collected data would be photogrammetrically processed and the photogrammetric analysis of the data represents a large fraction of the overall cost of $3,000 per river km. Thus, even this more conventional photogrammetric approach would be very expensive for monitoring the nearly one hundred archaeological sites within the Colorado River ecosystem (CRE). Alternatively, automated, digital photogrammetric technology (ISTAR; Table 2) provides 30-45 cm (RSME) vertical accuracy on bare ground, 1.3-m accuracy in dense vegetation, and corridor-wide topography, in addition to orthorectified imagery, at a cost of $625 per river km. The ISTAR system collects three panchromatic images simultaneously with different view angles, which allows derivation of elevation using automated softcopy photogrammetric technology. This system also simultaneously collects four color bands that are useful for mapping terrestrial physical and biologic resources. We will evaluate that elevation data during 2003 to determine its accuracy for canopy heights. If the ISTAR data provide relatively accurate canopy heights, then ISTAR technology may become the remote-sensing protocol for large-area requirements for the physical and biological resource programs and may also provide useful topographic data for geomorphic modeling of archaeological sites at no additional expense. We have found that low- and moderate-resolution LIDAR (Light Detection and Ranging) provides less accurate, less dense elevation data on bare ground than that provided by photogrammetric data. The density of photogrammetric elevation data is only limited by the resolution of the stereo imagery (assuming the data are collected with adequate viewing angles). Our recent evaluations of very high-resolution LIDAR showed that the data provide an 8 cm vertical accuracy and a 4-5 cm vertical precision on bare ground, which is close to the requirements for monitoring the arroyos and check dams near archaeological sites. Such accuracies cost about $6,200 per river km, but also provide useful data to all GCMRC programs.

2.3 Mapping Campsites and Beaches

The quality of 20 main campsites and beaches along the corridor is currently evaluated annually by field surveys that map each site's topography and amount of open space. The field surveys are performed by the fine-grained sediment team in the physical resource program, whose primary purpose is to map all storage sites for fine-grained sediment within the CRE. However, it is logistically impossible for ground surveys to obtain an accurate inventory within a given year for the entire CRE. This monitoring is better accomplished using remote-sensing approaches because (1) campsites are generally well exposed and the rather simple parameters that the ground surveys record for campsite habitability, (2) remote-sensing data can see most terrestrial storage sites for sediment, and (3) rather simple image-processing algorithms can be used to map the characteristics of these sites. Using the ISTAR digital elevation data and orthorectified, four-band color data that were acquired for the entire CRE during 2002, Mike Breedlove (personal communication, 2003) recently showed that these data could not only map all campsites and beaches, but could also accurately inventory all terrestrial fine-grained sediment storage sites, throughout the CRE in a period of a few months. His analysis used the color data to define the water's edge (Figure 3) and to define areas of non-vegetation that have high levels of surface reflectance (Figure 4). Local near-infrared-band variance separated smooth (fine-grained) and

rough (coarse-grained) surfaces (a fine-grained sediment map is shown in Figure 5). Elevation data were used to restrict the mapping of campsites and beaches to areas that are 10 meters or less in height above the water's edge, which is a criterion established for campsite inventories, but the analysis was actually performed up to the wall-rock/alluvium interface. These individual data sets were integrated to produce a CRE digital map of fine- and coarse-grained sediment deposits (Figure 6). Much of these analyses were largely automated computer processed, which was made possible by the calibrated, digital data provided by ISTAR. If this process was attempted using un-calibrated, aerial CIR photography, the time required to produce such a product would increase by a factor of 3-4 and the product would have higher positional errors making it less accurate for temporal analyses. This study found some limitations in that data, mainly due to the different viewing angles of the four ISTAR color detectors. For example, the different view angles produced non-coincident sun glint in the four bands over much of the water's surface, resulting in random, unnatural colors for the water. Thus, mapping the water's edge required a supervised approach, which is usually one of the simpler, automated remote-sensing analyses. ISTAR now uses a color-detector system in which three of the four color bands are collected through the same optics and therefore with the same view angle, but the NIR band (critical for mapping vegetation) is still collected at a different view angle. This improvement will make some aspects of camp-site/beach mapping more automated for rapid temporal analyses, but an optimal system would collect all band data with the same optics, which would not only make this type of mapping more unsupervised, more rapid, and less expensive, but would also produce more accurate temporal analyses. Despite these few problems, the resulting inventory map of campsites and beaches is the most complete and accurate database to date and provides a good foundation (database and approach) for improved monitoring in the future.

3.0 Biologic Resources

The primary objective of the biological resource program is to understand the cause/effect relations between Glen Canyon dam operations and the downstream aquatic and terrestrial biologic ecosystem, and to develop a model that can predict ecological effects for different dam operations. This objective is approached in three ways: (1) inventory of biologic resources and, together with related physical resource data, development of a conceptual model that links biotic and abiotic components; (2) research on and development of cause/effect relations between dam operations and the ecology and testing the validity of the observed relations under various dam operations; and (3) monitoring both long- and short-term ecosystem behavior to determine if models are predictive for both natural (tributary) and dam perturbations. Monitoring the biologic resources within the aquatic and terrestrial environments is a fundamental aspect of these objectives and therefore remote sensing approaches for detecting and mapping the various resource parameters were evaluated within this remote-sensing initiative.

3.1 Aquatic Environment

Parameters monitored in the aquatic environment are those deemed important for the survival of aquatic species. These parameters consist of the chemical and physical characteristics of the water, the aquatic foodbase, and the presence of warm backwater areas that serve as fish habitats.

3.1.1 Water Parameters

Water Resources Division of the USGS collects and analyzes data from water-gage stations and water samples at various locations within Lake Powell, the main channel, and within major tributaries. From the tailwaters to Lees Ferry, remote monitoring stations measure and

transmit every four hours the sediment load, turbidity, and water temperature in the main channel. Monthly water samples are collected at river miles 0, -3, -6, -9, -11, and –16 and the samples are analyzed for chlorophyll, phytoplankton, and zooplankton. Remote water monitoring stations also measure the above parameters at the same frequency within several tributaries (Paria River, Shinumo Creek, Tapeats Creek, Spenser Creek, Havasu Creek, Kanab Creek, Bright Angel Creek, Little Colorado River, and Diamond Creek) and within the main channel above the Glen Canyon dam, at Lee's Ferry, above the Little Colorado River confluence, near the Grand Canyon, above National Canyon, and above Diamond Creek. At Lake Powell, surveys are conducted quarterly (March, June, September, and December) to obtain profiles of water temperature and turbidity at approximately twenty stations north of Glen Canyon dam between river mile 2 to 263. Water samples are also collected at some of these sites and are analyzed for chlorophyll, phytoplankton, and zooplankton.

Numerous remote-sensing studies conducted within the last decade have developed algorithms to measure sediment load (as total suspended sediment), turbidity, chlorophyll a and b, total chlorophyll, and total dissolved solids (specific conductance), but the depth of measurement is limited to the depth of light penetration and such measurements cannot determine variations with depth (e.g., Goodin et al., 1993; McFeeters, 1996; George, 1997; Sathyendranath et al., 1997; Fraser, 1998a, b; Tassan, 1998). Most studies determined that multiple wavelength bands within the 0.420 μm and 0.710 μm wavelength region are necessary to obtain accurate estimates and that the algorithms to estimate the water parameters require periodic verification of their calibration. This latter requirement might suggest that remote sensing cannot benefit aquatic monitoring because it cannot replace *in situ* measurements that are necessary for remote-sensing calibration. However, the real strength of remote sensing is not the elimination of field verification, but rather the extrapolation of site-specific information to wide areas at a significant savings of time and cost. For example, the areal perspective provided by remote-sensing data can assist in determining the most representative sites for *in situ* measurement systems, which may not have been done for the existing water monitoring network. Chavez et al. (1997) used temporal remote-sensing data acquired under different environmental conditions within San Francisco Bay to help water resource personnel determine the most appropriate sites for their *in-situ* monitoring systems. In addition, remote-sensing data can be used to produce maps that show the distribution of particular parameters over large areas for a particular time period. *In-situ* measurement systems provide only point-source information, which might miss or misrepresent an event that has spatial variation. Remote-sensing algorithms that have been developed for lakes can map chlorophyll concentrations with a sensitivity of 3 μg/l (George, 1997). Algorithms have been developed specifically for the Colorado River that relate spectral radiance of the water to the water's chlorophyll content, turbidity, and suspended load, using water-gage data for calibration (Chavez et al, 2002a,b). The algorithms can now be used to produce water-parameter maps for parts or all of the CRE using the multispectral camera that Pat Chavez has purchased, whose bandwidths are optimized for mapping the aquatic environment, which was recommended by the remote-sensing PEP (Berlin et al., 1998).

3.1.2 Aquatic Foodbase

At 10-day intervals for 90 days each year, foodbase is determined within pool, cobble-riffle, shoreline, and nearshore environments. The foodbase surveys are performed at river miles -15.5, 0, 60, 64 , 138, and 205. For the pools, foodbase is examined at five locations along each of three transects; each transect is about 30 m apart. The five sampling locations along the transects include the thalweg, <28m^3/s, baseflow, lower varial, and upper varial zones. Cobble riffle sample collections occur within the deepest accessible zone, as well as the lower and upper varial zones. Population data are collected for five biotic classes. Associated data are also

collected, consisting of water temperature, dissolved oxygen, pH, specific conductance, substratum type, microhabitat conditions, total P and N, Secchi depth, water velocity, depth, site, and time of day. Shoreline habitats are sampled to determine (1) invertebrates in emergent vegetation, (2) fine sediment volume, and (3) tychoplankton. Nearshore habitats are surveyed to obtain (1) temperature profiles at 5-cm depth intervals within shoreline vegetation and 0.5 m from the shoreline and (2) surface (≤ 0.5 m depth) drift samples of coarse- (500 micron mesh) and fine-particulate (0.5 micron mesh) organic matter.

Although the remote-sensing PEP (Berlin et al., 1998) recommended that airborne multispectral image data be explored for mapping these parameters, most chemical constituents in water and other properties related to chemistry (pH) cannot be detected with airborne sensors. Even though certain elements and compounds do absorb in the visible through TIR wavelength region, their concentrations in water need to exceed 1 wt % for their detection. When aqueous chemical concentrations reach such high levels, such as in estuaries and lakes, it has been shown that their concentrations can be mapped (Chavez et al., 1997), but such techniques cannot provide depth-concentration profiles, which are obtained during GCMRC *in-situ* monitoring. In addition, an airborne remote-sensing approach for aquatic foodbase parameters would be limited to the clearer, shallower water areas, would provide only certain parameters (Alberotanza et al., 1999), such as algae, vegetation flotsum, plankton, organic matter, surface drift, total dissolved solids (specific conductance), and could not detect the biotic species that are monitored by GCMRC. Even though multispectral sensors exist that provide wavelength data appropriate for monitoring some of the foodbase parameters, obtaining such data through commercial vendors at the high frequency currently obtained by *in-situ* monitoring would cost so much that remote-sensing would not be a viable option for present foodbase monitoring. Pat Chavez tested this multispectral sensor by acquiring 3-cm image data within Glen Canyon to determine the ability of the data to map fish foodbase and nesting habitats. The results of this study will be available during the summer of 2003. If useful results are obtained, a similar sensor could be purchased by GCMRC ($15,000) and flown at relatively low cost to provide data for various monitoring requirements. However, orthorectified image data would be most useful, which requires expensive GPS and IMU instrumentation. Image data could be rectified using an existing controlled image base, but this georectification process is time consuming, would cost more than the data collection, and would provide at best only 1 m positional accuracy.

Remote sensing can provide wide-area monitoring for two other aquatic parameters: water surface temperature and substrate type. Mapping water surface temperature is discussed in the following section on warm backwaters; substrate mapping is discussed in a section within the physical resource program in which channel substrate is a primary collection parameter.

3.1.3. Warm Backwaters

One of the objectives of the CRE monitoring is the preservation of the native Humpback Chub, whose population has diminished due to the cold, low-flow water releases since construction of the Glen Canyon dam. Chub prefer warm (18-22 ºC), turbid, and sheltered water environments, such as return-current channels, shoreline embayments, and the mouths of tributaries. The presence and number of backwaters within or near return-current channels, shoreline embayments, and tributary mouths are monitored during quarterly, system-wide vegetation surveys, which map the presence of dry and wet marshes that contain different wetland vegetation. The temperatures within the backwater areas are monitored periodically by thermistor-string field surveys at selected backwater areas and by water gages at several sites within the CRE. By their nature, the surveys and gages sample a small portion of the CRE. Detection and mapping of these warm backwaters should be more easily accomplished using

appropriate remote-sensing data. We investigated this possible remote-sensing application by collecting a multispectral (12-band) data set containing two TIR bands for a 44-mile segment of the CRE between river miles 30 and 74 (coincident with a ground survey in the area). This 44-mile airborne survey took 20 minutes to complete using a helicopter flying at a 365 m AGL (above ground level). Even at this low AGL, the multispectral sensor could provide only 1-m spatial resolution. TIR image data record surface radiant temperature across the entire channel, which can augment site-specific thermistor surveys. Our TIR data were collected in early July 2000 when the ambient air temperature was so high (38˚C) that the TIR cooling system could not reach the required absolute zero degrees (for a 0.1 degree sensitivity), which resulted in a 0.3 degree sensitivity in the TIR image data, but even this sensitivity proved more than adequate to detect and map the warm backwater areas (Davis, 2002b). Derivation of water radiant temperature required calibration of the airborne sensor signals to water temperatures, which was accomplished using coincident water-gage temperature data. The airborne TIR data showed a linear relation with main-stem water temperature (Figures 7 and 8) and easily mapped all warm backwater areas within the 44-mile river segment, which included eddies with rather steep thermal gradients, tributary mouths with gradual and abrupt thermal gradients, eddies formed by reattachment bars, return-current channels, and isolated backwaters that are difficult to discern in visible-wavelength imagery (Figures 9 and 10). Although the 1-m spatial resolution (and possibly the 0.3 degree sensitivity) of the TIR imagery was insufficient for the detection of archaeological structures, it was found to be totally adequate for detection and mapping the warm-water areas within the 44-mile study area. Unfortunately, the 44-mile study area covered by the multispectral data only included wet marshes. Therefore, we could not test the capability of these data for discriminating and mapping dry and wet marsh areas based solely on the 1-m reflectance band data.

At the present time, the limiting factor for multispectral sensors is their spatial resolution, which is not better than 50 cm. Additional protocols of the physical resource program, and possibly of the biologic resource program, require a higher spatial resolution (≤ 20 cm). These additional requirements are discussed in following sections. Without any additional applications of multispectral data at resolutions near 50-100 cm, the cost ($530 per river km) for such data for just mapping warm backwaters would be difficult to justify. However, there may be additional needs for this lower resolution, multispectral image data in order to more accurately and efficiently inventory the terrestrial vegetation resources within the CRE. This issue is addressed in the following section.

3.2 Terrestrial Environment

The biological resource program periodically monitors the composition, area, and volume of vegetation habitats within the CRE each year. Composition is monitored to determine changes in plant populations due to the invasion of exotic (non-native) species and to dam flow operations during the year. Area and volume are primary indicators of the suitability of vegetation stands as faunal habitats. Monitoring of these characteristics is performed mostly by ground surveys.

Parameters monitored in the terrestrial environment are those deemed important for bank stabilization, aquatic and terrestrial faunal habitats, tribal botanical resource, and recreation. Prior to 2002, vegetation type, area, and height were mapped annually at 11 sites (river miles, 6, 43.5, 50.5, 55, 68.5, 71.5, 93, 123, 194, 209, and 243) using aerial photographs and field studies. In addition, downslope growth rates of equisetum, juncus, and phragmites were measured along selected transects on monthly basis over a four-month period. The monthly field studies also monitored growth or removal of exotic plants, such as tamarisk ramosissima and alhagi camelorum (camelthorn), and sample low-elevation areas for changes in seed abundance and

type. Surveys now consist mostly of random samples throughout the CRE and of culturally significant plants (exotic/invasive species and ethnobotanical species) during April, May, and September. Vegetation of interest includes acacia, equisetum/sedge, redbud (Cercis occidentalis), tamarisk (tamarix ramosissima), arrowweed (tessaria sericea), bermuda and red brome monotypic grasses, hackberry (celtis reticulata), cliffrose, desert brome, mesquite, coyote willow (salix exigua), baccharis seepwillow (baccharis emoryi and salicifolia). Before 2000, photographic prints were used to manually trace the distribution of vegetation species, based on a visual interpretation of CIR color and texture. All derived polygons were then field checked. The collection of orthorectified imagery now makes this process more efficient and accurate. More advanced remote-sensing data and analysis methods should be able to increase the area covered and reduce the time required for field surveys, but this will depend on the capability of the remote-sensing data that can be acquired for the CRE within GCMRC's remote-sensing budget.

Several factors control the spectral reflectance of vegetation; these include water, chlorophyll a (absorbs at 0.430 μm and 0.662 μm) and b (absorbs at 0.453 μm and 0.642 μm), assessory pigments (e.g., Beta carotene and lycopene that absorb between 0.460 μm and 0.550 μm), nitrogen, lignin (cell wall polymer), cellulose (40-60% of cell walls), and open pore space. Numerous studies have been performed over the past three decades to determine the most appropriate data and analysis methods to accurately detect and map these vegetation characteristics using remotely sensed data. Recent research has determined the following relations.

1. There is a strong linear correlation between chlorophyll (a+b) and (1) the ratios 0.750 μm/0.700 μm and 0.750 μm/0.550 μm and the green vegetation index (Gitelson and Merzlyak, 1997); (2) the 0.700 μm and 0.735 μm reflectance and their band ratio (Gitelson et al., 1999); (3) the first derivative of the green vegetation index (Elvidge and Chen, 1995); (4) the perpendicular vegetation index (Richardson and Wiegand, 1997); (5) the first derivative of the 0.721 μm band (Blackburn, 1999); and (6) the band ratios 0.836 μm/0.817 μm and 0.969 μm/0.931 μm, the first derivative of the 0.750 μm band, and the second derivative of the 0.753 μm band (Blackburn and Steele, 1999). Blackburn and Steele (1999) also found good correlations between their wavelength band ratios and derivatives and the carotenoid content and that the derivative of 0.721 μm band correlated well with total chlorophyll, chlorophyll a, and chlorophyll b, but not so well with carotenoid content.

2. Penuelas et al. (1997) found some correlation between the 0.900 μm/0.970 μm band ratio and plant water content, but it was very weak, but Hardy and Burgan (1999) found a good correlation between NDVI and plant moisture.

3. Kokaly and Clark (1999) found good correlations between spectral reflectance centered at 1.730 μm, 2.100 μm, and 2.300 μm with nitrogen and cellulose, but not with lignin.

4. Spectral reflectance from vegetation is affected by soil and litter cover, illumination angle, and shadows. Methods have been devised to mitigate these effects (Lee and Marsh, 1995; Garcia-Haro et al., 1996; Todd and Hoffer, 1998; Blackburn, 1999; Pinder and McLeod, 1999; Yu et al., 1999; and Quackenbush et al., 2000).

5. Vegetation classification accuracies greater than 80% have been obtained using remotely sensed data (Butt et al., 1998; Purevdorj et al., 1998; Coulter et al., 2000). Use of seasonal data improves classification for deciduous vegetation (Grignetti et al., 1997;

Mickelson et al., 1998). Additional and narrower wavelength bands increase classification accuracy (Elvidge and Chen, 1995; May et al., 1997; Green et al., 1998). Airborne imagery provides better accuracy than spaceborne imagery due to its higher resolution (Rowlinson et al., 1999; Zhu et al., 2000).

All of this research points to the distinct possibility that terrestrial vegetation surveys can become more automated, extensive, and less expensive using remote-sensed data and image-processing algorithms. Therefore, the remote sensing initiative investigated various airborne technologies for mapping the community-level compositions and deriving accurate canopy elevations of habitats.

3.2.1 Vegetation mapping

For vegetation composition at the community level, we evaluated different types and resolutions of image data that were acquired during the remote-sensing initiative (Davis et al., 2002c). The data that were evaluated included 11-cm CIR film (July 2000), 30.5-cm CIR film (March 2000), 28-cm CIR film (acquired during overcast conditions in September 2000), 30.5-cm digital CIR imagery (September 1999), and 100-cm digital, 9-band multispectral (July 2000) image data. Vegetation texture was derived from each data set and used with the color information in various supervised image classifiers to produce vegetation maps at five study areas that were previously mapped by ground surveys (Kearsley and Ayers, 2000). The study areas were located at river miles 43.1, 51, 55.5, 68.2, and 71.4. The vegetation maps produced using the airborne image data were compared to the ground survey maps to determine the accuracies and relative merits of the different types and resolutions of image data for mapping CRE vegetation communities. The resulting classification maps produced for study area RM 68.2 are shown in Figures 11-17. The results of this investigation are summarized in the following items that were extracted from Davis et al. (2002c).

1. The intrinsic reflectance of vegetation is an important factor in discrimination of the riparian vegetation within the CRE. Thus, digital sensors that record a large dynamic range and maintain radiometric fidelity provide higher mapping accuracies than photographic film. Although image data acquired under overcast sky conditions produced less shadowing within vegetation, the resulting lower reflectance of the vegetation reduced the classification accuracies from these data over that obtained from image data acquired under clear sky conditions. In addition, it is best to obtain image data near the summer solstice in order to minimize shadows within vegetation, but also shadows cast by the canyon walls. Even at the solstice, there are areas within the CRE that need to be acquired within one hour of noon in order to minimize shadows from steep canyon walls (Figures 18 and 19).

2. Vegetation texture is an important factor in vegetation map accuracies. Texture was found to increase mapping accuracies by 20-30 absolute percent over accuracies obtained from vegetation mapping that used just color reflectance information. Mapping accuracy is the percentage of picture elements for a particular vegetation alliance or collection of alliances that are correctly identified. Texture is much better defined within the vegetation at higher spatial resolutions and is best derived from image resolutions near 20 cm or higher resolution.

3. Calibrated, 9-band multispectral image data (1-m resolution) produced higher map accuracies than higher resolution (11-cm), un-calibrated CIR film, *which shows the importance of radiometric calibration for vegetation mapping*. Reducing the number

of multispectral bands used to map vegetation to only four wavelength bands did not greatly reduce mapping accuracies over those obtained using the full 9-band set. The four most useful bands for mapping the CRE riparian vegetation were centered near the wavelengths 0.53-54 μm, 0.066-0.67 μm, 0.70 μm, and 0.79-0.82 μm. These are close to the wavelengths selected for the early Landsat Multispectral Scanner System (Landsat MSS), which was primarily designed for vegetation monitoring.

4. The use of a Global Positioning System (GPS) and an Inertial Measuring Unit (IMU) that provides 30-cm positional accuracies should be used with DEM data to orthorectify the image data in order to provide accurate area and volume estimates.

5. Phase angle during image data collection should be kept to a narrow range ($\leq 10^{\circ}$) because canopy reflectance values can change at different solar incidence angles and sensor viewing angles.

6. Subsequent field work is required to reach an 80% mapping accuracy, but the field work would be much less intensive and invasive than current field surveys for vegetation.

7. Remote sensing will not eliminate the need for the current random sampling of vegetation within the CRE because understory is a key component in these field surveys and remote-sensing data even at 6-cm resolution cannot identify, and in most cases see, the understory.

We have not yet found an imaging system that can provide the four wavelength bands listed in item 3 above with acceptable spatial resolutions. We did locate a 4-band imaging system operated by ISTAR Americas that provides three of the four desired wavelength bands (not the band centered at 0.70 μm), in addition to a blue wavelength band, at 44-cm spatial resolution. This system was used to collect the 2002 annual image and DEM data for the entire CRE. The positional accuracy of the orthorectified image data was found to be about 30 cm, which is better than most other image data acquired by GCMRC to date and acceptable for biologic monitoring purposes. The 44-cm spatial resolution was less than desired, but our preliminary vegetation analyses using these data show that texture derived from this 44-cm data still added 10-25% to the classification accuracies for various vegetation alliances. We did encounter a problem with saturation in the critical NIR image data, which means that the recorded NIR brightness for some vegetation alliances were similar even though their NIR ground reflectance spectra show that they are distinctly different. This is a calibration issue and is the *main reason that correct sensor calibration is a critical factor in the list above*.

Some vegetation alliances were found difficult to discern using the 4-band ISTAR data, which raises an important issue for future vegetation mapping. Is a sensor that provides additional useful wavelength bands at the expense of spatial resolution (and derived texture) better for future vegetation inventories than a sensor that provide a few bands but higher spatial resolution? Before the next data collection for vegetation inventory, this question needs to be answered so that mapping can be less time consuming and more accurate. Higher order multispectral data (referred to as hyperspectral data) were acquired for small areas within the CRE in order to evaluate these data. HYDICE (an Navy experimental sensor) acquired 206 bands at 1.5-m resolution within Glen Canyon, but the data proved to be too noisy (poorly calibrated) to use for vegetation classification. AVIRIS (a NASA instrument) acquired 220 bands at 4 m resolution, but occurrences of some important vegetation alliances are much smaller than an AVIRIS picture element. We hope that a well-calibrated, hyperspectral data set can be acquired

in the near future at a few different resolutions in order to resolve this issue, preferably using a commercially available system so that we could confidently employ the system once collection specifications were determined.

3.2.1 Canopy elevation and volume

Currently, vegetation stand volume is estimated from the stand's area, which can be obtained from correctly orthorectified imagery, and from spot vegetation height measurements, which may be limited to the more accessible parts of a stand. Two remote-sensing approaches, photogrammetry and LIDAR, were investigated that potentially could produce more accurate (representative) stand volumes. For this evaluation, we examined photogrammetric data produced from 1:4,000-scale photography and two sets of LIDAR data acquired using different LIDAR sensors that collected points at a 1.5-m and 3.75-m spot spacings. The LIDAR data were evaluated as a potential method for mapping canopy volumes because neither LIDAR data set provided ground elevations within our CRE vegetated test areas. We therefore thought that these LIDAR data might at least provide canopy elevations. [Our assessment of LIDAR for ground elevation is discussed in the following section within the physical resource program.] Based on our assumption that stand volume could be under-/over-represented by 20% using current field sampling technique, we set this level of accuracy as the minimum accuracy for the remote-sensing data.

Our analyses of the photogrammetric and low-to-moderate resolution LIDAR elevation data (Davis et al., 2002a and submitted) showed that photogrammetry is much more accurate for mapping canopy elevations than are either of the two LIDAR surveys. We found that (1) 67% of the photogrammetric spot elevations were within 20% of ground-surveyed canopy elevations, (2) only 38% of the high-resolution (1-m spot spacing) LIDAR data met this accuracy, and (3) less than 5% of the moderate-resolution (3.75-m spot spacing) LIDAR data met this criterion (Figure 20). The new ISTAR airborne technology that we employed in June of 2002 for the entire CRE produced a 1-m digital surface model (DSM), which is a digital elevation model for the reflected surface, that should include the vegetation canopy within dense stands. These data are currently being evaluated for canopy heights, which will require that the DSM data accurately represent both the canopy and surrounding bare ground. These DSM data were produced without human intervention using automated softcopy photogrammetry and therefore the cost is relatively low ($625 per river km) compared to more conventional photogrammetric analyses. On the other hand, we are currently evaluating very high-resolution LIDAR data for topography and canopy height for vegetated areas. We have already found these data to be extremely accurate on bare surfaces (8 cm) and hope this also holds for the vegetation. However, the cost for these LIDAR data ($6,200 per river mile) may preclude its use for large-area volume estimates. A less-expensive ($2,100 per river mile), high-resolution LIDAR sensor, which provided 17 cm vertical accuracy on bare ground, is also being evaluated and may provide an acceptable medium.

4.0 Physical Resources

The physical resources program provides information and assessments of dynamic hydrologic and geomorphic processes resulting from Glen Canyon dam operations that directly and indirectly affect the CRE. The overall objective of the program is ecosystem sustainability of hydrologic and geomorphic processes and interactions and long-term conservation of sediment in main-stem and riparian environments. The habitats of concern include channel environments (cobble and gravel bars, debris fans, and talus shorelines) where benthic organisms occur and which are used by spawning fish; aquatic near-shore habitats (sandy shorelines and backwaters) that are used by juvenile native fish and that provide substrates for plants; terrestrial habitats that

support riparian flora and fauna; terrestrial substrates used by recreational visitors; and terrestrial substrates that support and preserve cultural resources up to the stage associated with pre-dam river terraces. This overall objective is being approached by three program elements, which also have implications for biological and cultural resources.

1. Long-term monitoring of fine-grained sediments in key storage settings documenting system-wide changes in these deposits (morphology, volume, area distribution, and grain-size characteristics) relative to dam operations and natural tributary inputs.

2. Long-term monitoring and evaluation of coarse-grained sediment inputs (with respect to volume, grain-size, and topographic changes within debris fans, eddies, cobble bars, and the channel substrate) from tributary debris flows and Glen Canyon dam operations relative to system-wide, coarse-sediment mass balance and distributions of aquatic and terrestrial habitats.

3. Developing or refining existing stream-flow and suspended-sediment transport models, considering a subset of river reaches grouped by their common characteristics and behavior, to better predict average sand-bar deposition and erosion responses to varied discharge rates, fine-grained sediment supply, and thermal conditions, and to better understand coupled suspended-sediment and stream-flow processes along the main channel.

Grain size is an important parameter, especially with respect to the 10 lowest size classes within the sand, silt, and clay categories. However, these fine grain sizes are also the most difficult to detect with remote sensing due to the small size of the particles. Past monitoring within this program concentrated on just 4-5 reaches within the first 100 river miles, on the assumption that these sites adequately represented corridor changes from dam operations. Monitoring within this program has now been expanded to 11 reaches that are distributed throughout 230 miles of the corridor. As in the biologic resource program, the parameters that are monitored by the physical resource program can be separated into two categories: aquatic and terrestrial.

4.1 Aquatic Environment

Unlike the biologic resource program, the physical resource program is concerned mainly with the inorganic (geologic) components within the aquatic environment, which are easier to detect and monitor using remote-sensing data.

4.1.1. Water parameters

Water parameters monitored within this program consist of main-stem and tributary flow rate, sediment load, turbidity, temperature, and grain-size distribution of suspended sediment. The first four of these parameters are measured mainly with stream gages, whose data are transmitted by telemetry to the Flagstaff Field Center. The gaging stations are located at river miles 0, -3, -6, -9, -11, and -16; downstream within the Paria River, Shinumo Creek, Tapeats Creek, Spenser Creek, Havasu Creek, Kanab Creek, Bright Angel Creek, Little Colorado River, and Diamond Creek; and within the main channel above the Little Colorado River confluence, near the Grand Canyon, above National Canyon, and above Diamond Creek. In the recent past, grain-size distributions were only measured from collected water samples. The remote-sensing PEP suggested that in-stream optical devices be explored for measuring turbidity (Berlin et al.,

1998), but turbidity was already recorded by the gaging stations. However, grain-size distribution within the suspended sediment, which is not obtained by the conventional water-gaging stations, is now being continuously monitored using LISST (Laser In-Situ Scattering and Transmissometry) submersible instruments that measure particle concentration, particle size spectra, pressure, and temperature. These instruments are portable and are easily relocated. Spatial water temperature is measured with strings of thermistors that are deployed by boat crews. Our previous discussion on mapping warm backwater areas showed that airborne TIR data can provide rapid, wide-area, surface water temperature maps for the CRE, but the cost of these spatial data are high relative to the point-specific data provided by the *in-situ* detectors, especially high-frequency data collections. Use of remote-sensing data for mapping the water temperature will obviously be determined by the specific requirements of the program within any given year.

Although stream instrumentation is the most accurate method for obtaining sediment load, and turbidity, the instruments provide only point-specific data and relatively few points within the CRE. Airborne image data, calibrated by these *in-situ* instrurments, have the potential for producing regional water-parameter maps for improved understanding of the spatial relations between sediment transport and deposition within the CRE. Multispectral, visible-wavelength image data have been used to estimate turbidity and total suspended sediment load using ground calibration data to relate spectral response to absolute water values (e.g., Whitlock et al., 1978; Goodin et al., 1993; Jerome et al., 1996; Sathyendranath et al., 1997; Fraser, 1998a, 1998b; Pozdoyakov et al., 1998; Tassan, 1998). Some of the better correlations between turbidity or total suspended sediment and spectral response have been obtained in the 0.695-0.720 micrometer wavelength region (Goodin et al., 1993; Tassan, 1998; Fraser, 1998a), but this wavelength region does not provide the greatest water penetration.

Chavez et al. (2002a,b) correlated radiance-ratio measurements of the main stem at selected CRE locations with concentrations of total suspended sediment concentrations (TSSC; mg/l) and silt/clay ratios that were obtained from nearby water-gage stations. They found good correspondence (correlation coefficient of 0.95; Figure 21) for these two data sets, but not for sand concentration (correlation coefficient of 0.60; Figure 21). The observed relations were used to map TSSC concentrations and silt-clay ratios for segments of the CRE that were imaged with CIR sensors in September of 2000 (Figure 22).

Spectral response due to total suspended load or turbidity is affected by mineral composition and quantity and dissolved organic matter, all of which affect the backscatter and absorption coefficients of water. Thus, the relations developed by Chavez may need to be established at various locations within the CRE for corridor-wide application. Chavez (personal communication, 2003) believes that just three locations within the CRE are necessary in order to capture the variations produced by different tributary inputs. The relations that he has developed for visible-wavelength image data can now be used to calibrate airborne sensors to produce maps of these parameters throughout the CRE. Relatively inexpensive ($15,000) digital camera systems (such as that used by Chavez) are available that can record these required wavelengths, which would allow data collection at any time for the cost of aircraft and pilot time (about $350 per hour using a BOR aircraft and pilot). This helicopter-mounted instrument can image about 100 miles of the river corridor in two hours because the aircraft can follow the course of the corridor, but care needs to be taken during turns so that the aircraft does not produce roll, which results in off-nadir imagery. Although data collection is inexpensive, post-processing of these data without GPS and IMU data will add to these costs. This factor is discussed in more detail in the next section.

4.1.2. Channel substrate

Channel substrate parameters consist of main-stem and tributary bathymetry, fine- versus coarse-grain-size distribution on beds, median grain-size distribution in vertical profiles of river beds, and thickness of beds. Only the first two of these parameters can be approached using airborne remote-sensing data. Bathymetry within the main stem is currently obtained using a backscatter multibeam instrument that provides fine-scale (3 cm) topography, as recommended by the physical resource PEP (Wohl et al., 1999). Bathymetry of shallow, limited near-shore environments that cannot be surveyed with this instrument is measured by ground-survey crews. Although the goal is to map the substrate bathymetry throughout the corridor every five years, processing of the backscatter data is time consuming and the monitoring is behind schedule.

Alternative airborne remote-sensing techniques include the SHOALS LIDAR and optical image data. The physical resource PEP (Wohl et al., 1999) recommended that SHOALS (*S*canning *H*ydrographic *O*perational *A*irborne *L*idar *S*urvey) be considered for bathymetric surveys. The SHOALS LIDAR system is a dual-beam laser system that obtains water depth by differencing the distances recorded from the green wavelength laser (substrate) and the near-infrared laser (water surface). Recent studies have shown that the combination of SHOALS bathymetry and color aerial photography can greatly assist in the mapping of coastal substrate and coral reefs (Chavez and Field, 2000a, 2000b; Chavez et al., 2000a, 2000b), but those waters are relatively clear. The water penetration of SHOALS is constrained by turbidity and, therefore, will have limited application within the CRE (Irish and Lillycrop, 1999). Two optical-image approaches for mapping bathymetry derive (1) relative water depth from images acquired at two wavelengths and (2) absolute water depth from stereo-image pairs. The first technique has been used in a variety of clean, standing water bodies (Lyzenga, 1978, 1981; Bagheri et al., 1998; Bryant and Gilvear, 1999; Roberts and Anderson, 1999; Woodruff et al., 1999; Durand et a., 2000). This technique requires two wavelength bands because reflectance from the substrate can change with the substrate composition and images of two different wavelengths can be used to separate and map water depth and bottom composition, as long as both wavelength signals are reflected from the substrate. The maximum water depth that can be determined using this method is limited by the maximum penetration depth of light in the longest wavelength region and by the optical properties of the water. The suspended sediment within the Colorado River will limit the application of this technique to a very small fraction of the CRE that generally has clear water. Sun glint from rapids will create problems in this approach for submerged cobble bars or debris flows. The photogrammetric approach using stereo-pair images, which was suggested by the remote-sensing PEP (Berlin et al., 1998), is extremely difficult to apply in water due to corrections for refraction and would be limited in its application to clear-water regions. We investigated the use of stereo image data to derive substrate elevations for shallow, calm-water areas that had ground truth bathymetry and found that the lack of texture on sandy substrates precluded image correlation between the stereo images, which is necessary for derivation of topography. Therefore, the backscatter multibeam approach appears to be the most viable approach for channel bathymetry despite its data processing limitation.

Grain-size distribution on the channel substrate is currently mapped using a combination of side-scan sonar and underwater videography The sonar beam scans across the channel substrate producing a single image strip that has different perspective views on each side of the sonar image (centered on the boat position). Such imagery is extremely difficult to orthorectify and mosaic due to a lack of the sonar's fish pointing characteristics (pitch, roll, and yaw) and point-perspective distortions. Consequently, side-scan sonar has not proven to be a productive tool for imaging the substrate. In addition, the resulting rectified sonar image data have positional accuracies of only 2-3 m at best. Videography is used in conjunction with the side-scan sonar surveys to record the surface characteristics of the substrate, which was initially

recommended by the remote-sensing PEP (Berlin et al., 1998), but the panel subsequently recommended that videography be replaced with alternative sensors. New software (QTC Multiview) for processing backscatter multibeam data can supposedly map bed composition, but the software has not yet been fully evaluated to determine its mapping accuracy for grain-size distribution on the channel floor.

There are airborne imaging approaches that may provide good water penetration in order to image the channel substrate under clear water conditions. This approach is rather simple and rapid in its image processing, is cost-effective, and provides wide-area coverage with positional accuracies of at least 1 meter. Photographic film acquired with long exposures or digital image data acquired with a high-gain state provide maximum water penetration, but digital cameras that can record a larger range of radiance provide better image data for channel substrates. In August and September of 2000, an experiment was performed using a digital (CCD) panchromatic imaging system that acquired main-stem image data above Lees Ferry using a high-gain detector setting (equivalent to increasing the exposure time on photographic film). The two image acquisitions bracketed a spike flow in early September; the resulting image data clearly show morphologic detail on the channel substrate and clearly show changes in channel sand storage due to the spike-flow release (Figures 23-25; Chavez et al., 2002a). The image data appear superior to the image data produced by side-scan sonar. Although this technique requires relatively clear water for substrate imaging, there are periods when sediment input is quite low (such as 2002 and 2003). The present condition of low sediment input has allowed the physical resource program to extend this experiment to include the first 100 miles of the CRE using Pat Chavez's CIR sensor whose wavelengths are optimized for water penetration. The three wavelength bands were acquired at different gain states. The blue-green band was acquired at high-gain for water penetration, the red band at moderate gain for moderate water penetration, and the NIR band at normal gain to provide land data for image registration. Data were acquired at 300 m AGL within the Grand Canyon producing CIR data with 15-cm spatial resolution. The high-gain image data clearly showed locations of various types of sediment storage within the channel, where the water depth allowed light penetration to the substrate. In fact, variation in grain size is also easily seen in that data, as evidenced by the image mosaic of a channel segment south of the LCR confluence (Figure 26). Although these data will be examined in detail this summer, our preliminary evaluation of these data show that it requires about one hour to georectify each image to an existing controlled image base. At 15-cm resolution, there are about 1000 overlapping images that cover the first 100 miles of the CRE. Thus, without accurate GPS and IMU data for each image to allow automated rectification, the true cost of useable data needs to include one-half year of salary for the image rectification, but that will only produce 1 m positional accuracy. We are in the process of testing software that is especially designed for more automated image rectification, which is also relevant for rectifying some of the more useful historical data sets.

4.1.3 Main-stem water elevation

During 2002, water resources personnel (Tucson, Arizona) noticed a correlation between one of the LIDAR elevation data sets (acquired in 2000) over the CRE main stem and the historical main-stem elevations that were measured by a ground survey in the early 1900's. They also noticed at some locations that the LIDAR main-stem elevations were at least 1 m higher than the historical water profile and that these locations coincided with riffles or rapids. The LIDAR data used in that comparison were acquired with a NIR laser system. Although LIDAR is not commonly used to measure water surface elevation, the SHOALS LIDAR does use a NIR laser source to measure water-surface elevation, as well as a green-wavelength laser to measure substrate elevation. Thus, water surface elevations might be obtained from conventional LIDAR

data. In order to verify this observation, Davis et al. (2002b) compared the March 2000 LIDAR elevation data over the main stem channel with corresponding water-edge elevations obtained from coincident ground surveys at four long-term monitoring sites. They found a high degree of correlation between the LIDAR water elevations and the surveyed water-edge elevations. The LIDAR elevations over the main-stem channel showed a vertical root-mean-square error (RMSE) value of 30 cm (Figure 27), assuming that ground-surveyed water-edge elevations accurately reflected the water's surface elevation at the center of the channel. Thus, the LIDAR data were found to closely represent water-surface elevations and may in fact be useful in monitoring changes in submergent debris flows or cobble bars. The majority of the LIDAR elevations (90%) at most sites were within 40-50 cm of the surveyed water-edge elevations (Figure 27) and, therefore, LIDAR elevation differences between any two time periods would have to exceed 40-50 cm before being considered significant.

4.2. Terrestrial Environment

On land, the physical resource program monitors change in fine- and coarse-grained sediment storage, which is represented by debris flows, cobble bars, river terraces, and different types of sand bars. The basic parameters measured consist of geomorphology and topography. These parameters are monitored at active sand bars in the New High Water Zone, the return-current channels within fan/eddy complexes (backwaters), and the pre-dam river terraces with cultural resources, both on a historical (annual) basis and on a short-term, experimental-event basis. Study sites number about 35 between river mile -6 and 225, but many of these are camp sites and camping beaches; there are 11 main monitoring sites for sediment that average 2 miles in length. Geomorphology is interpreted and mapped using stereo imagery. Before 2000, scientists within the program used aerial photographic data that had no pointing or positional information, which made rectification and orthorectification very difficult, time-consuming, and error prone. The remote-sensing PEP recommended that future data be acquired with GPS (Global Positioning System) and IMU (Inertia Measurement Unit) data. This panel also recommended an image resolution 1-5 m for sand-bar mapping, but we have found that image resolution for the physical resource program was more a function of required vertical accuracy than resolving power for geomorphic mapping.

Before the remote-sensing initiative, all topographic data were acquired by field survey measurements, which is not only expensive but also time consuming, both of which limited the area that could be monitored within any given year. Since 2000, various alternative airborne approaches have been tested, the results of which are discussed below. As additional study sites were added or when more historical data were required to extend the period of observation, photogrammetry and geomorphic mapping were applied to historical photographic data. The historic photogrammetric analyses partly overlap time periods of land-based topographic surveys to provide ground truth data for photogrammetry. Before 2000, almost every annual image acquisition consisted of analog film and prints, which degrade over time, were lost or misplaced, and were extremely difficult to use by non-resident scientists. Thus, preservation and access of the historical image archive were two critical factors considered within the remote-sensing initiative. An operational airborne approach for topography must satisfy the most stringent vertical accuracy requirements within the GCMRC programs. This requirement resides within the physical resource program and is 25 cm, which is based on the minimum amount of change in sand bar height that is deemed "significant" and needs to be recorded (Schmidt et al., 1999). This elevation accuracy value was our targeted objective with all the various topographic remote-sensing evaluations that we performed during the past two years (Table 2).

Surficial geology of terraces and debris flows are mapped into units based on elevation (terrace level), hill slope, grain size, relative age, and composition. Historically, this information was extracted from (poorly rectified) aerial photographs using photointerpretation and field investigations. In general, debris flows are monitored and mapped on an annual, system-wide basis, whereas terrace deposits at long-term monitoring sites for fine-grained sediment are generally mapped once and monitored annually. Water resources personnel who monitor CRE debris flows have examined hyperspectral data to determine if mass movement could be predicted from the surficial geologic compositions provided by hyperspectral data. Although this is an intriguing problem, the remote-sensing initiative focused on a more fundamental issue to determine the type of data that is most appropriate for detecting and mapping debris flows.

One of the primary objectives of the remote-sensing initiative was to determine if there were better cost-effective, data-collection approaches for all the various parameters that are monitored by the physical resource program so that scientists could be more productive and their data would be at least as accurate as that obtained by past approaches. The most appropriate data would provide the highest mapping capability. Overall, there are four remote-sensing issues that needed to be resolved for this program and they are addressed in the following section.

4.2.1. Preservation of GCMRC Image Archive

An initial step in the remote-sensing initiative was an inventory of all image data that had been collected by GCMRC. During this process, we discovered that the film for one annual image collection had been lost and could not be located. We also observed that the photographic print collection was deteriorating due to age (discoloration) and use (markings, tears, wrinkles). In addition, access to the archive required a physical presence into order to view, select and duplicate necessary data. The initiative therefore strongly recommended that all future image collections either be obtained with digital sensors or be immediately scanned to digital format. The initiative also strongly recommended that the original photographic film be converted to digital imagery and, in the case of lost film, that the prints be digitally scanned. Within the initiative, Davis et al. (2002b) determined by a series of scan tests that a scan resolution of 15 microns per picture element was adequate to retain all of the information in the photographs (compare Figures 28 and 29); a scan resolution higher than 15 microns produces too much image noise to be useful in photogrammetry. In addition, evaluations of various data compression engines during the remote-sensing initiative determined that the best compression software was Gzip because it is lossless, free-ware, and not copyrighted. At this time, the film library is being converted to digital format by the IT program and, since the beginning of the initiative, all image data collections have been delivered in digital format and have been duplicated for archival preservation. An ArcIMS system has been implemented by the IT program which allows easy access to most of the collected digital data.

4.2.2. Most suitable image data for geomorphology

As far as future data collections, scientific review of image data collected during the remote-sensing initiative at different spatial resolutions showed that 15-20 cm resolution was sufficient for geomorphic mapping of physical resources. We found that digital, orthorectified panchromatic imagery with 18-cm resolution can be acquired at about one-half the cost of color imagery. However, evaluations of different types of image data for mapping physical resources showed that CIR imagery discriminates surface materials better than panchromatic data (compare Figures 30 and 31) and allows more accurate digital classification of sand bars and debris flows that does panchromatic imagery (Davis et al., 2002b). In fact, CIR imagery (Figure 31) was found to be better than true-color imagery (Figure 29) for mapping sand bars and debris flows,

mainly because CIR imagery allows more complete removal of vegetation cover, which in turn allows more accurate determination of geologic surface textures (Davis et al., 2002b). Surface texture was found to be a very important characteristic for distinguishing smooth sand bars and rough debris flows (Davis et al., 2002b), which was also found in other surficial-geologic studies (Shih and Schowengerdt, 1983; Anys et al., 1994)

4.2.3. Airborne approaches for ground topography

In March and in August-September of 2000, GCMRC collected LIDAR data with different collection parameters to evaluate the ability of LIDAR to provide topography at acceptable vertical accuracies on bare surfaces and on vegetated surfaces at the GCMRC sediment long-term monitoring sites. The March data were collected with the ALMS (Aeroscan Laser Mapping System) sensor at a spot spacing of 3.75 m and a spot diameter of 1.5 m. The August-September data were collected with the RAMS (Remote Airborne Mapping System) sensor at a 1-m spot spacing and a 0.5-m spot diameter; these data were acquired both in August and in September over the same four long-term monitoring sites using the same collection parameters to evaluate the precision of LIDAR elevation data. Photogrammetric data were derived from stereo image data (1:4,000-scale photography) that were collected in September 2000 for one of the four study areas. Ground-survey elevation transects were performed at the sites during the LIDAR surveys and stakeout surveys were conducted at selected LIDAR point locations after the LIDAR surveys on different types of bare surfaces and within vegetated terrain. The LIDAR data sets and the photogrammetry data set were compared to the ground survey data to determine each data set's vertical accuracy. Various analyses were performed on these data over a two-year period (e.g., Davis et al., 2002a; Mietz et al., 2002), culminating in a final detailed evaluation of these data (Davis et al., submitted).

Our evaluations of high-resolution photogrammetry and of different resolution and replicate LIDAR data with respect to GCMRC monitoring requirements for sediment deposits provided the following conclusions:

1. The low- and moderate-resolution LIDAR elevation data sets that we investigated on relatively flat, bare-sand surfaces were offset *above* the true ground surfaces at our four study areas (Figures 32-34). Without correction for these vertical offsets, almost all the LIDAR data sets have RMSE values greater than our desired 20 cm and greater than contractor specifications (15 cm); many of the data sets have RMSE values in the range of 40-100 cm. Vertical offsets have also been reported in previously published evaluations of LIDAR data, which suggest that some LIDAR surveys are no more independent of ground control than photogrammetric surveys.

2. After correction of the low- and moderate-resolution LIDAR data sets for their observed vertical offsets, the resulting bare-sand elevation data for the moderate-resolution LIDAR surveys produced better vertical accuracies (RMSE = 9-26 cm in August and RMSE = 13-36 cm in September) than the lower resolution LIDAR survey (RMSE = 26-103 cm) and the photogrammetric survey (RMSE = 32 cm; Figure 35). However, the higher photogrammetric error was due to isolated editing errors by the photogrammetrist (Figure 36).

3. Photogrammetry produced more accurate ground elevations on the cobble bars (RMSE = 16 cm) and on the vegetated sand surfaces (RMSE = 75 cm: Figure 37) than did either LIDAR survey.

4. The low-resolution, March LIDAR survey produced better elevation accuracies within the vegetated terrain (RMSE = 14-189 cm; Figure 37) than the moderate-resolution, August LIDAR survey (RMSE = 58-279 cm; Figure 37). This is attributed to the March collection period during leaf-off conditions and to the smaller scan angle used during the lower resolution LIDAR survey.

5. In terms of reproducibility, which is an important consideration in a monitoring program, our analyses of replicate collections of the moderate-resolution LIDAR data showed an average RMSE value of 29 cm for bare-ground surfaces in our four study areas (after correction for vertical offsets). In terms of vegetated terrain, the reproducibility of these data averaged 95 cm (RMSE). Thus, the RAMS moderate-resolution LIDAR data are both inaccurate and imprecise in CRE vegetated terrain, which is one reason we rank the performance of moderate-resolution LIDAR *below* that of photogrammetry for our requirements at this time.

6. Our recent evaluations of high- (1.5 points/m^2) and very-high (10 points/m^2) resolution LIDAR data on bare ground showed vertical accuracies of 17 cm and 8 cm, respectively, much higher accuracies than the photogrammetry data or lower resolution LIDAR data. In particular, the very high-resolution LIDAR data was found to have very high precision (reproducibility) of 4-5 cm and to have essentially no vertical offsets. Figure38 shows the correspondence between the very high-resolution LIDAR elevations and ground surveyed elevations for points on bare ground, near vegetation, and within vegetation. Within the densely vegetated areas, the accuracies of both high resolution LIDAR data sets decreased, but this may be a result of our processing. Visual inspection of these data sets within vegetation suggests that more rigorous (smarter) processing may be able to reduce the observed 0.7-1.3 m errors found in these data. An advantage of the very high-resolution LIDAR system is that it achieves very high accuracy without any ground control and is therefore non-invasive, except for the 100-m flight AGL required to obtain the high density data. Although the cost for the very high-resolution LIDAR data is $6,200 per river km, its high accuracy makes it useful for several monitoring requirements across all GCMRC programs and, therefore, may be quite cost effective.
7. Overall, vertical accuracies from different airborne topographic mapping approaches increase with increasing cost and therefore decreasing surface area that can be mapped. ISTAR automated photogrammetry can cover the entire canyon system at 44 cm accuracy for $625/km, manual photogrammetry can map specific areas at 25-30 cm accuracy for $3,000/km, and high-resolution LIDAR can map specific areas at 8-17 cm accuracy for $2,100-$6,200/km. Sediment monitoring will require one of the latter two technologies, whereas system-wide resource monitoring will require the ISTAR system.

4.2.4. Spatial resolution for terrestrial photogrammetr*y*

Stereo image data collections during 2000 included digital panchromatic (18-cm resolution), CIR film (10-cm resolution), and true-color (6-cm resolution) film. The true-color imagery was scanned at three different resolutions (resulting in 6, 8, and 16-cm resolution images) to determine the optimal minimum scan resolution to maintain high vertical accuracy. Photogrammetric analyses of these data were performed by the U.S. Geological Survey and by Pacific Western Technologies (PWT). Our evaluations of the resulting photogrammetric elevation data (Davis et al., 2002b) showed that image resolution needs to be near 6 cm or 1:4,000-scale photography (Figures 39-40; Davis et al., 2002b) to produce elevation data with vertical accuracies of 25 cm or better, which is the smallest change in sand-bar elevation that is deemed "significant" (Schmidt et al., 1999). Digital panchromatic stereo imagery with 18-cm

resolution produced very high elevation errors (RMSE = 53 cm; Figure 39; Davis et al., 2002b), but it is difficult to acquire higher resolution digital data using airborne digital sensors. In addition, the dimensions of CCD arrays need to be at least 10,000 by 10,000 to support accurate photogrammetric analysis. Industry is currently developing such cameras, but it will take a few years for the technology to be proven viable. In the meantime, data to support GCMRC photogrammetric needs will have to be acquired as film, which requires expensive post-collection scanning and rectification if orthorectified imagery is needed.

5.0 Further Evaluations

Although the remote-sensing initiative is officially over, we still need to evaluate some remaining data and some analysis systems that will answer unresolved issues. The types of data for further evaluations consist of photogrammetric data from ISTAR and the two high-resolution LIDAR data sets. This analysis will resolve the accuracies of these data for topography within vegetated areas and for canopy volume. GCRMC should proceed to establish a set of fixed, photo-identifiable points within the CRE (with accurate N, E, and elevation values) in order to verify future airborne topographic surveys and to develop a photogrammetric method that is based on these points instead of control panels. We will also evaluate the ability of the Chavez multispectral camera for mapping main-stem sediment storage within the first 100 miles of the CRE. The QTC software should also be examined to determine if it can map sediment characteristics from backscatter multibeam data, but there is no time for this evaluation this fiscal year. An additional evaluation should also be performed on a well-calibrated, multispectral or hyperspectral data set for mapping vegetation species within the CRE to determine the accuracy tradeoffs between number of spectral bands and spatial resolution.

6.0 Summary of Remote-Sensing Protocols

Protocols for remote-sensing data collection are divided into three categories based on their different collection requirements. The categories include terrestrial image data, aquatic image data, and digital surface models (both ground and canopy elevations).

Protocols	Terrestrial Image Data	Aquatic Image Data	Digital Surface Models
Wavelength bands	At a minimum, green (0.55 μm), red (0.65 μm) , and 1st NIR (0.80 μm) [for vegetation, 2nd NIR near 0.7 μm]	High-gain blue-green (0.50 μm) and TIR	ISTAR DSM for wide-area surveys; high-resolution LIDAR or photogrammetry for specific areas
Resolution or scale	≤ 20 cm	≤ 20 cm	1 m (ISTAR); ≥ 10 points/m^2 (LIDAR); or 1:4,000-scale film
Positional accuracy	≤ 30 cm	≤ 30 cm	≤ 30 cm
Vertical accuracy	n.a.	n.a.	≤ 25 cm
Time of year	Summer solstice	Summer solstice	Summer solstice (ISTAR); any time for LIDAR
Time of day	10:30 AM – 2 PM (more restricted in	10:30 AM – 2 PM (more restricted in	10:30 AM – 2 PM (more restricted in certain

	certain areas)	certain areas) (TIR = 1-2:30 PM)	areas)
Format	Calibrated digital; orthorectified or at least with image φ, κ, α	Calibrated digital; orthorectified or at least with image φ, κ, α	Calibrated x, y, z text files
Radiometric calibration	≤ 3%	≤ 3% (TIR ≤ 0.1°)	n.a.
Bit size of digital data	8-bit minimum 11 or 12-bit preferred	8-bit minimum 11 or 12-bit preferred	32-bit

7.0 Positive Effects of the Remote Sensing Initiative

1. Established detailed scope of work (SOW) for airborne data collections, including image, photogrammetric, and LIDAR data. The SOW should only require minor modifications for future data collections based on particular data requirements for a given year.
2. Established the image data characteristics that need to be obtained for overall GCMRC protocols. These characteristics include spatial resolution, band number and wavelengths, positional accuracy, preference for digital sensors that can record a large dynamic range, and calibrated sensors with 2-3% radiometric accuracy (see above table).
3. Established the optimal period for airborne image data collection. This was found to be the summer solstice when wall shadows are minimal, but also includes time-of-day restrictions on data collection (Figures 19-20).
4. Established the best airborne approach for terrestrial topography. Very high-resolution LIDAR for specific areas and ISTAR DSM data for wide-area analyses seems to be the most appropriate approaches for non-invasive topographic and canopy volume mapping.
5. Established the protocols for digital archiving the GCMRC photographic archive. The photographic library records the changes that have occurred within the CRE over the past 20 years. It is in serious danger of further degradation due to misuse and misplacement of photos. This library is also one of the least accessible data sets due to its format. Conversion of this library to digital format has now commenced.
6. Because all data are now delivered in digital format and are stored in an accessible on-line archive, cooperators are now making more and better use of airborne data. When these data provided in rectified form, cooperators are able to perform more accurate analyses in a much shorter time, thus increasing their productivity. Because of this, use of airborne data is ever increasing in all the monitoring programs.

8.0 Future Challenges for the GCMRC Remote Sensing Program

1. Finding a good contracting vehicle. This is by far the most difficult and frustrating challenge facing GCMRC airborne data collection. The existing remote-sensing QBS (Quality Based Selection) contract within the USGS has cumbersome management controls with a large overhead charge (17%). In addition, the existing QBS contract personnel appear to be more sympathetic to commercial profit margins than to USGS science requirements. GCMRC needs to establish its own (QBS) contract for their monitoring needs.
2. Enforcement of established standards for delivered data and delivery schedules. This may never get easier unless future data are collected by a set of contractors who become familiar with GCMRC standards and expectations.

3. Enforcement of the statement of work for airborne data collections. This needs attention during each data collection so that contractors do not relax the specifications.
4. Keeping up with latest remote-sensing technologies for GCMRC protocols, which change within a given year. This is a never-ending process, but also a critical process in order to ensure that the best (or acceptable) data are collected for GCMRC protocols and at a reasonable price. Performing this function for GCMRC requires that personnel within GCMRC (preferably Information Technology) actually research new data to better understand its true capabilities and limitations. In many instances we have found the claims made by remote-sensing firms to be overly optimistic or not applicable to the CRE. Only after interrogating data and questioning commercial firms on specific issues did we receive more accurate or realistic statements from commercial firms.
5. Maintaining the ever-increasing volume of collected data so that it is safe and accessible. The most critical factor here is preservation of data. Duplicate copies of data need to be maintained where one copy is never used except to restore a damaged shelf copy. It is not critical that original data be kept on-line, as long as data can be viewed (browse files) and requested for digital transfer.
6. Historically, the river stage for collection of remote-sensing data has been at a low steady flow rate of 8,000 cfs. With increasing energy costs, we have made every effort to reduce the time required for data collections in order to minimize loss of dam revenue from the low flows. In 2003, we found that even the most simple, conventional data collection using a framing camera and film can fail (due to a shutter malfunction). In order to reduce the financial risk of possible failure, and to allow a second data collection, it would be prudent to institute a liability clause in the remote-sensing contract, requiring companies to compensate BOR for its lost revenue in case of equipment or personnel failure. Such a clause will undoubtedly increase the cost for data collections.

References Cited

Alberotanza, L., Brando, V. E., Ravagnan, G., and Zandonella, A., 1999, Hyperspectral aerial images. A valuable tool for submerged vegtation recognition in the Orbetello Lagoons, Italy: Int. Jour. Remote Sensing, v. 20, p. 523-533.

Anders, P., and panel members, 2001, Final Report of the Aquatic Protocol Evaluation Program Panel, 43 pp.

Anys, H., Bannari, A., He, D. C., and Morin, D., 1994, Texture analysis for the mapping of urban areas using airborne MEIS-II images: Proc. First International Airborne Remote Sensing Conference and Exhibition, Strasbourg, France, v. 3, p. 231-245.

Bagheri, S., Stein, M., and Dios, R., 1998, Utility of hyperspectral data for bathymetric mapping in a turbid estuary: Int. Jour. Remote Sensing, v. 19, p. 1179-1188.

Berlin, G. L., Ambler, J. R., Hevley, R. H., and Schaber, G. G., 1977, Identification of a Sinagua agricultural field by aerial thermography, soil chemistry, pollen/plant analysis, and archaeology: American Antiquity, v. 42, p. 588-600.

Berlin, G. L., and panel members, 1998, Final Report of the GCMRC Remote Sensing Protocols Review Panel, 18 pp.

Blackburn, G. A., 1999, Relationships between spectral reflectance and pigment concentrations in stacks of deciduous broadleaves: Remote Sensing of Environ., v. 70, p. 224-237.

Blackburn, G. A., and Steele, C. M., 1999, Towards the remote sensing of matorral vegetation physiology: Relationships between spectral reflectance, pigment, and biophysical characteristics of semiarid bushland canopies: Remote Sensing of Environ., v. 70, p. 278-292.

Bryant, R. G., and Gilvear, D. J., 1999, Quantifying geomorphic and riparian land cover changes either side of a large flood event using airborne remote sensing: River Tay, Scotland: Geomorphology, v. 29, p. 307-321.

Butt, A. Z., Ayers, M. B., Swanson, S., and Tueller, P. T., 1998, Relationship of stream channel morphology and remotely sensed riparian vegetation classification: Rangeland Management and Water Resources, American Water Resources Association Technical Publication Series, TPS-98-1, p. 409-416.

Chavez, P. S., and Field, M., 2000a, Use of digitized aerial photographs and airborne laser bathymetry to map and monitor coral reefs: Proc. International Coral Reef Conference, October, 2000, Bali, Indonesia, 1 p.

Chavez, P. S., and Field, M. E., 2000b, Correction for water depth brightness variation in aerial photographs using spatial filtering and laser bathymetry in clear coastal waters, Molokai, Hawaii: Proc. International PACON 2000 Conference, June, 2000, Honolulu, Hawaii, 1 p.

Chavez, P. S., Sides, S. C., and Velasco, M. G., 1997, Mapping sediment concentration in San Francisco Bay using Landsat Thematic Mapper multitemporal satellite images. Proc.

U.S. Geological Survey Workshop on San Francisco Bay Studies, Menlo Park, California, 1 p.

Chavez, P. S., Sides, S. C., Velasco, M. G., Isbrecht, J., and Soltesz, D., 2002a, Use of digital aerial images to map and detect change in the benthic habitat of the Colorado River. Fifth International Airborne Remote Sensing Conference, Environmental Research Institute of Michigan, Miami, Florida, May, 2002.

Chavez, P. S., Sides, S. C., Velasco, M. G., Topping, D. J., Hornewer, N., and Soltesz, D., 2002b, Use of field instruments and remotely sensed images to monitor suspended sediment concentrations of the Colorado River. Fifth International Airborne Remote Sensing Conference, Environmental Research Institute of Michigan, Miami, Florida, May, 2002.

Coulter, L., Stow, D., Hope, A., O'Leary, J., Turner, D., Longmire, P., Peterson, S., and Kaiser, J., 2000, Comparison of high spatial resolution imagery for efficient generation of GIS vegetation layers: Photog. Engr. Remote Sensing, v. 66, p. 1329-1335.

Davis, P. A., 2002a, Review of remote-sensing and GIS approaches as alternative ecological monitoring tools for the Grand Canyon Monitoring and Research Center. Report to Grand Canyon Monitoring and Research Center, 101 p.

Davis, P. A., 2002b, Evaluation of airborne thermal-infrared image data for monitoring aquatic habitats and cultural resources within the Grand Canyon. U.S. Geological Survey Open-File Report 02-367, 94 p.

Davis, P., Manone, M., Mietz, S., Kohl, K., Rosiek, M., Hazel, J., Kaplinski, M., and Gonzales, M., 2002a, Evaluation of LIDAR and photogrammetry for monitoring volume changes in riparian resources within the Grand Canyon, Arizona. Pecora 15/Land Satellite Information IV Conference, Nov. 10-14, Denver, CO., 6 p.

Davis, P. A., Mietz, S. N., Manone, M. F., Kaplinski, M. A., Kohl, K. A., Gonzales, F. M., Hazel, J. E., Rosiek, M. R., and Galuszka, D. M., Evaluation of airborne LIDAR and photogrammetric surveys for monitoring sediment and vegetation resources within the Colorado River ecosystem, Arizona. Submitted to ISPRS Photogrammetry and Remote Sensing, submitted, 40 p.

Davis, P. A., Rosiek, M. R., and Galuszka, D. M., 2002b, Evaluation of airborne image data and LIAR main stem data for monitoring physical resources within the Colorado River ecosystem. U.S. Geological Survey Open-File Report 02-469, 35 p.

Davis, P. A. Staid, M. I., Plescia, J. B., and Johnson, J. R., 2002c, Evaluation of airborne image data for mapping riparian vegetation within the Grand Canyon. U.S. Geological Survey Open-File Report 02-470, 65 p.

Doelle, W. H., and panel members, 2000, Final Report: Cultural Resource Program Assessment, http://www.gcmrc.gov/pep/Cult_PEP.htm

Durand, D., Bijaoui, J., and Cauneau, F., 2000, Optical remote sensing of shallow-water environmental parameters: A feasibility study: Remote Sensing of Environ., v. 73, p. 152-161.

Elvidge, C. D., and Chen, Z., 1995, Comparison of broad-band and narrow-band red and near-infrared vegetation indices: Remote Sensing of Environ., v. 54, p. 38-48.

Fraser, R. N., 1998a, Hyperspectral remote sensing of turbidity and chlorophyll a among Nebraska Sand Hills lakes: Int. Jour. Remote Sensing, v. 19, p. 1579-1589.

Fraser, R. N., 1998b, Multispectral remote sensing of turbidity among Nebraska Sand HIlls lakes: Int. Jour. Remote Sensing, v. 19, p. 3011-3016.

Garcia-Haro, F. J., Gilabert, M. A., and Melia, J., 1996, Linear spectral mixture modelling to estimate vegetation amount from optical spectral data: Int. Jour. Remote Sensing, v. 17. P. 3373-3400.

George, D. G., 1997, The airborne remote sensing of phytoplankton chlorophyll in the lakes and tarns of the English Lake District: Int. Jour. Remote Sensing, v. 18, p. 1961-1975.

Gitelson, A. A., Buschmann, C., and Lichtenthaler, H. K., 1999, The chlorophyll fluorescence ratio F_{735}/F_{700} as an accurate measure of the chlorophyll content in plants: Remote Sensing of Environ., v. 69, p. 296-302.

Gitelson, A. A., and Merzlyak, M. N., 1997, Remote estimation of chlorophyll content in higher plant leaves: Int. Jour. Remote Sensing, v. 18, p. 2691-2697.

Goodin, D. G., Han, L., Fraser, R. N., Rundquist, D. C., Stebbins, W. A., and Schalles, J. F., 1993, Analysis of suspended solids in water using remotely sensed high resolution derivative spectra: Photog. Engr. and Remote Sensing, v. 59, p. 505-510.

Green, E. P., Clark, C. D., Mumby, P. J., Edwards, A. J., and Ellis, A. C., 1998, Remote sensing techniques for mangrove mapping: Int. Jour. Remote Sensing, v. 19, p. 935-956.

Grignetti, A., Salvatori, R., Casacchia, R., and Manes, F., 1997, Mediterranean vegetation analysis by multi-temporal satellite sensor data: Int. Jour. Remote Sensing, v. 18, p. 1307-1318.

Hardy, C. C., and Burgan, R. E., 1999, Evaluation of NDVI for monitoring live moisture in three vegetation types of the western U.S.: Photog. Engr. Remote Sensing, v. 65, p. 603-610.

Holroyd, E. W., 1995a, Thermal infrared (FLIR) mosaics of the Little Colorado River. Bureau of Reclamation Technical Service Center Technical Memorandum 8260-95-01, 34 p.

Holroyd, E. W., 1995b, Temperatures and warm springs along the Little Colorado River. Bureau of Reclamation Technical Service Center Technical Memorandum 8260-95-03, 7 p.

Hussein, S. A., 1982, Infrared spectra of some Egyptian sedimentary rocks and minerals: Modern Geology, v. 8, p. 95-105.

Irish, J. L., and Lillycrop, W. J., 1999, Scanning laser mapping of the coastal zone: the SHOALS system. ISPRS Journal of Photogrammetry and Remote Sensing 54, 123-129.

Jerome, J. H., Bukata, R. P., and Miller, J. R., 1996, Remote sensing reflectance and its relationship to optical properties of natural waters: Int. Jour. Remote Sensing, v. 17, p. 3135-3155.

Johnson, J. R., Lucey, P. G., Horton, K. A., and Winter, E. M., 1998, Infrared measurements of pristine and disturbed soils 1. Spectral contrast differences between field and laboratory data: Remote Sensing of Environ., v. 64, p. 34-46.

Jones, J., and panel members, 2001, Final Report of the Protocol Evaluation Panel for the Grand Canyon Monitoring and Research Center Integrated Water Quality Program, 50 pp.

Kearsley, M. J. C., and Ayers, T. J., 2000, Riparian vegetation monitoring in the Colorado River corridor 1998 to 1999. Report to Grand Canyon Monitoring and Research Center, Biologic Program, U.S. Geological Survey, Flagstaff, Arizona, 47 p.

Kokaly, R. F., and Clark, R. N., 1999, Spectroscopic determination of leaf biochemistry using band-depth analysis of absorption features and stepwise multiple linear regression: Remote Sensing of Environ., v. 67, p. 267-287.

Lee, C. T., and Marsh, S. E., 1995, The use of archival Landsat MSS and ancillary data in a GIS environment to map historical change in an urban riparian habitat: Photog. Engr. Remote Sensing, v. 61, p. 999-1008.

Liszewski, M., Davis, P. A., Mietz, S., Chavez, P. S., and Gonzales, M., 2001, Remote sensing of natural and cultural resources in the Colorado River ecosystem at the Grand Canyon: ASPRS Meeting, Measuring the Earth - Digital Elevation Technologies and Applications, St. Petersburg, FL, 1 p

Lyzenga, D. R., 1978, Passive remote sensing techniques for mapping water depth and bottom features: Applied Optics, v. 17, p. 379-383.

Lyzenga, D. R., 1981, Remote sensing of bottom reflectance and water attenuation parameters in shallow water using aircraft and Landsat data: Int. Jour. Remote Sensing, v. 2, p. 71-82.

May, A. M. B., Pinder, J. E., and Kroh, G. C., 1097, A comparison of Landsat Thematic Mapper and SPOT multi-spectral imagery for the classification of shrub and meadow vegetation in northern California, U. S. A.: Int. J. Remote Sensing, v. 18, p. 3719-3728.

MacFarlane, W. W., Pederson, J. L., and Petersen, P. A., 2002, Testing the limits of photogrammetry to monitor erosion of archaeological sites in Grand Canyon. 2002 Annual Meeting, Geological Society of America.

McFetters, S. K., 1996, The use of the Normalized Difference Water Index (NDWI) in the delineation of open water features: Int. Journ. Remote Sensing, v. 17, p. 1425-1432.

Mickelson, J. G., Civco, D. L., and Silander, J. A., 1998, Delineating forest canopy species in the northeastern United States using multi-temporal TM imagery: Photog. Engr. Remote Sensing, v. 64, p. 891-904.

Mietz, S., Davis, P., Kohl, K., and Manone, M., 2002, An evaluation of LIDAR vertical accuracy in Grand Canyon, Arizona. 22nd Annual ESRI International User Conference, 13 p.

Nash, D. B., 1985, Detection of bedrock topography beneath a thin cover of alluvium using thermal remote sensing. Photog. Engr. and Remote Sensing 51, 77-88.

Penuelas, J., Pinol, J., Ogaya, R., and Filella, I., 1997, Estimation of plant water concentration by the reflectance Water Index WI (R900/R970): Int. Jour. Remote Sensing, v. 18, p. 2869-2875.

Petersen, P. A., Pederson, J. L., and MacFarlane, W. W., 2002, Gully erosion of archaeological sites in Grand Canyon – Photogrammetry and GIS used in geomorphic studies. 2002 Annual Meeting, Geological Society of America.

Pinder, J. E., and McLeod, K. W., 1999, Indications of relative drought stress in Longleaf Pine from Thematic Mapper data: Photog. Engr. Remote Sensing, v. 65, p. 495-501.

Podzdnyakov, D. N., Kondratyev, K. Ya., Bukata, R. P., and Jerome, J. H., 1998, Numerical modelling of natural water colour: Implications for remote sensing and limnological studies: Int. Jour. Remote Sensing, v. 19, p. 1913-1932.

Purevdorj, T., Tateishi, R., Ishiyama, T., and Honda, Y., 1998, Relationship between percent vegetation cover and vegetation indices: Int. Jour. Remote Sensing, v. 19, p. 3519-3535.

Quackenbush, L. J., Hopkins, P. F., and Kinn, G. J., 2000, Developing forestry products from high resolution digital aerial imagery: Photog. Engr. Remote Sensing, v. 66, p. 1337-1346.

Richardson, A. J., and Wiegand, C. L., 1977, Distinguishing vegetation from soil background information: Photog. Engr. Remote Sensing, v. 43, p. 1541-1552.

Roberts, A. C. B., and Anderson, J. M., 1999, Shallow water bathymetry using integrated airborne multi-spectral remote sensing: Int. Jour. Remote Sensing, v. 20, p. 497-510.

Rowlinson, L. C., Summerton, M., and Ahmed, F., 1999, Comparison of remote sensing data sources and techniques for identifying and classifying alien invasive vegetation in riparian zones: Water SA, v. 25, p. 497-500.

Sathyendranath, S., Subba Rao, D. V., Chen, Z., Stuart, V., Platt, T., Budgen, G. L., Jones, W., and Vass, P., 1997, Aircraft remote sensing of toxic phytoplankton blooms: A case study from Cardigan River, Prince Edward Island: Canadian Jour. Remote Sensing, v. 23, p. 15-23.

Schmidt, J. C., Grams, P. E., and Leschin, M. F., 1999, Variation in the magnitude and style of deposition and erosion on three long (8-12 km) reaches as determined by photographic analysis. In Webb, R. H., Schmidt, J. C., Marzolf, G. R., and Valdez, R. A. (Eds.), The Controlled Flood in Grand Canyon, American Geophysical Union, Geophysical Monograph Series 110, 185-204.

Shih, E. H. H., and Schowengerdt, R. A., 1983, Classification of arid geomorphic surfaces using Landsat spectral and textural features: Photog. Engr. Remote Sensing, v. 49, p. 337-347.

Tassan, S., 1998, A procedure to determine the particulate content of shallow water from Thematic Mapper data: Int. Jour. Remote Sensing, v. 19, p. 557-562.

Todd, S. W., and Hoffer, R. M., 1998, Responses of spectral indices to variations in vegetation cover and soil background: Photog. Engr. Remote Sensing, v. 64, p. 915-921.

Urquhart, N. S., and panel members, 2000, Report of a Peer Review Panel on Terrestrial Aspects of the Biological Resources Program of the Grand Canyon Monitoring and Research Center, 54 pp.

Whitlock, C. H., Witte, W. G., Usry, J. W., and Gurganus, E. A., 1978, Penetration depth at green wavelengths in turbid waters: Photog. Engr. and Remote Sensing, v. 4, p. 1405-1410.

Wohl, E. E., and panel members, 1999, Final Report of the Physical Resources Monitoring Peer Review Panel, 12 pp.

Woodruff, D. L., Stumpf, R. P., Scope, J. A., and Pearl, H. W., 1999, Remote estimation of water clarity in optically complex estuarine waters: Remote Sensing Environ., v. 68, p. 41-52.

Yu, B., Ostland, I. M., Gong, P., and Pu, R., 1999, Penalized discriminant analysis of *in situ* hyperspectral data for conifer species recognition: IEEE Trans. Geosci. and Remote Sensing, v. 37, p. 2569-2577.

Zhu, Z., Yang, L., Stehman, S. V., and Czaplewski, R. L., 2000, Accuracy assessment for the U.S. Geological Survey regional land-cover mapping program: New York and New Jersey region: Photog. Engr. Remote Sensing, v. 66, p. 1425-1435.

Table 1. Remote-sensing technologies tested or investigated based on their potential to provide desired ecosystem parameters at required accuracies. Some technologies were eliminated based on resolution limitations and some environmental parameters are not listed because current technologies cannot provide that information, based on published results and expert opinion. The **top row** indicates whether the technology can (YES) or cannot (NO) measure a parameter, can measure a parameter with limitations (LIMITED), or was not tested (NO TEST). The **middle row** gives comments. The **bottom row** indicates a cost estimate ($/river km) for processing data to provide the ecosystem parameter.

Sensor Data	Aquatic Resources				Terrestrial Resource Parameters					Cultural Resource Parameters		Data Collection Cost ($/river km)
	Suspended Materials	Water Temperature	Substrate Unit Mapping	Bathymetry	Vegetation Type	Vegetation Area	Vegetation Volume	Geomorphic Unit Mapping	Ground Topography	Arroyo Mitigation	Small Resource Monitoring	
1-band, B&W Panchromatic	NO	NO	LIMITED	NO	NO	LIMITED	LIMITED	LIMITED	YES	LIMITED	NO	
			mod. depth/clear			ambiguous	ISTAR/film	ambiguous	ISTAR/film			
			200			50	625[1]/3,000	100	625[1]/3,000	22,000[3]		345[1]-1,100
3-band Natural Color	LIMITED	NO	LIMITED	NO	NO	YES	YES	YES	YES	NO TEST	YES	
	susp. Sed.		mod. depth/clear				only film		only film			
	??		200			50	3,000	100	3,000		300	475[1]-1,100
3-band Color Infrared	LIMITED	NO	LIMITED	NO	YES	YES	YES	YES	YES	NO TEST	YES	
	susp. Sed.		shallow		Suitable	Best	only film	Best	only film		Best	
	??		200		400	50	3,000	100	3,000		300	475[1]-1,100
Multispectral (≤ 10 bands)	NO TEST[2]	NO	LIMITED	NO	YES	NO TEST	NO TEST	YES	NO	NO	NO	
			mod. depth/clear		4-band Best							
					400			100				600-800
Hyperspectral (>10 bands)	NO TEST[2]	NO	LIMITED	NO	NO TEST	NO TEST	NO TEST	NO TEST	NO	NO	NO	
			mod. depth/clear									
												3,500
Thermal	NO	YES	NO	NO	NO	NO	NO	NO	NO	NO	LIMITED	
		TOD[4]									TOD[4]/resolution	
		200									10	600-800
Near-IR	NO	NO	NO	NO	NO	NO	LIMITED	NO	LIMITED	NO	NO	450 @ 1.5 m
							only dense veg.?		bare grnd, water			2,100 @ 0.8 m
							200		200			6,200 @ 0.4 m
Green LIDAR	NO	NO	NO	NO	NO	NO	NO	NO	NO	NO	NO	

[1] These costs also provide orthorectified CIR image data.
[2] Funding limitations precluded further testing.
[3] Includes both collection and analysis costs.
[4] TOD = time of day.

Table 2. Image and topographic data collected and evaluated during the GCMRC Remote Sensing Initiative.

Image Data Type	Spatial Resolution	Rectified	Horizontal Accuracy	GPS IMU	Collection Date	Conditions	Coverage (RM)	Target Programs	Comments
HYDICE digital 206-band HS	150 cm	No	n.a.	yes	Aug., 1998	clear	-10 - +9	P, B	Too noisy to use.
Emerge digital CIR	30 cm	Yes	6-8 m	yes	Sept., 1999	clear	entire corridor	All	Sub-sampled surface radiance.
CIR film	30 cm	Yes	1-2 m	yes	Mar., 2000	p. cloudy	entire corridor	All	Collected resolution did not provide requested 30 cm horizontal accuracy. Shadows.
ED digital B&W	30 cm	No	n.a.	yes	Mar., 2000	p. cloudy	entire corridor	All	
CIR film	11 cm	No	n.a.	yes	June, 2000	clear, windy	entire corridor	All	GPS/IMU did not work properly.
Bechtel 12-band MS	100 cm	Yes	2-3 m	yes	July, 2000	clear	+30 - +74	All	
EQ digital B&W	18 cm	Yes	30 cm	yes	Aug., 2000	clear	-15 - +90	P	
EQ digital B&W	18 cm	No	n.a.	yes	Aug., 2000	clear	-15 – 0	P	High-gain state for channel substrate.
CIR film	28 cm	No	n.a.	no	Sept., 2000	overcast	-15 - +90	P, B	Best surface color data without shadows.
EQ digital B&W	18 cm	Yes	30 cm	yes	Sept., 2000	clear	-15 - +90	P	
EQ digital B&W	18 cm	No	n.a.	yes	Sept., 2000	clear	-15 - 0	P	High-gain state for channel substrate.
EQ digital B&W and Emerge CIR	18 cm	Yes	n.a.	yes	May, 2001	clear	entire corridor	All	Failed - contractor misrepresented experience with Emerge detector
ISTAR digital B&W and CIR	22 and 44 cm	Yes	25 cm	yes	May, 2002	clear	entire corridor	All	First to follow restricted flight window.
B&W film	6 cm	No	n.a.	no	May, 2003	clear	entire corridor	All	Failed - shutter malfunction.
Chavez digital CIR	8 and 15 cm	No	n.a.	no	May, 2003	clear	-15 - +90	P, B	High-gain state for channel substrate.
Topographic Data Type	**Spatial Resolution**	**Unadjusted Vertical Accuracy**	**Adjusted Vertical Accuracy**	**GPS IMU**	**Collection Date**	**Vegetation Conditions**	**Coverage (RM)**	**Target Programs**	**Comments**
ED LIDAR	3.75 m	44-103 cm	26-103 cm	yes	Mar., 2000	Leaf-off	entire corridor	All	
EQ LIDAR	1.5 m	14-33 cm	9-26 cm	yes	Aug., 2000	Leaf-on	5 LTM reaches	P, B	Provided few multiple returns in vegetation.
Natural-color film	6 cm	28 cm	n.a.	no (panels)	Sept., 2000	Leaf-on	2 LTM reaches	P, B	
EQ LIDAR	1.5 m	22-53 cm	13-36 cm	yes	Sept., 2000	Leaf-on	5 LTM reaches	P, B	Provided few multiple returns in vegetation.
B&W film	3 cm	6-10 cm	n.a.	no (panels)	Mar., 2002	n.a.	4 arch. sites	C	
ISTAR B&W	22 cm	45 cm	30 cm	yes	June, 2002	Leaf-on	entire corridor	All	Entirely by softcopy photogrammetry.
B&W film	6 cm	25-30 cm	n.a.	yes (panels)	June, 2002	Leaf-on	11 LTM reaches	P	
B&W film	3 cm	20 cm	n.a.	yes (panels)	Oct., 2002	n.a.	4 arch. sites	C	Some image blurring – flew too fast
3Di LIDAR	0.8 m	17 cm	n.a.	yes	Nov., 2002	Leaf-off	4 LTM reaches	P, B	
Chance LIDAR	0.3 m	8 cm	n.a.	yes	May, 2003	Leaf-on	2 LTM reaches	P, B	Densest possible LIDAR data.

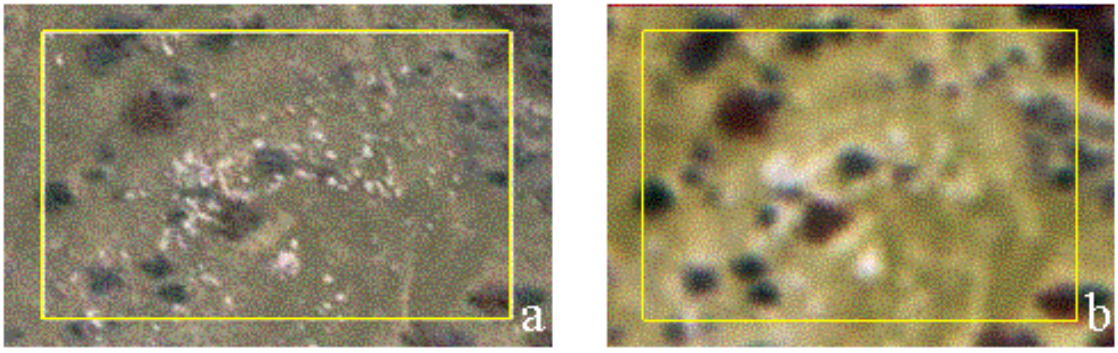

Figure 1. Archaeological structure on the northwest side of Unkar delta shown on natural-color images at (a) 11-cm and (b) 100-cm resolution. Image width is 27.9 meters. Multiple archaeological foundations are easily visible at 11-cm resolution, but are not uniquely discernable from natural alluvial surface materials at 100-cm resolution.

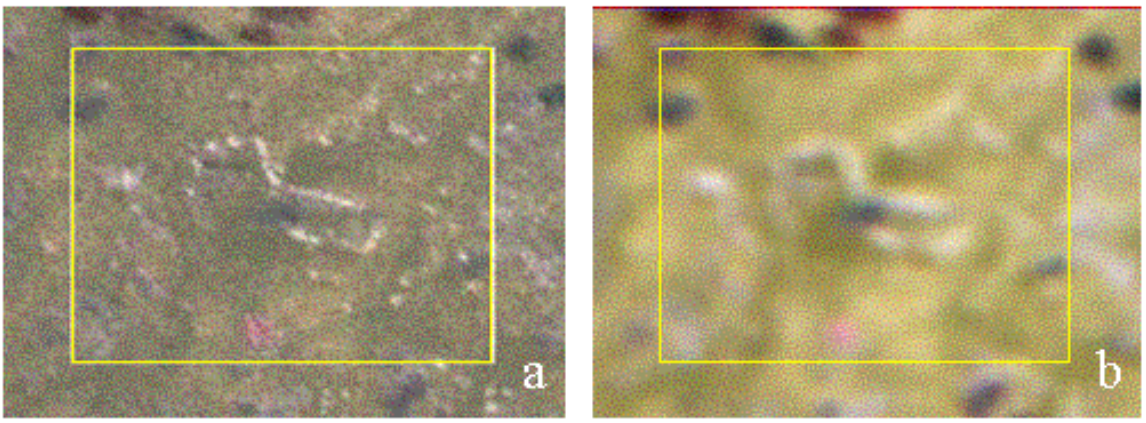

Figure 2. Archaeological structure on west side of Unkar delta shown on imagery at (a) 11-cm and (b) 100-cm resolution. Image width is 21.9 meters. An archaeological foundation is easily visible at 11-cm resolution, but much less distinguishable from natural alluvial surface features (produced by surface runoff) at 100-cm resolution.

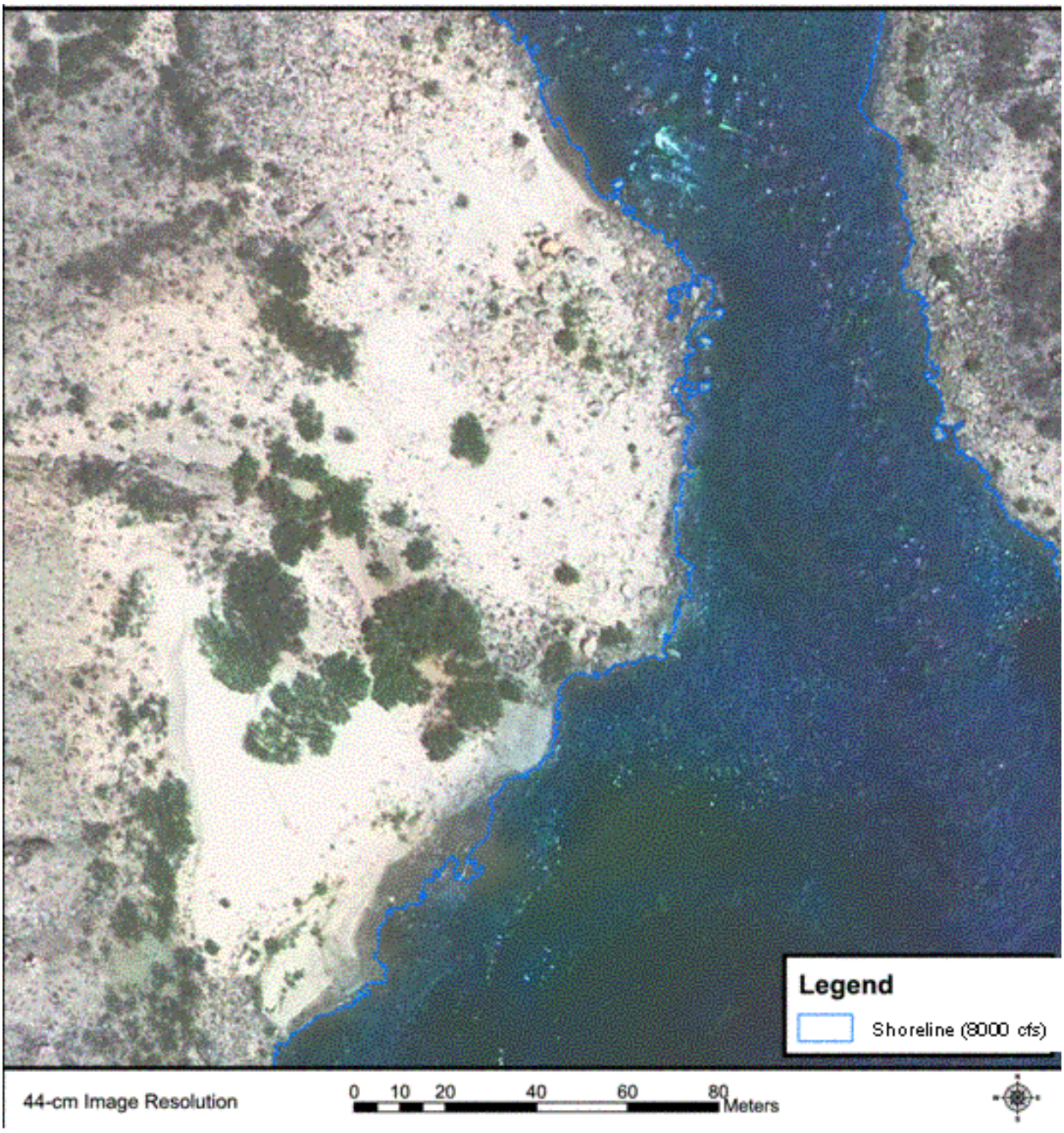

Figure 3. Natural-color image of the Malgosa Canyon area (RM 58) produced from ISTAR image data collected May 2002. Shoreline at 8,000 cfs is indicated by blue line, vegetation is green, and young sand deposits are bright white.

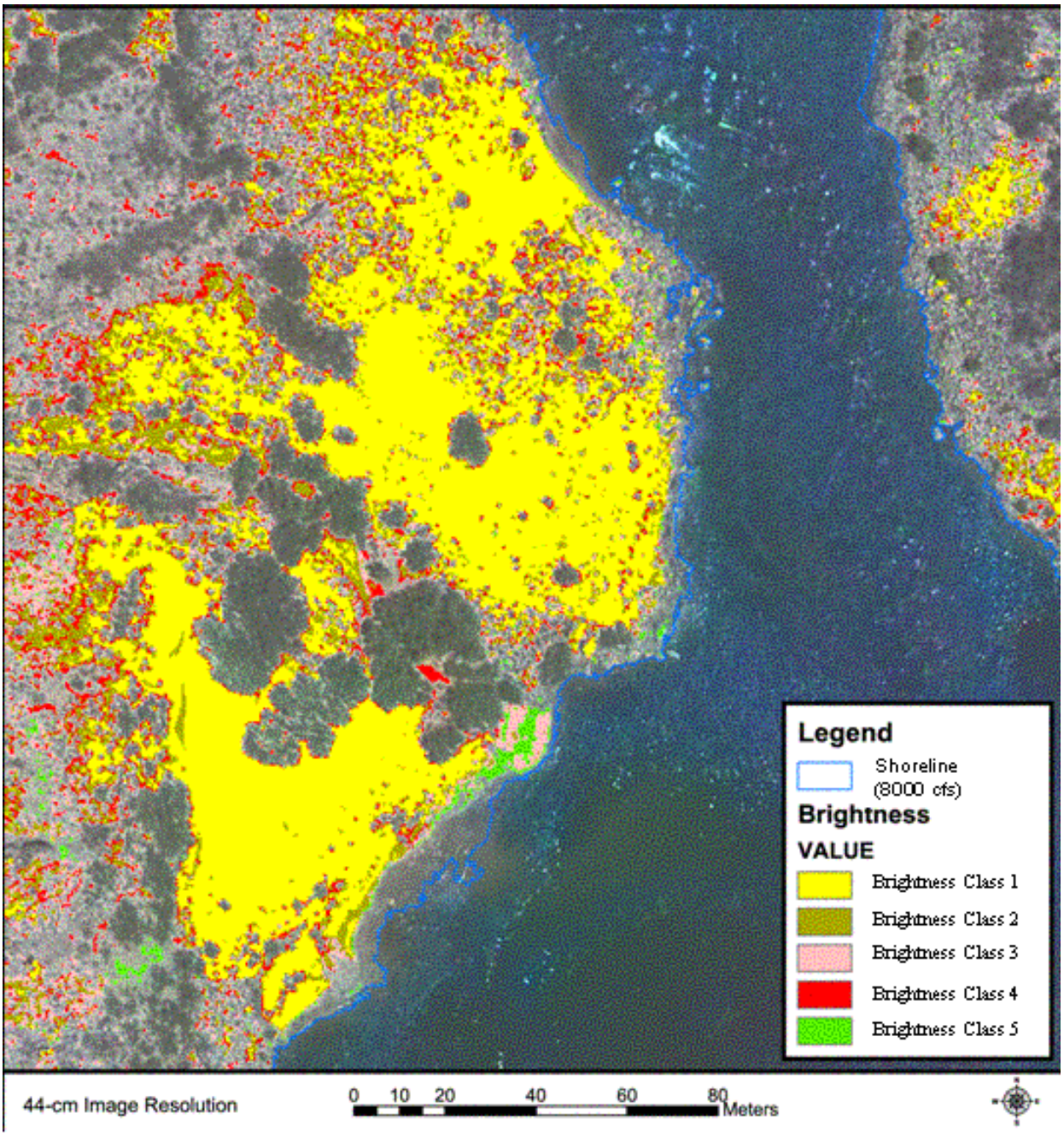

Figure 4. Distribution of inorganic materials of different ranges of brightness (albedo) based on spectral signatures in the ISTAR four-band image data. Brightness classes superposed on the natural-color image shown in Figure 3. Shoreline at 8,000 cfs is indicated by blue line.

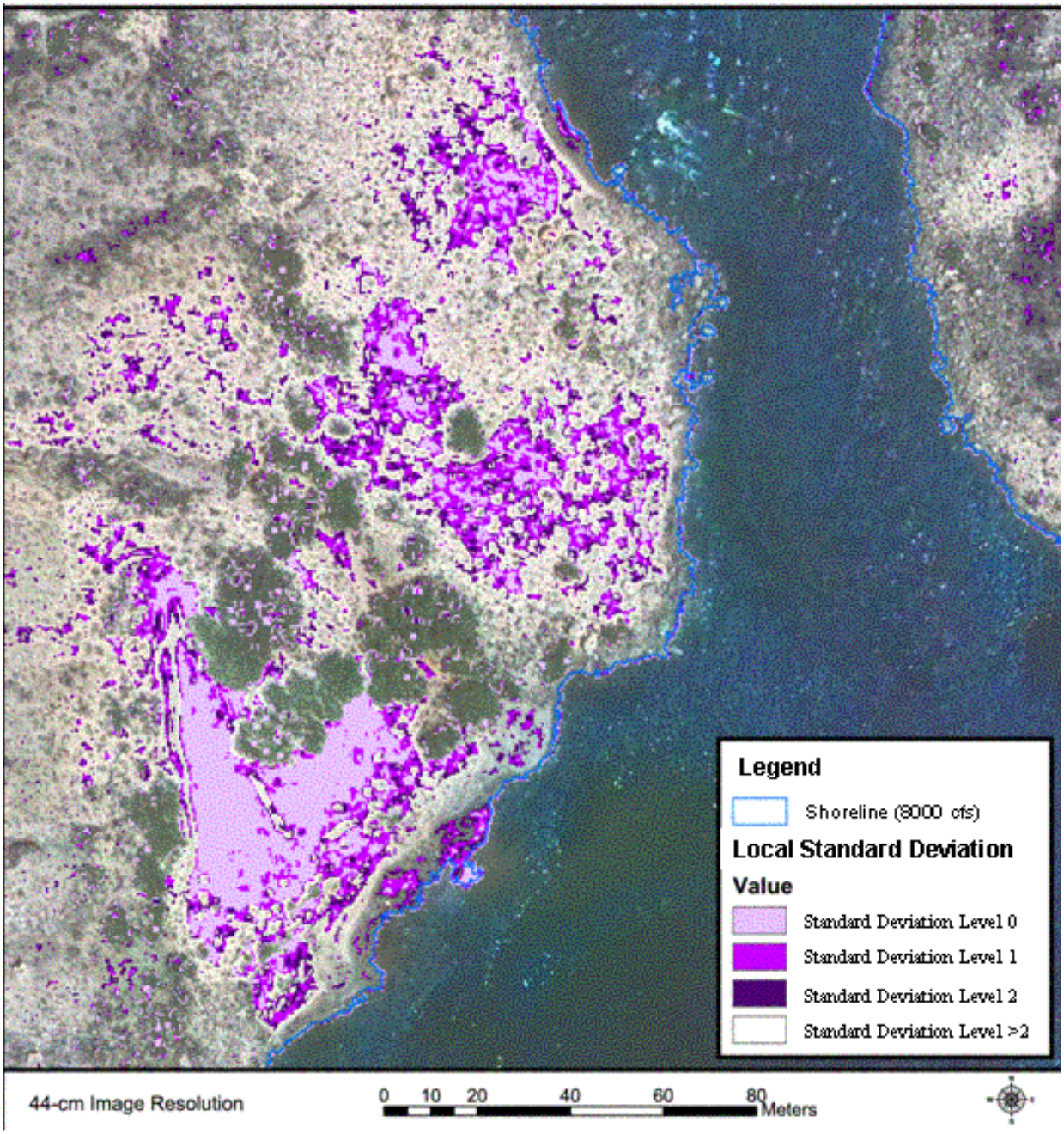

Figure 5. Distribution of surfaces with different relative textures (roughness) based on the average variance in near-infrared-band reflectance within an areal dimension that was found optimal for separating smooth and rough surfaces. Roughness classes are superposed on the natural-color image shown in Figure 3. Shoreline at 8,000 cfs is indicated by blue line.

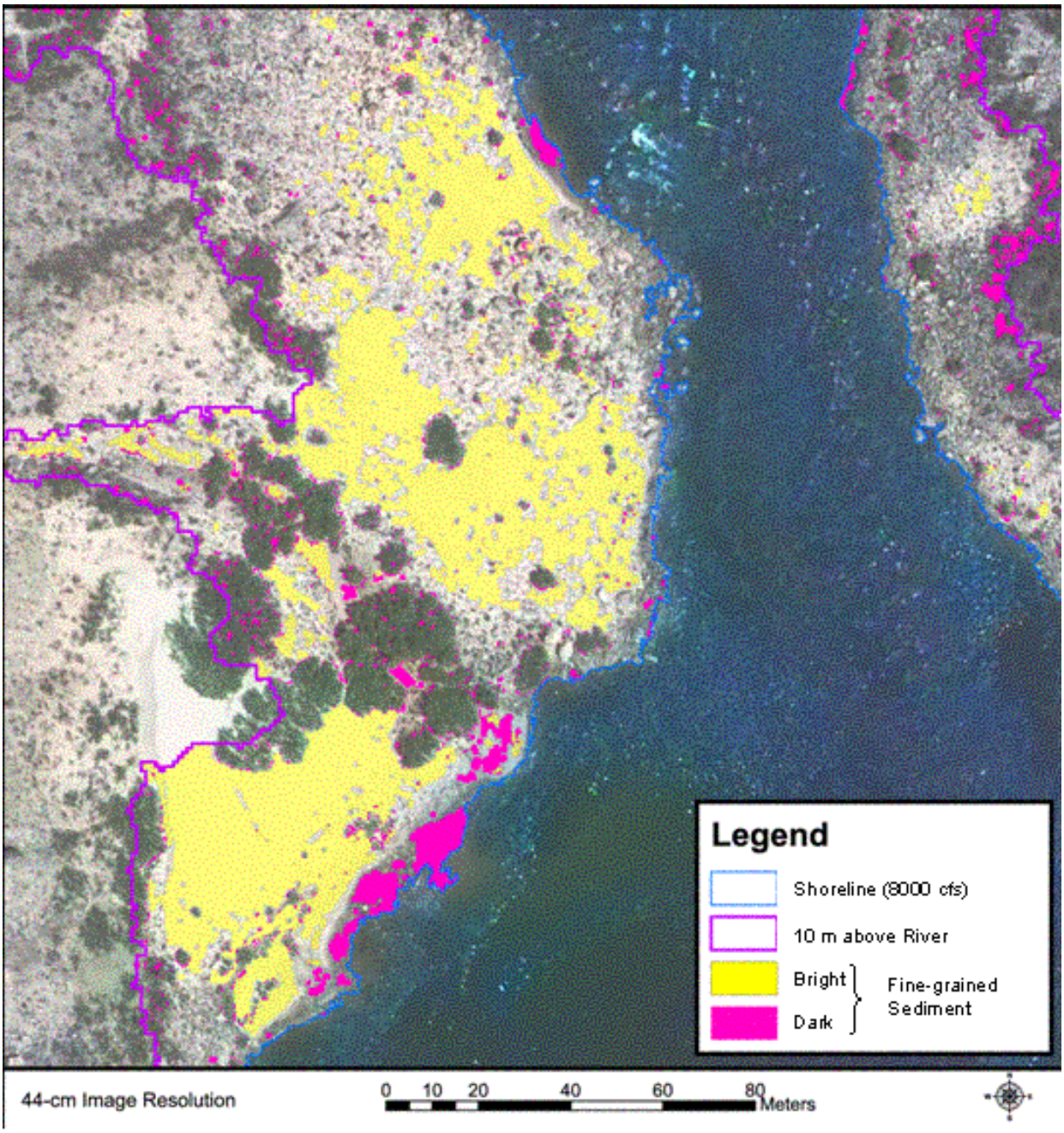

Figure 6. Distribution of near-shore, bright and dark, fine-grained inorganic surface materials based on surface brightness, color, texture, and elevation data. Sediment classes are superposed on the natural-color image shown in Figure 3. Shoreline at 8,000 cfs is indicated by blue line; area within 10 meters of elevation above the water's edge is indicated by a orchid-colored line.

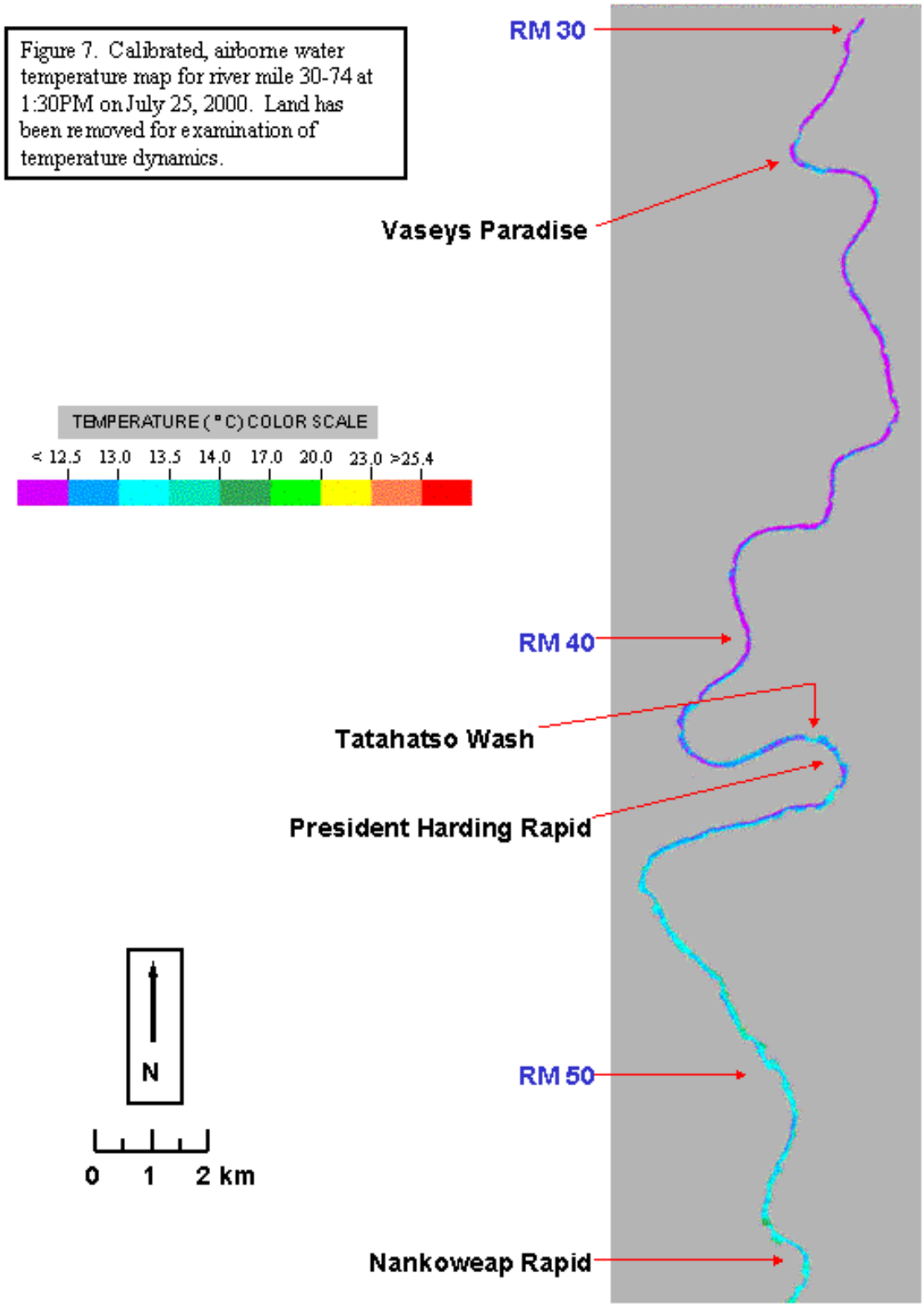

Figure 7. Calibrated, airborne water temperature map for river mile 30-74 at 1:30PM on July 25, 2000. Land has been removed for examination of temperature dynamics.

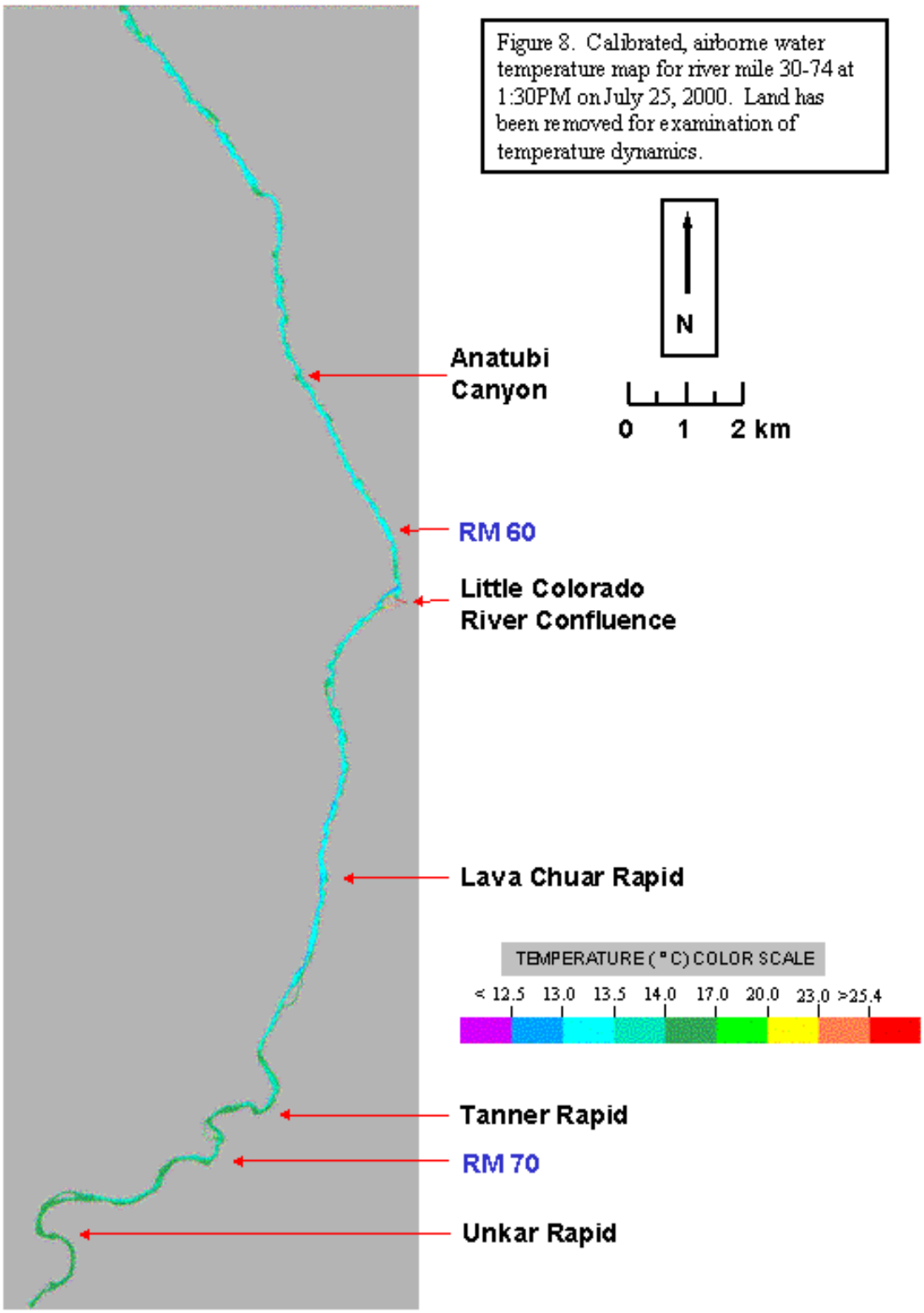
Figure 8. Calibrated, airborne water temperature map for river mile 30-74 at 1:30PM on July 25, 2000. Land has been removed for examination of temperature dynamics.
N
0 1 2 km
Anatubi Canyon
RM 60
Little Colorado River Confluence
Lava Chuar Rapid
TEMPERATURE (°C) COLOR SCALE
< 12.5 13.0 13.5 14.0 17.0 20.0 23.0 >25.4
Tanner Rapid
RM 70
Unkar Rapid

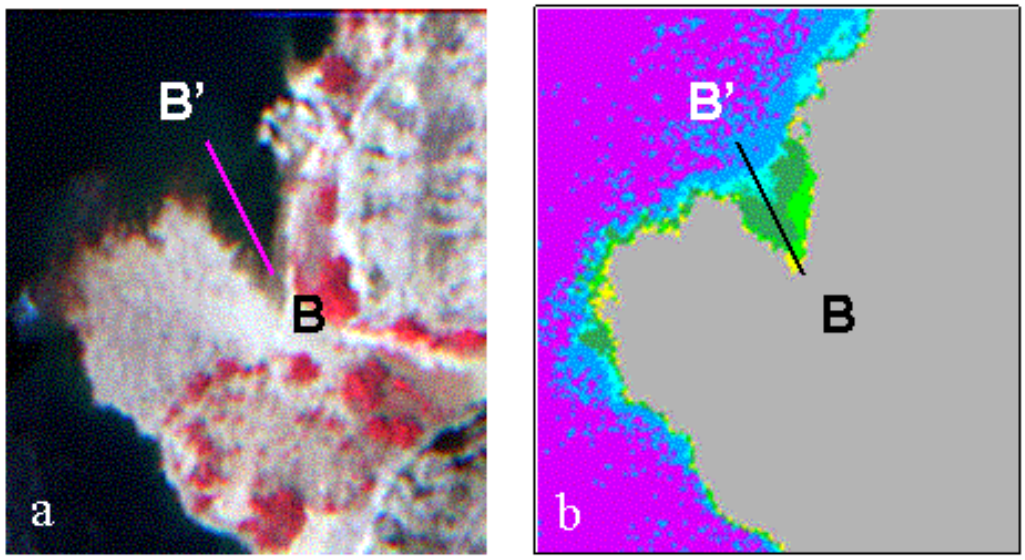

Figure 9. Color-infrared image (a) and color-coded airborne water-temperature map (b) of the left bank of the Colorado River at the mouth of Tatahatso Wash (river mile 43.2). Image width is 128 meters. On (b) land is gray and water colors correspond to temperature scale shown below.

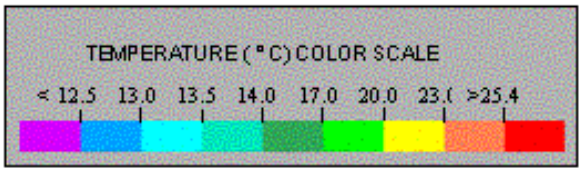

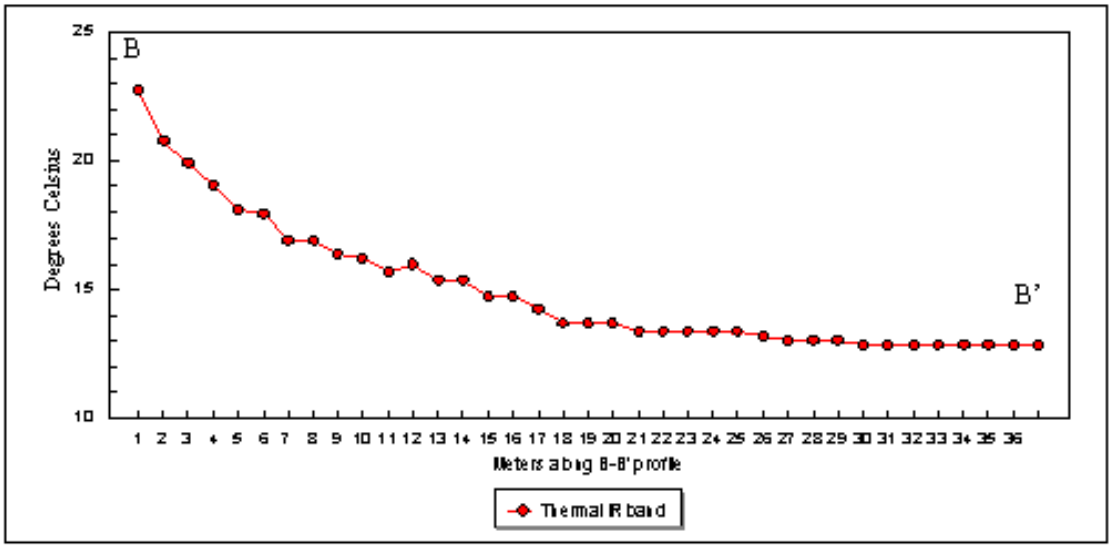

Figure 10. Calibrated, airborne water temperatures along profile B-B'.

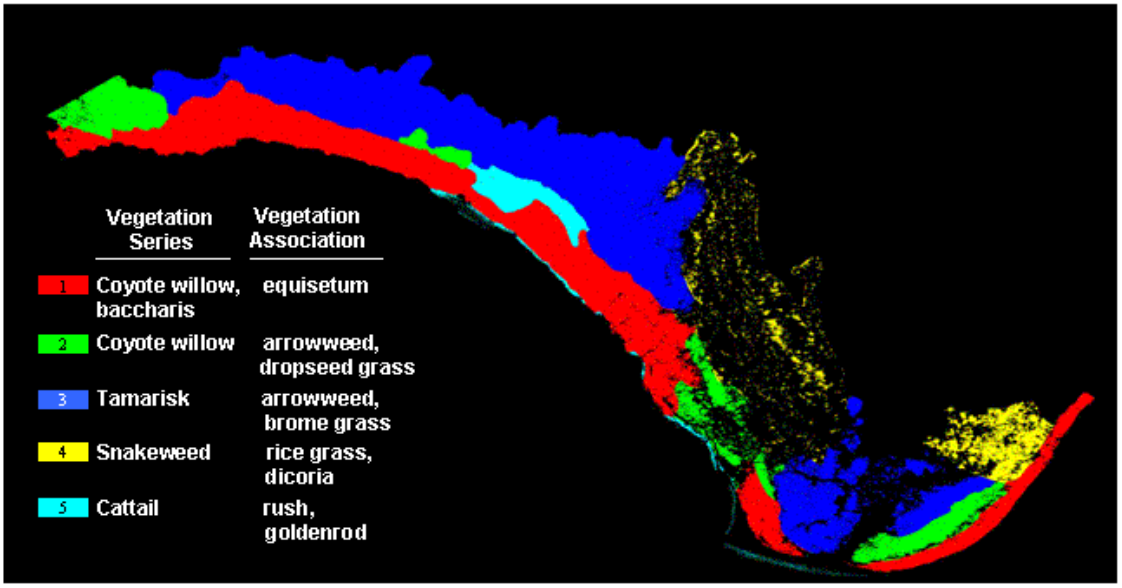

Figure 11. Vegetation map of study site RM68.2 produced from field observations by Kearsley and Ayers (2000). Map excludes bare ground.

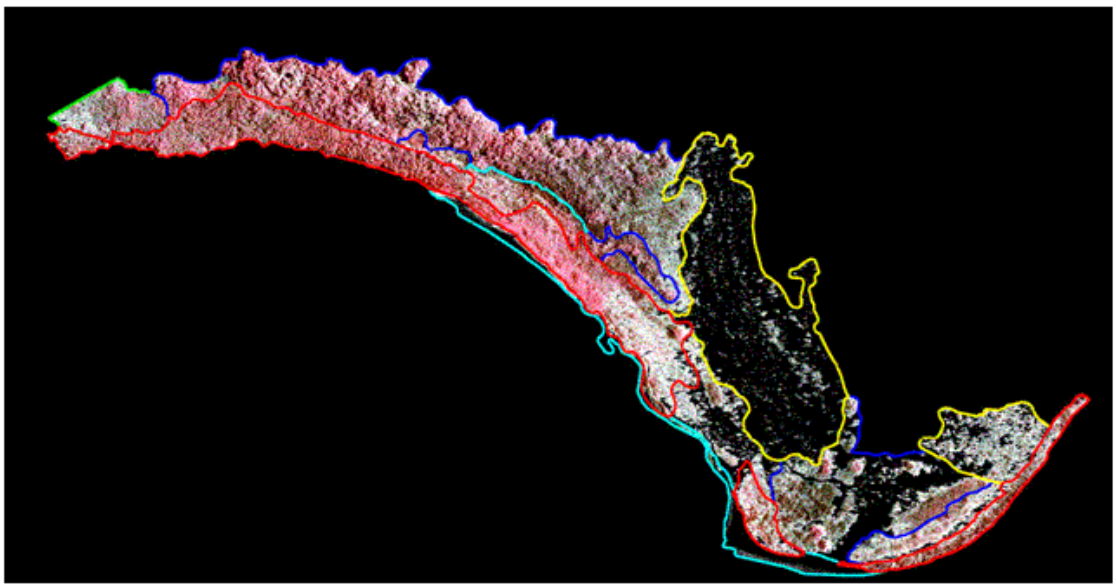

Figure 12. Vegetation unit outlines superposed on CIR image of study site RM68.2. Image excludes bare ground.

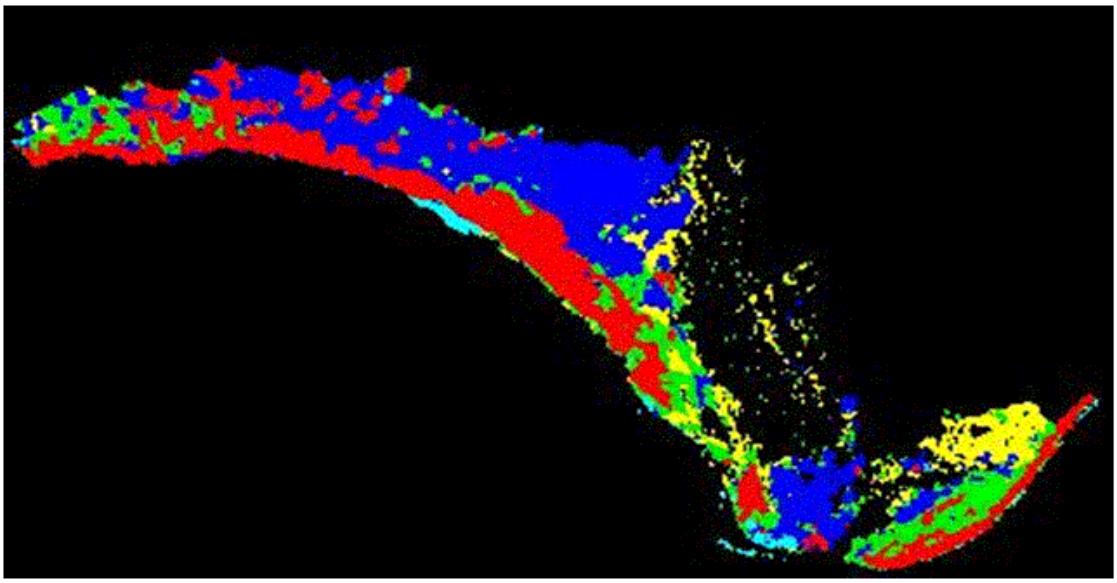

Figure 13. Vegetation classification map of study site RM68.2 produced from maximum likelihood classification of Daedalus multispectral band data (acquired at 100-cm resolution in July, 2000) and derivative texture data. Map excludes bare ground. Classification accuracy is 67.0% for the Kearsley and Ayers vegetation units.

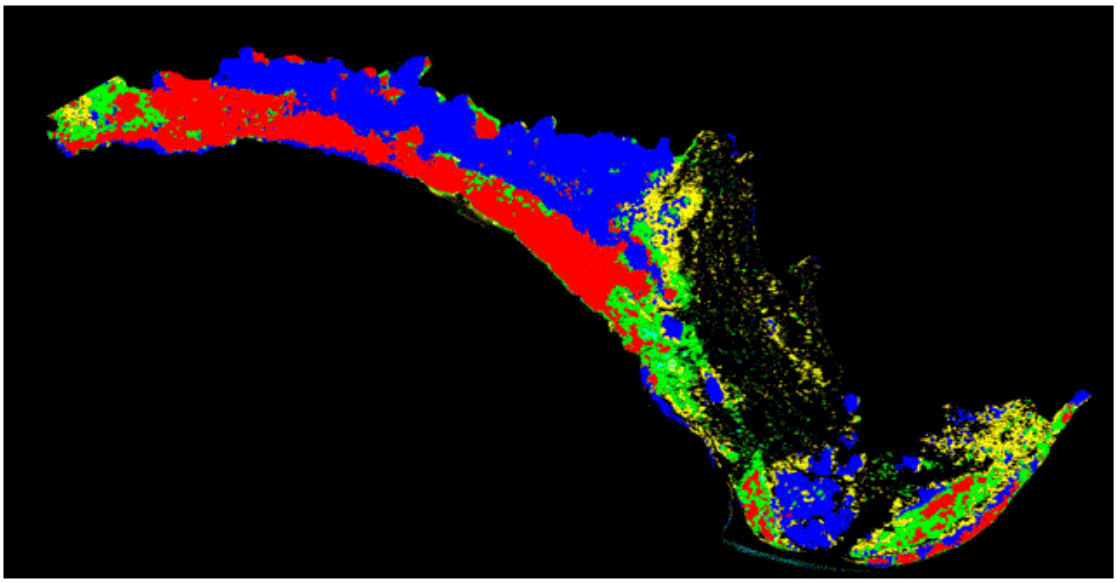

Figure 14. Vegetation classification map of study site RM68.2 produced from maximum likelihood classification of color-infrared (CIR) band data (acquired at 11- resolution in July, 2000) and derivative texture data. Map excludes bare ground. Classification accuracy is 62.6% for Kearsley and Ayers vegetation units.

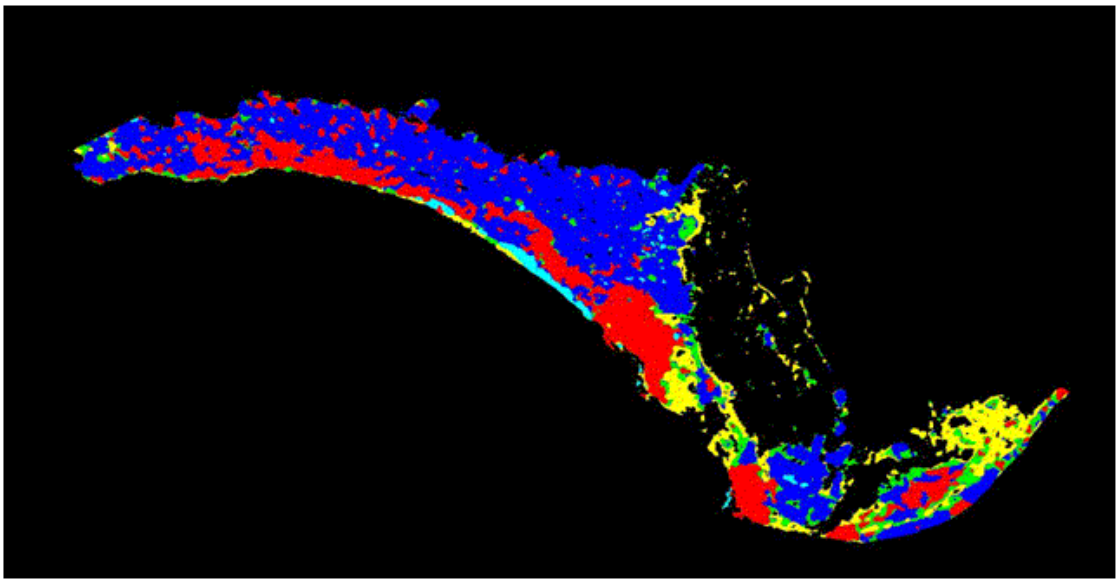

Figure 15. Vegetation classification map of study site RM68.2 produced from maximum likelihood classification of Emerge color-infrared (CIR) band data (acquired at 30.5-cm resolution in September, 1999) and derivative texture data. Map excludes bare ground. Classification accuracy is 59.2% for the Kearsley and Ayers vegetation units.

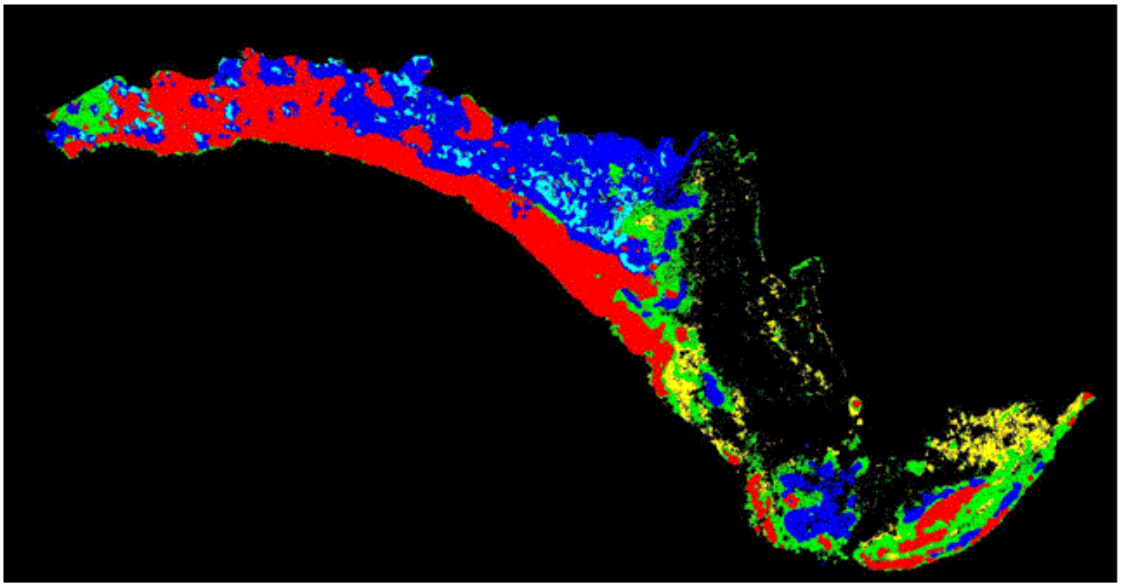

Figure 16. Vegetation classification map of study site RM68.2 produced from maximum likelihood classification of color-infrared (CIR) band data (acquired at 28-cm resolution in September, 2000) and derivative texture data. Map excludes bare ground. Classification accuracy is 58.0% for the Kearsley and Ayers vegetation units.

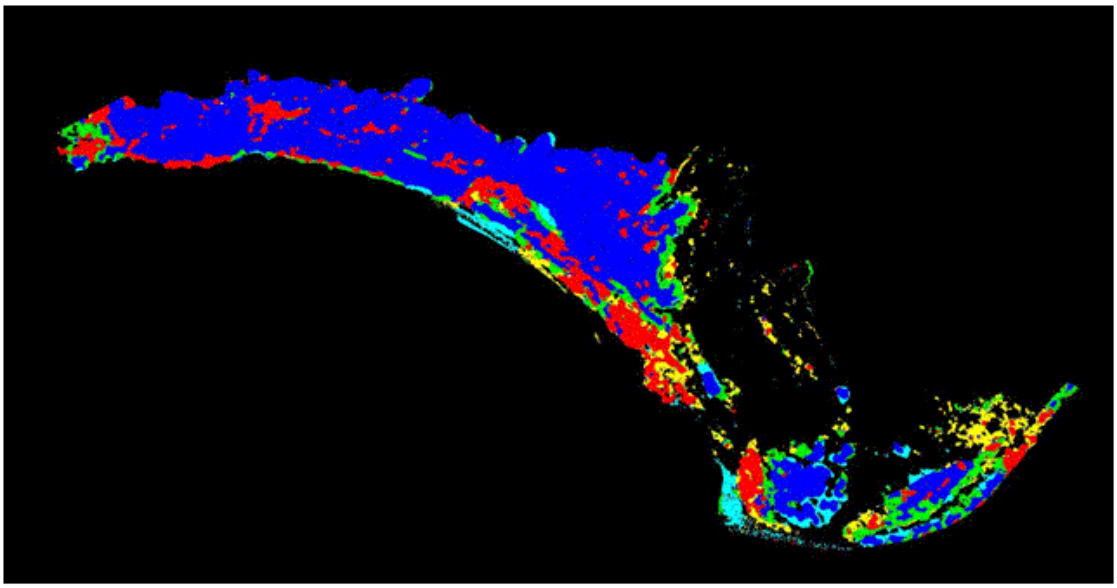

Figure 17. Vegetation classification map of study site RM68.2 produced from maximum likelihood classification of color-infrared (CIR) band data (acquired at 30.5-cm resolution in March, 2000) and derivative texture data. Map excludes bare ground. Classification accuracy is 53.8% for the Kearsley and Ayers vegetation units.

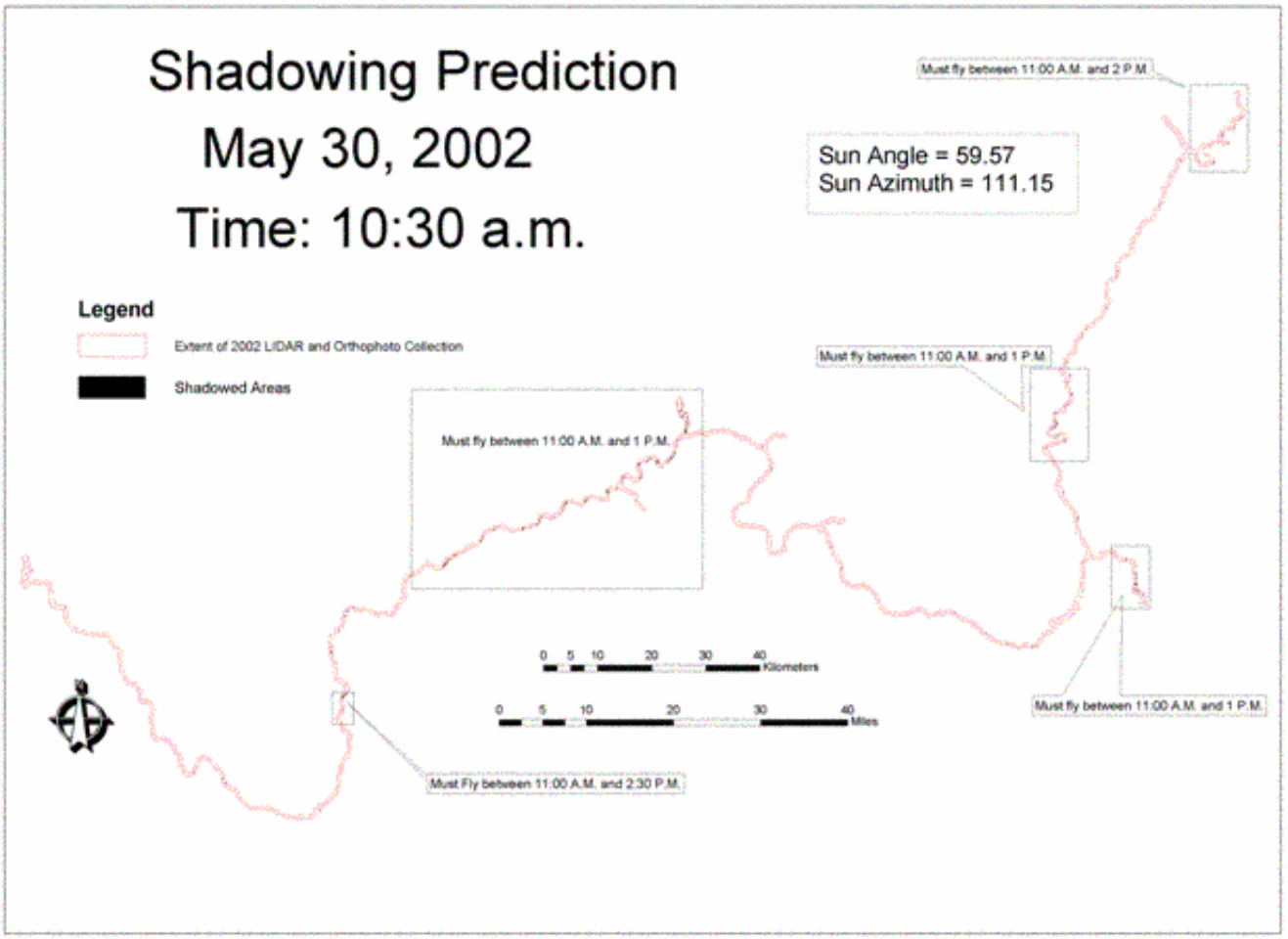

Figure 18. Results from shadow analysis for May 30, 2002 at 10:30 AM. Red line indicates limits of corridor monitoring. Black areas within red zone indicates shadows at the designated time and day. This analysis was used to establish the earliest time on a given day for shadow-fee data collection for most of the corridor. Some areas (boxes) are more constrained.

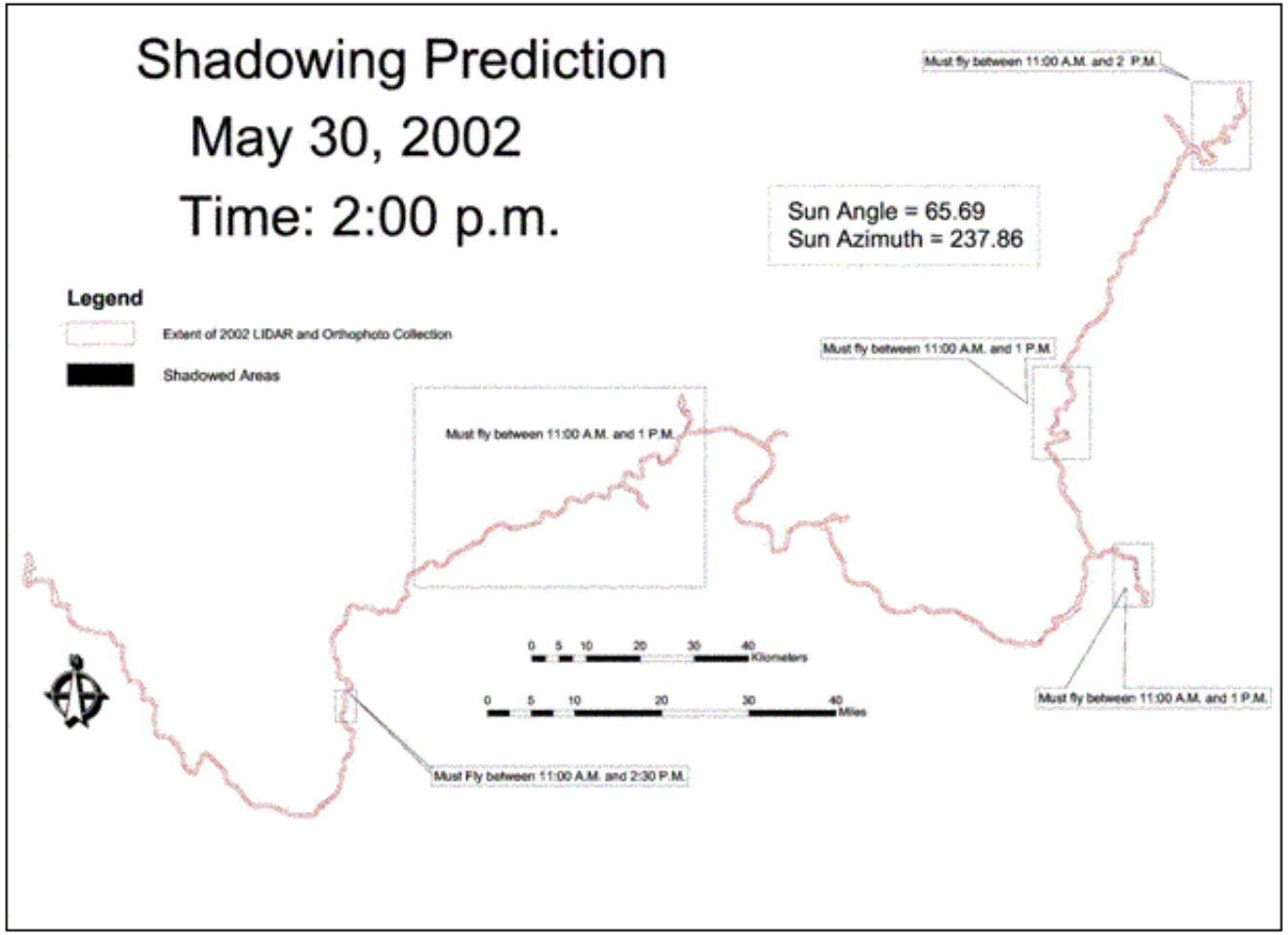

Figure 19. Results from shadow analysis for May 30, 2002 at 2:00 PM. Red line indicates limits of corridor monitoring. Black areas within red zone indicates shadows at the designated time and day. This analysis was used to establish the latest time on a given day for shadow-fee data collection for most of the corridor. Some areas (boxes) are more constrained.

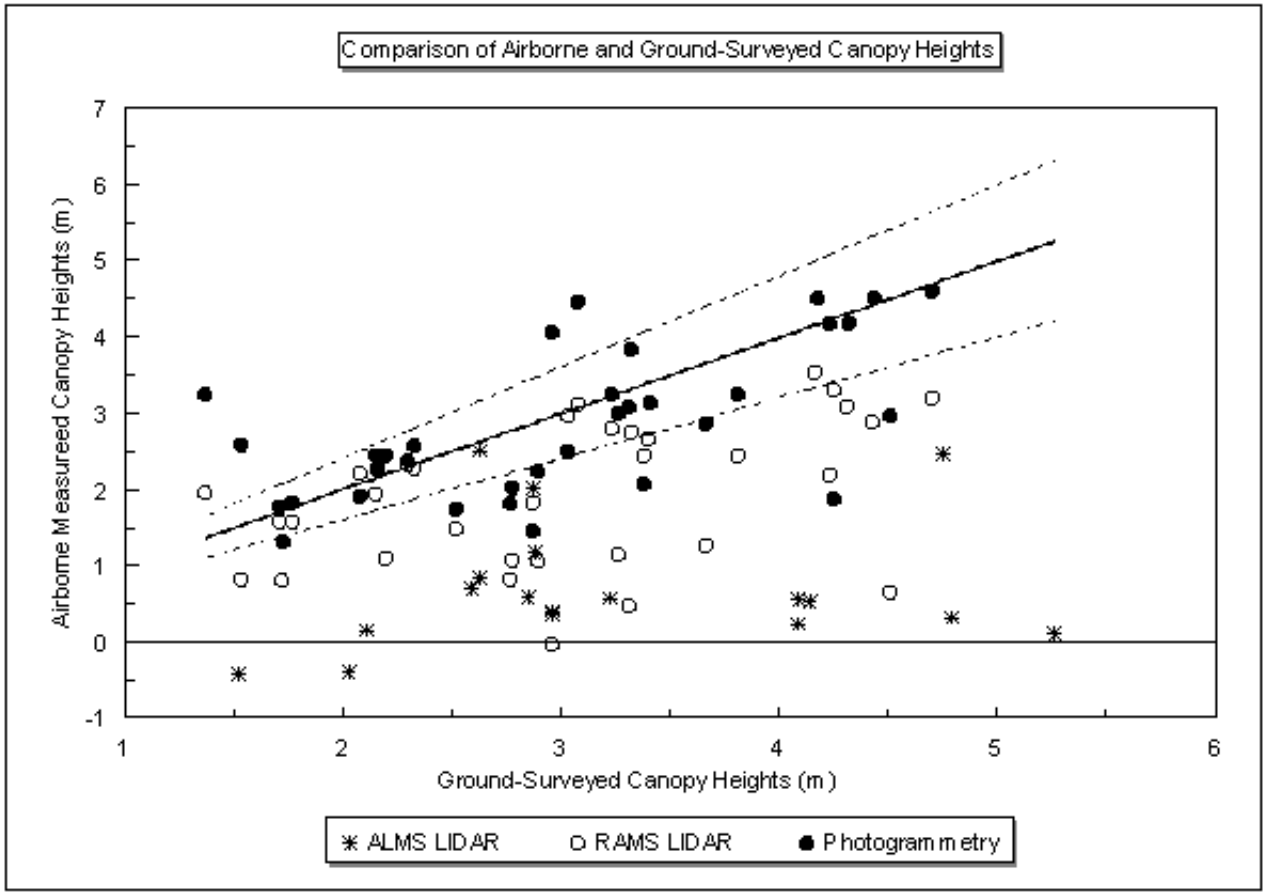

Figure 20. Scatter plot of airborne-derived and ground-surveyed canopy heights. Solid line represents perfect agreement between airborne-derived and ground-surveyed canopy heights. Dashed lines represent the 20% error limit on height measurements.

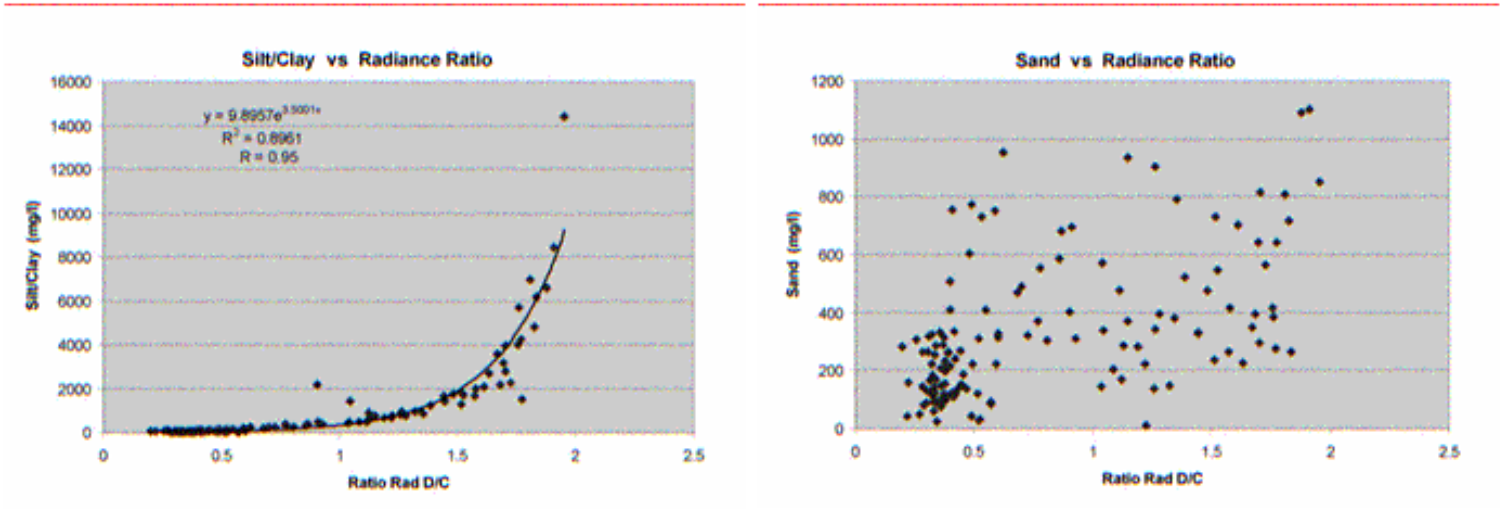

Figure 21. Relation between radiance ratios derived from ground measurements and (a) silt-clay and (b) sand concentrations that were recorded by water gages (Chavez et al., 2002b).

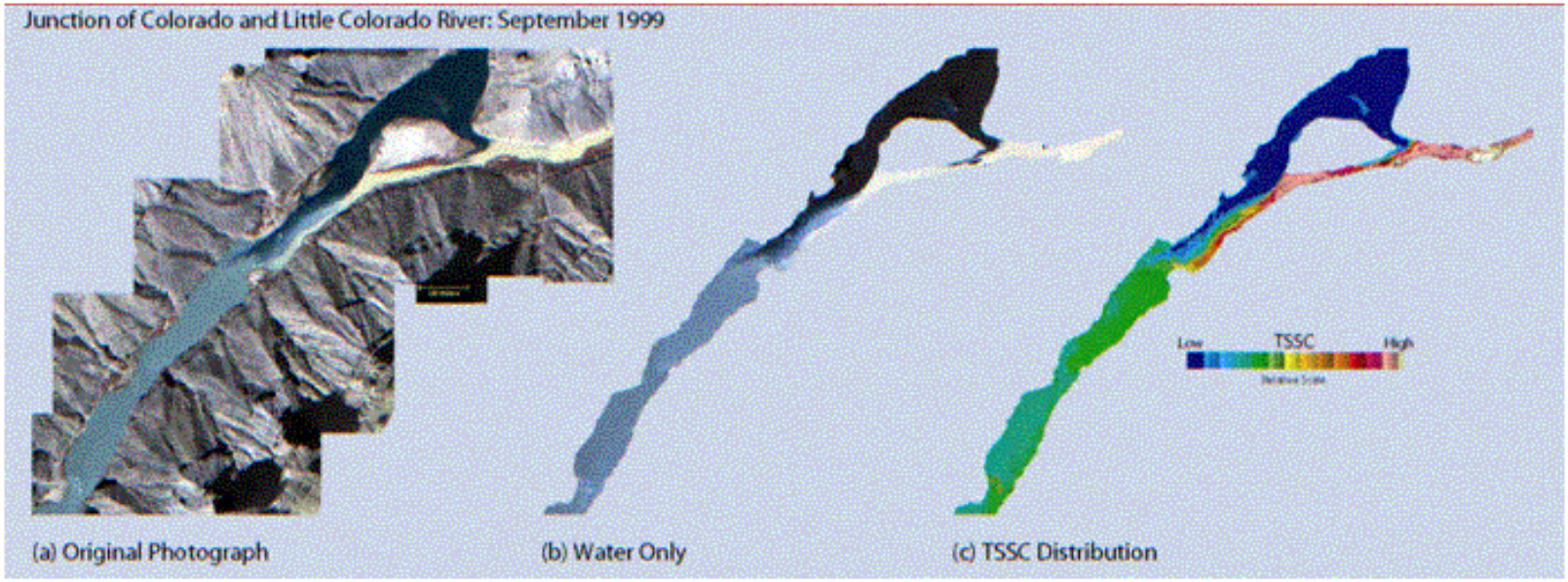

Figure 22. Color-infrared (CIR) image data acquired in September, 2000 for the upper 100 miles of the CRE shown in (a) for all surfaces and in (b) for only water areas. The airborne CIR imagery were used to extrapolate site-specific, ground-measured total suspended sediment concentrations (TSSC) to an entire river reach (c) south of the Little Colorado River confluence (Chavez et al., 2002b).

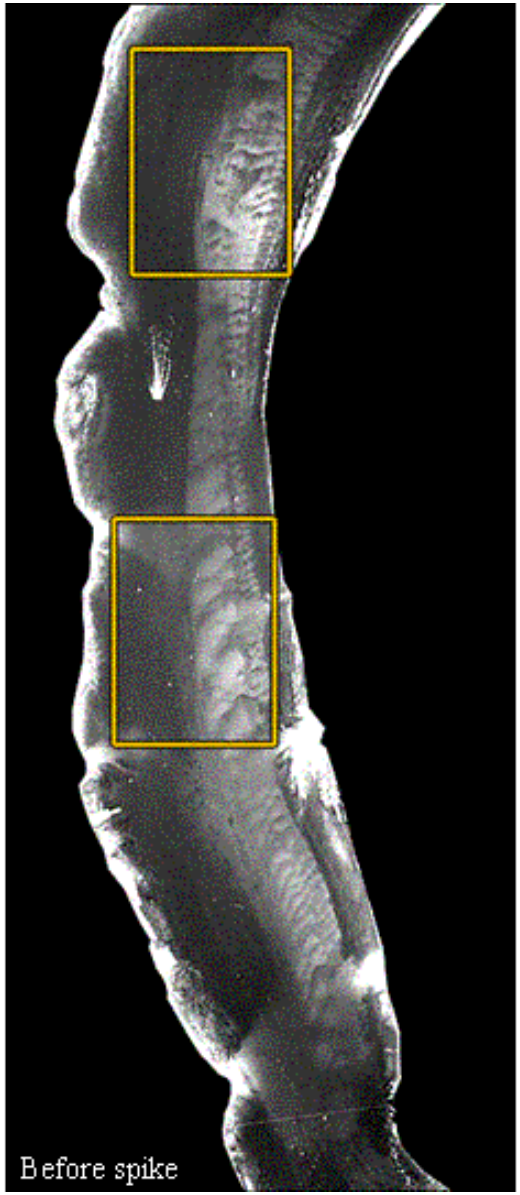

Figure 23. High-gain panchromatic images of a part of the main channel in Glen Canyon acquired in August, 2000 (left image) before the flow spike in early September, 2000 and one week later after the flow spike (right image). Both imagers were contrast stretched to more clearly show substrate information, at the expense of land surfaces (Chavez et al., 2002a). Boxed areas are shown at higher resolutions in the next figures.

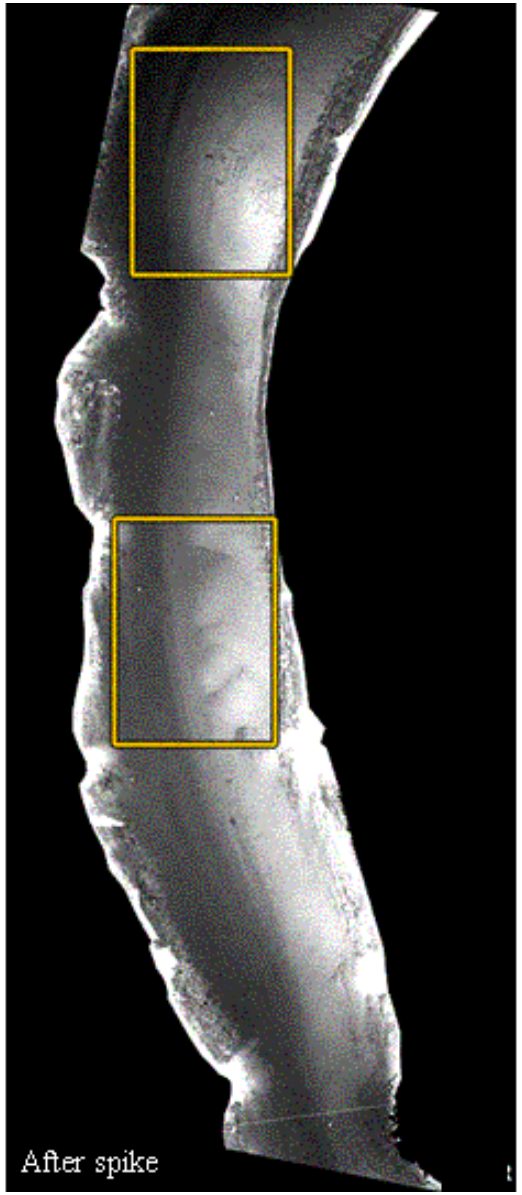

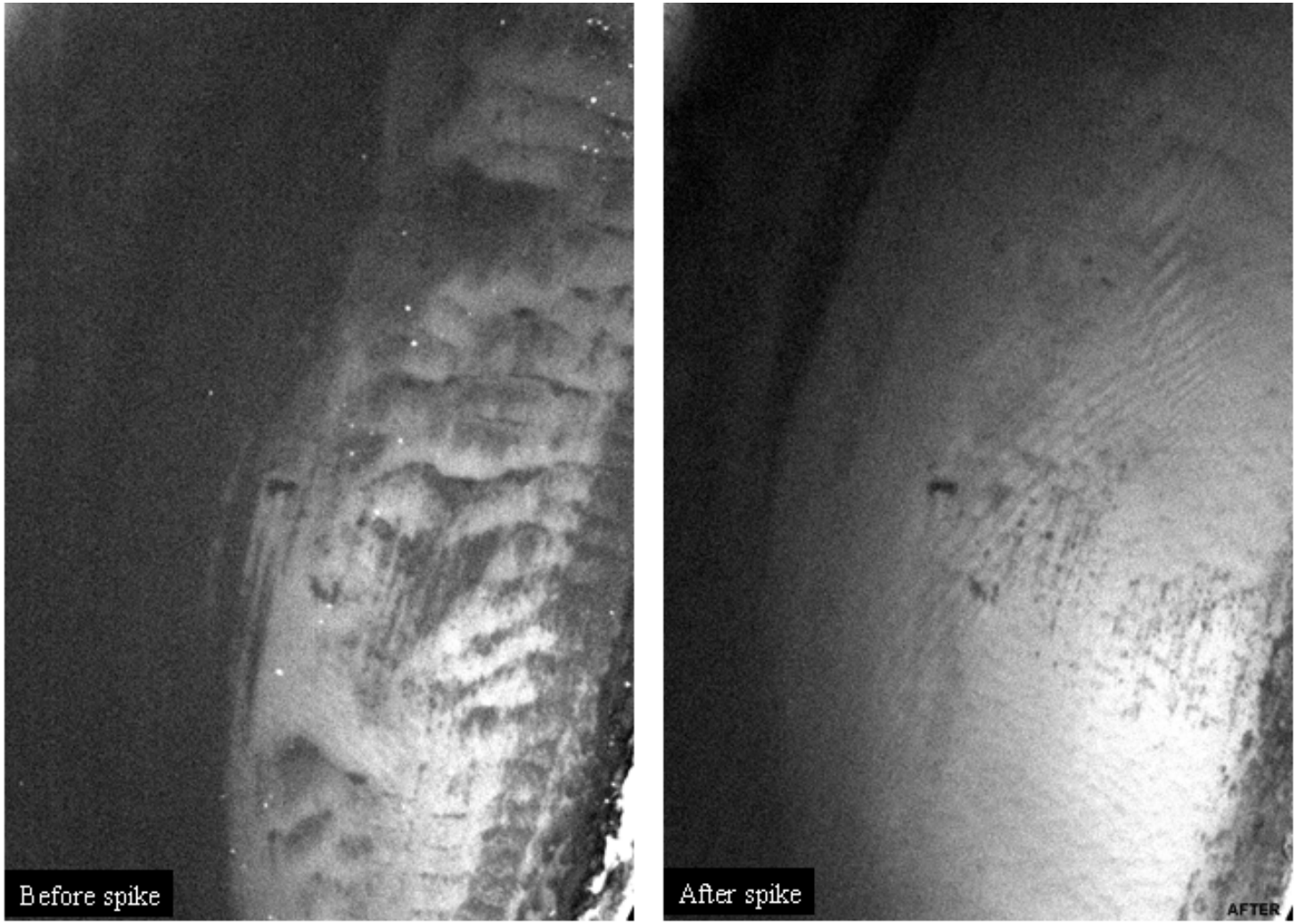

Figure 24. High-gain panchromatic images, contrast stretched to show detail on channel substrate before (left image) and after (right image) the high-flow spike in September, 2000 (Chavez et al., 2002a). Images are the upper subarea shown in Figure 19.

Figure 25. High-gain panchromatic images, contrast stretched to show detail on channel substrate before (left image) and after (right image) the high-flow spike in September, 2000 (Chavez et al., 2002a). Images are the lower subarea shown in Figure 19.

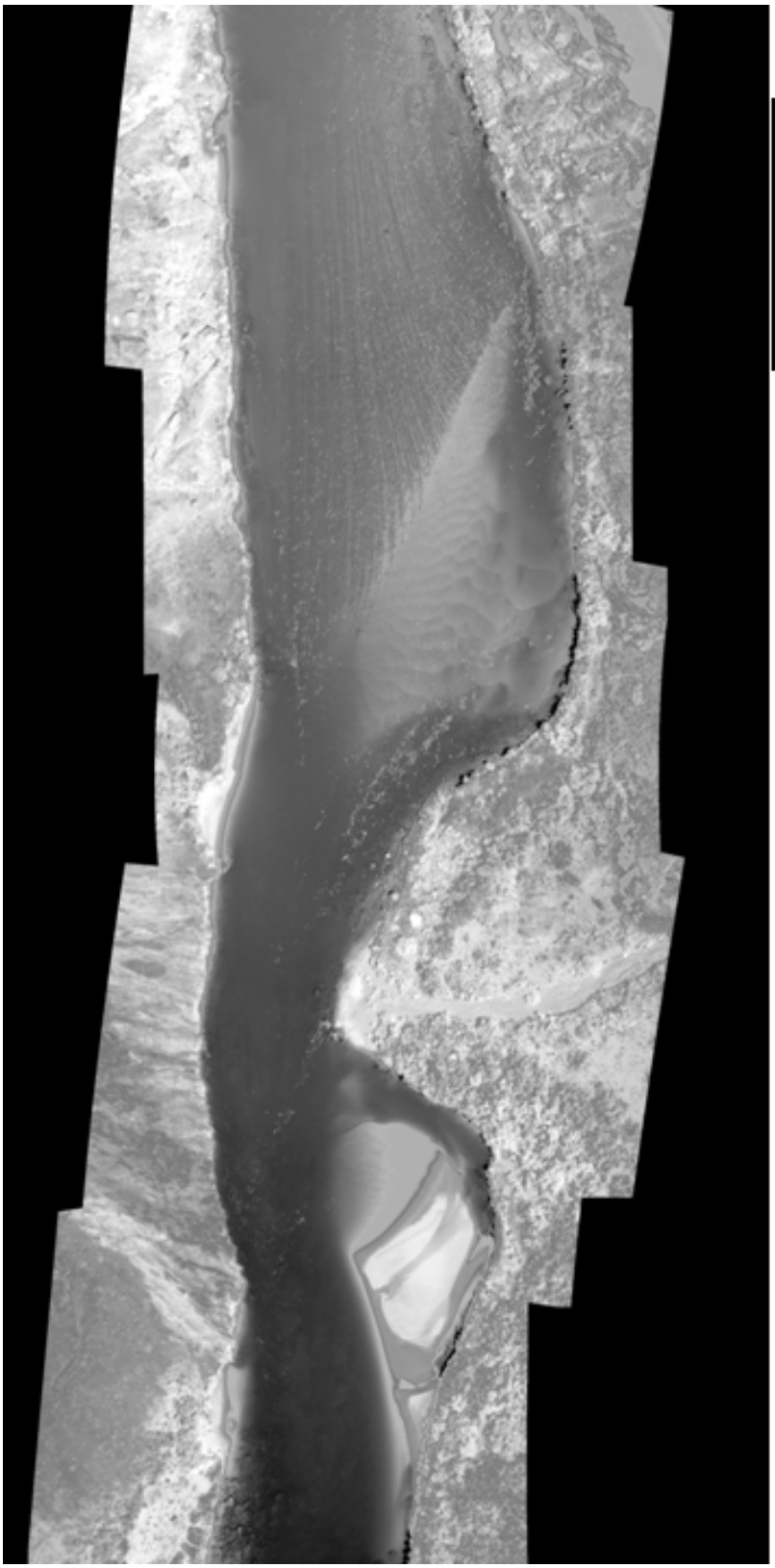

Figure 26. Image showing morphology of channel substrate compiled from high-gain, blue-green image of water areas and a normal-gain, near-infrared image of land areas. Area is south of LCR confluence near river mile 65.

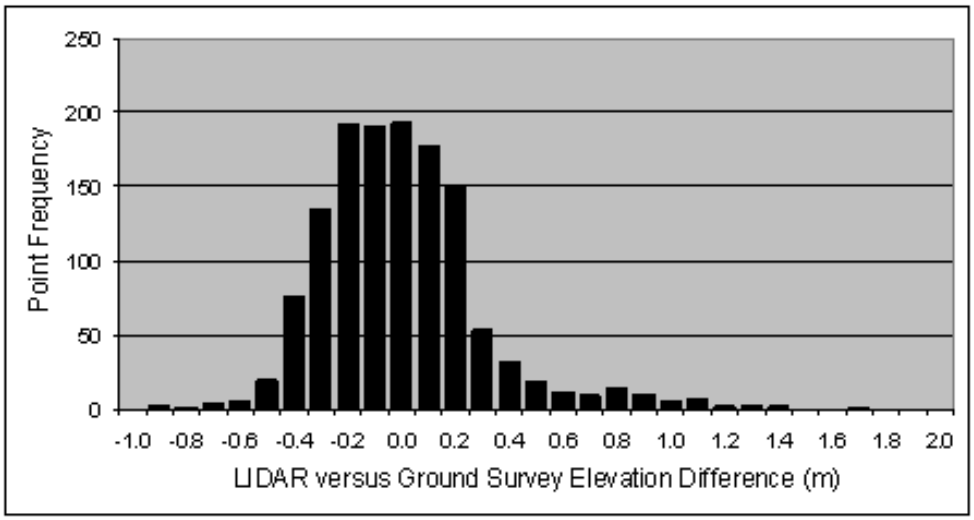

Figure 27. Point frequency distribution of differences between LIDAR elevations on the main-stem and ground-survey elevations of the adjacent water's edge.

Figure 28. Natural-color image (16-cm resolution produced by a 40-micron scan of 1:4,000-scale film) of debris flow surface at RM 43 study area. Vegetation is green. Geologic materials have their natural colors with little or no saturation. Image represents the original orientation (no geometric resampling) and the original color balance of the scanned image. Four-foot control panel near image center has a black-and-white hourglass shape.

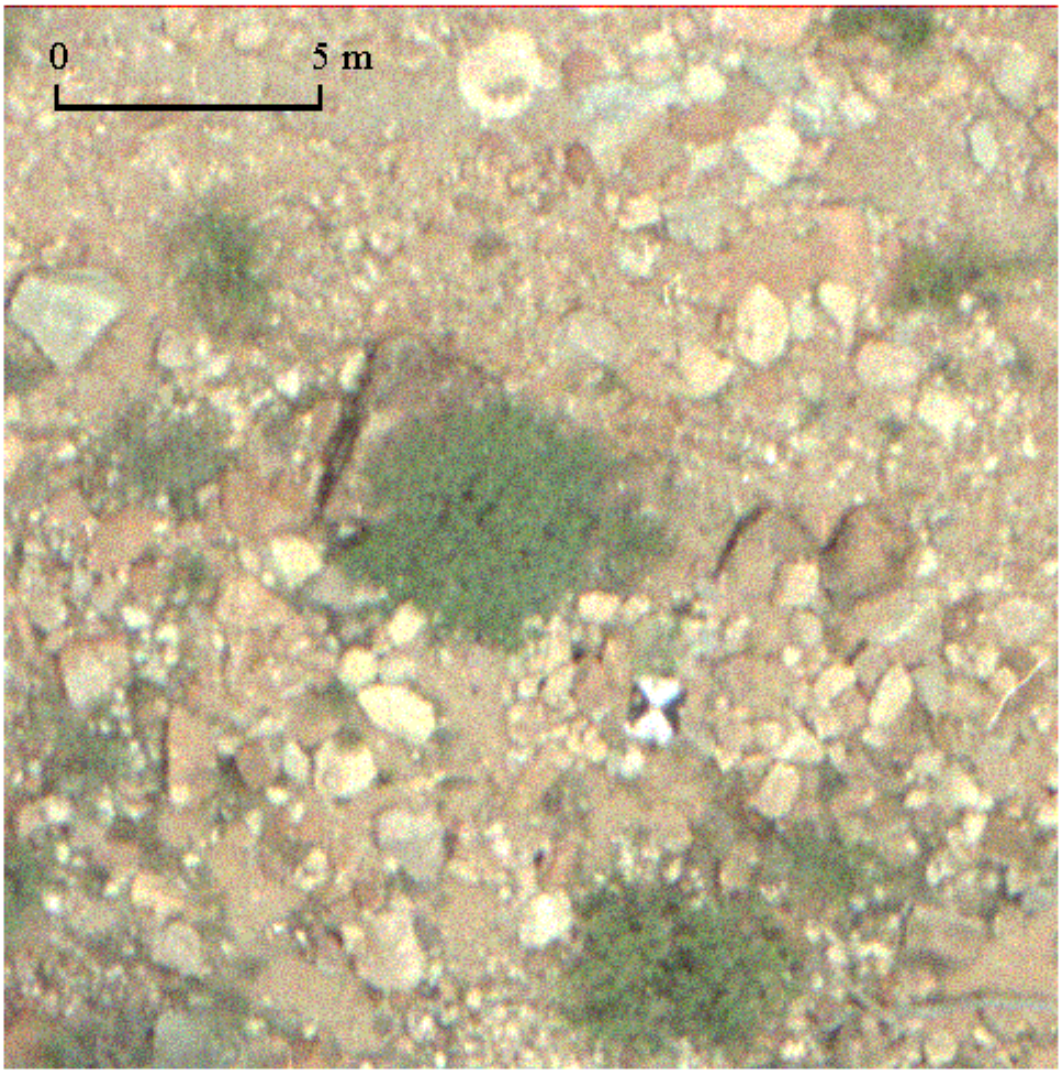

Figure 29. Natural-color image (6-cm resolution produced by a 15-micron scan of 1:4,000-scale film) of debris flow surface at RM 43 study area. Vegetation is green. Geologic materials have their natural colors with little or no saturation. Image represents the original orientation (no geometric resampling) and the original color balance of the scanned image. Scan resolution is near the limit of the film's resolution. Four-foot control panel near image center has a black-and-white hourglass shape.

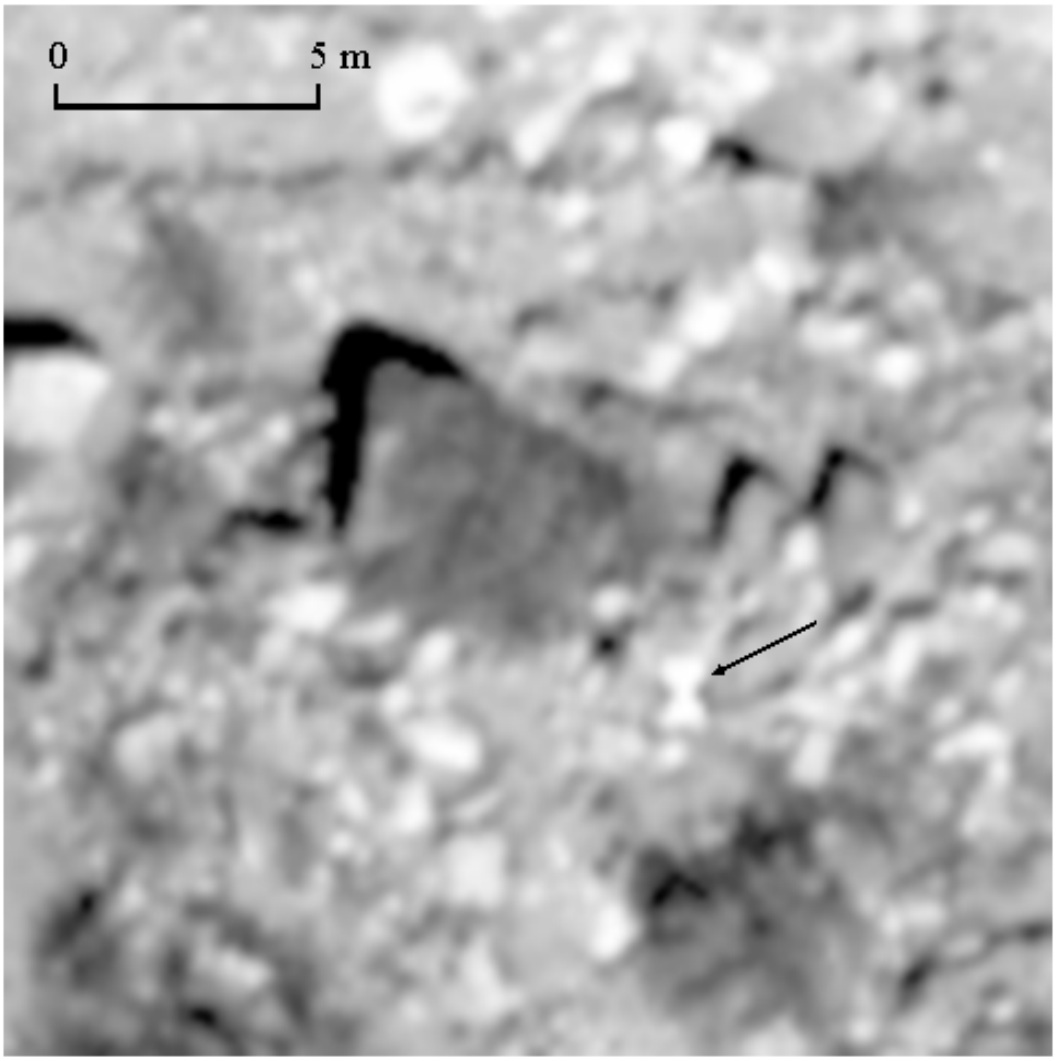

Figure 30. Digital panchromatic image (18-cm resolution) of debris flow surface at RM 43 study area. Vegetation is dark and difficult to distinguish from shadows cast by large rock fragments and even some of the rock fragments themselves. Differences between geologic materials are also difficult to distinguish. This image is a portion of an orthorectified mosaic and has therefore been resampled to some degree. Four-foot control panel near image center (indicated by arrow) has a white hourglass shape.

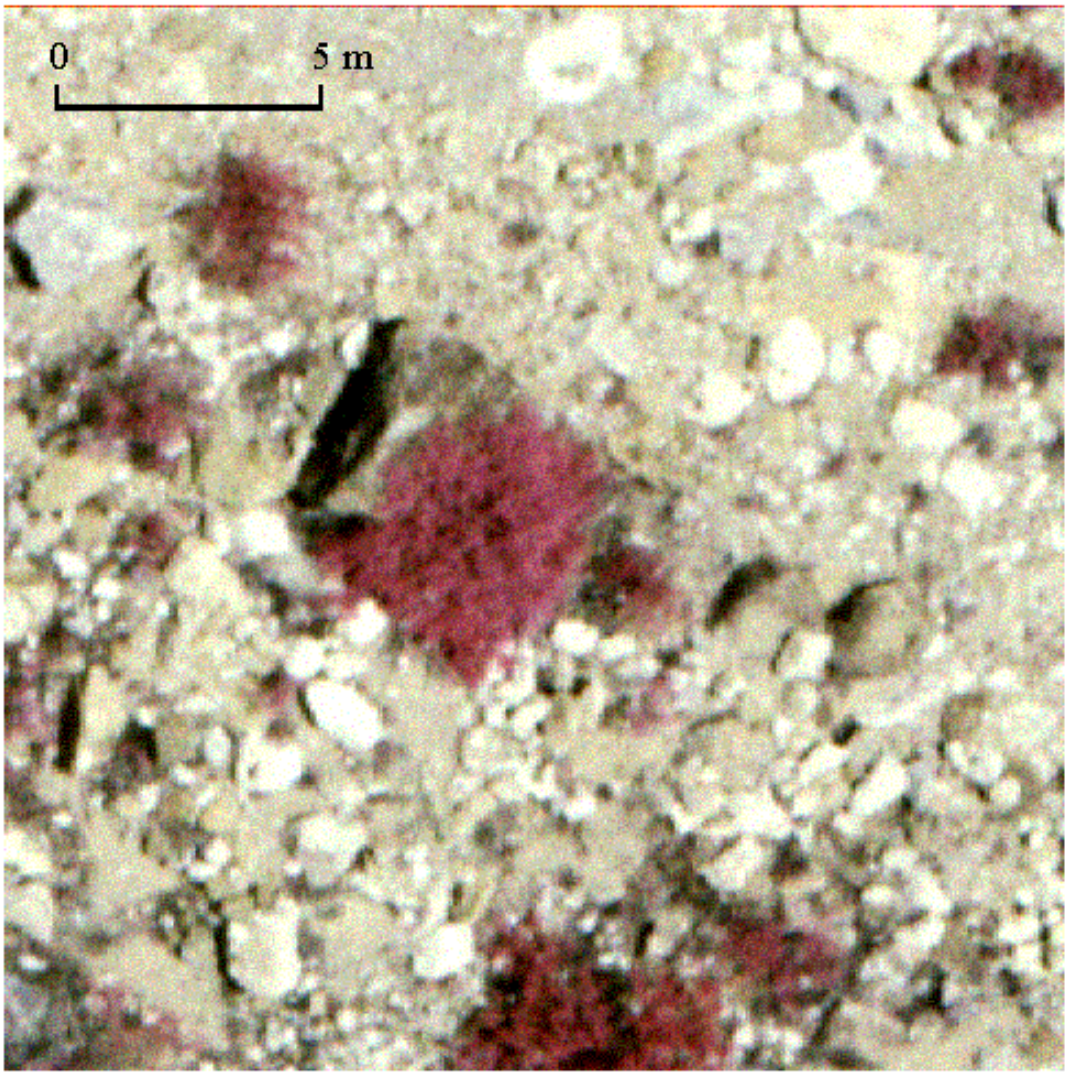

Figure 31. Color-infrared (CIR) image (10-cm resolution produced by a 21-micron scan of 1:4,800-scale film) of debris flow surface at RM 43 study area. Vegetation has very distinct shades of red. Some geologic materials tend to be washed out or saturated white. Image represents the original orientation (no geometric resampling) and the original color balance of the scanned image. Control panel visible on previous images (Figures 23-25) was not present on surface during this image acquisition.

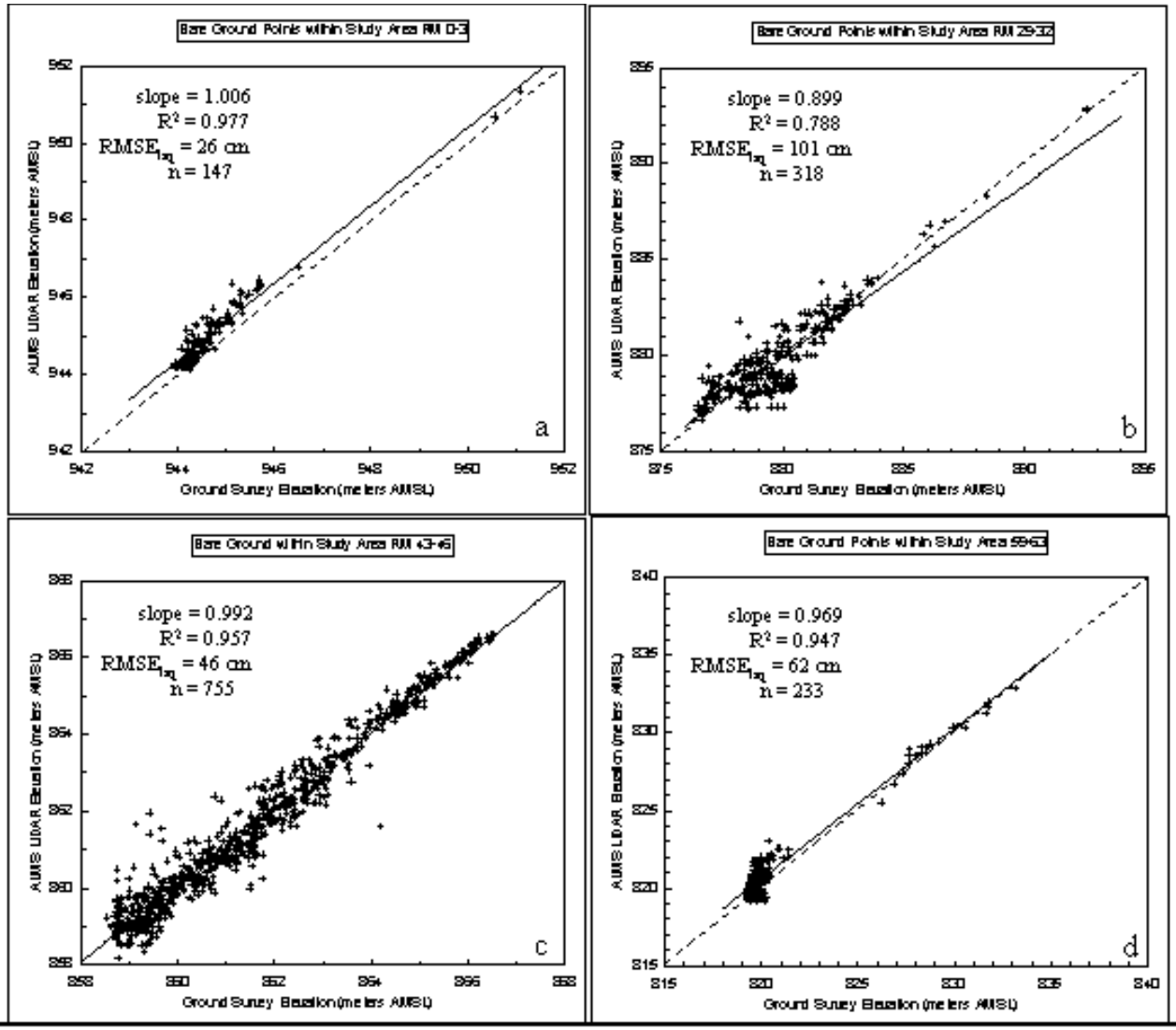

Figure 32. Scatter plots of March 2000 ALMS LIDAR elevations and ground survey elevations on bare ground for study areas (a) RM 0-3, (b) RM 29-32, (c) RM 43-46, and (d) RM 59-63. Solid lines are least-squares regression lines; dashed lines represent perfect agreement between LIDAR and ground-survey elevations.

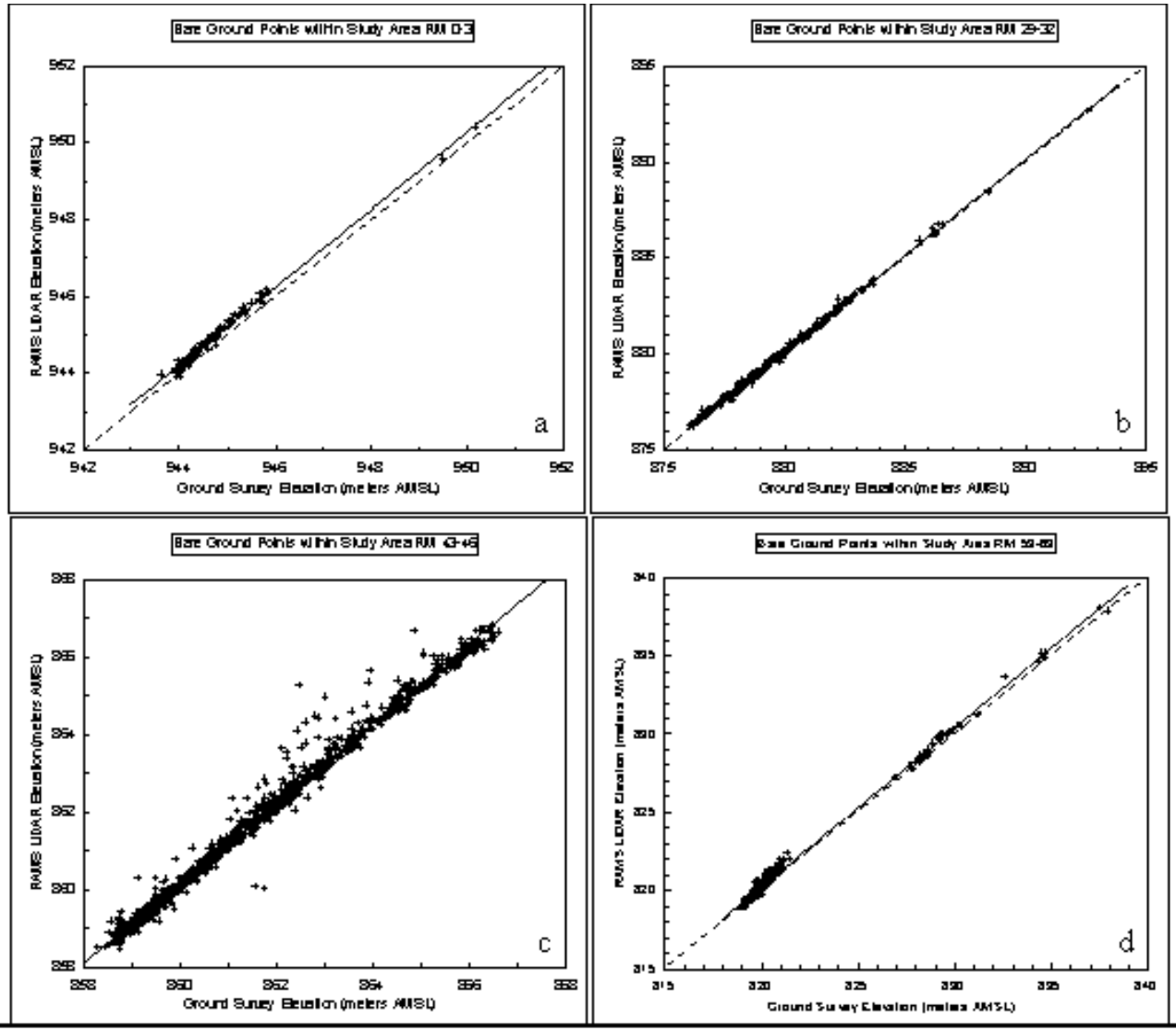

Figure 33. Scatter plots of August 2000 RAMS LIDAR elevations and ground survey elevations on bare ground for study areas (a) RM 0-3, (b) RM 29-32, (c) RM 43-46, and (d) RM 59-63. Solid lines are least-squares regression lines; dashed lines represent perfect agreement between LIDAR and ground-survey elevations.

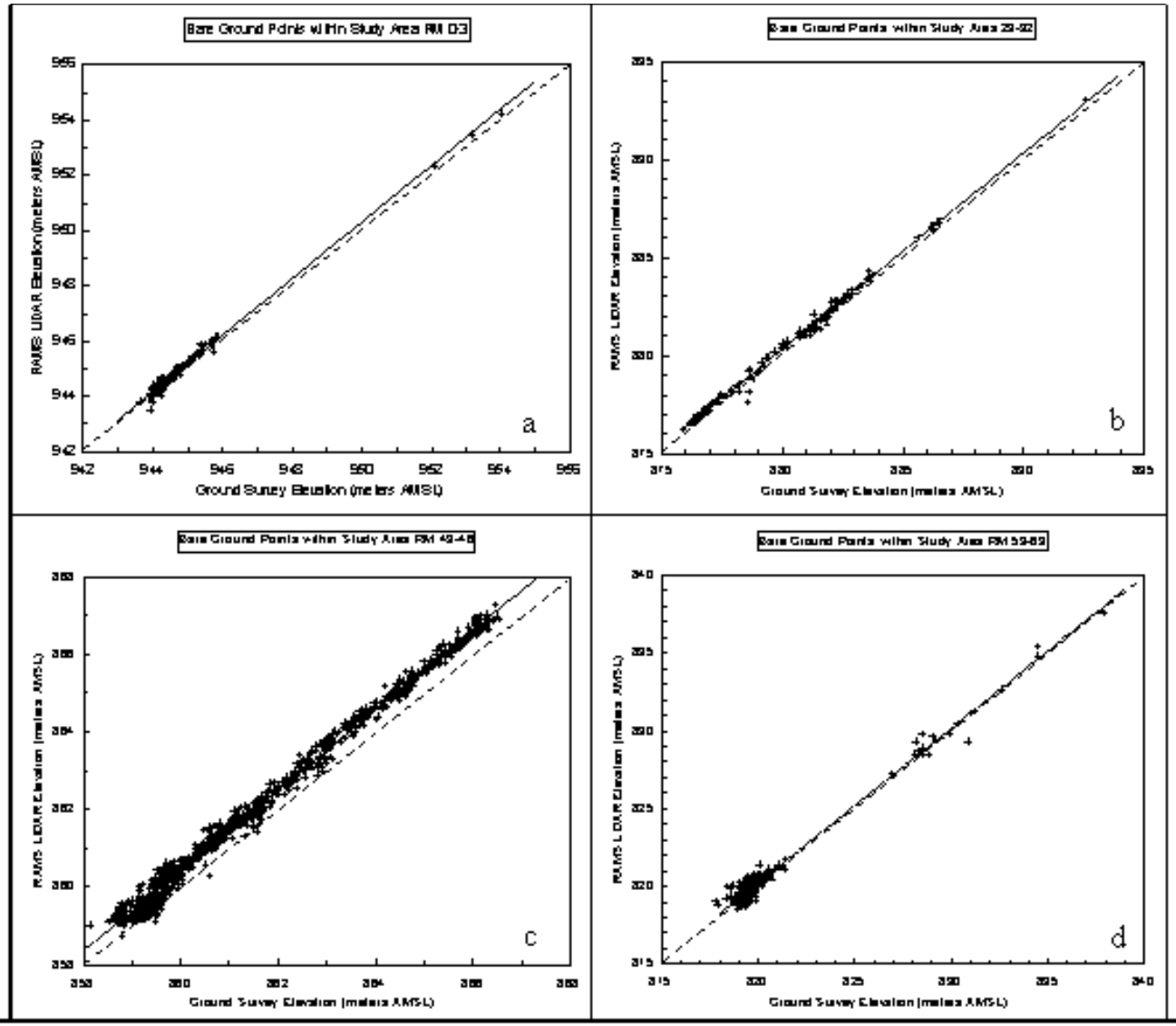

Figure 34. Scatter plots of September 2000 RAMS LIDAR elevations and ground survey elevations on bare ground for study areas (a) RM 0-3, (b) RM 29-32, (c) RM 43-46, and (d) RM 59-63. Solid lines are least-squares regression lines; dashed lines represent perfect agreement between LIDAR and ground-survey elevations.

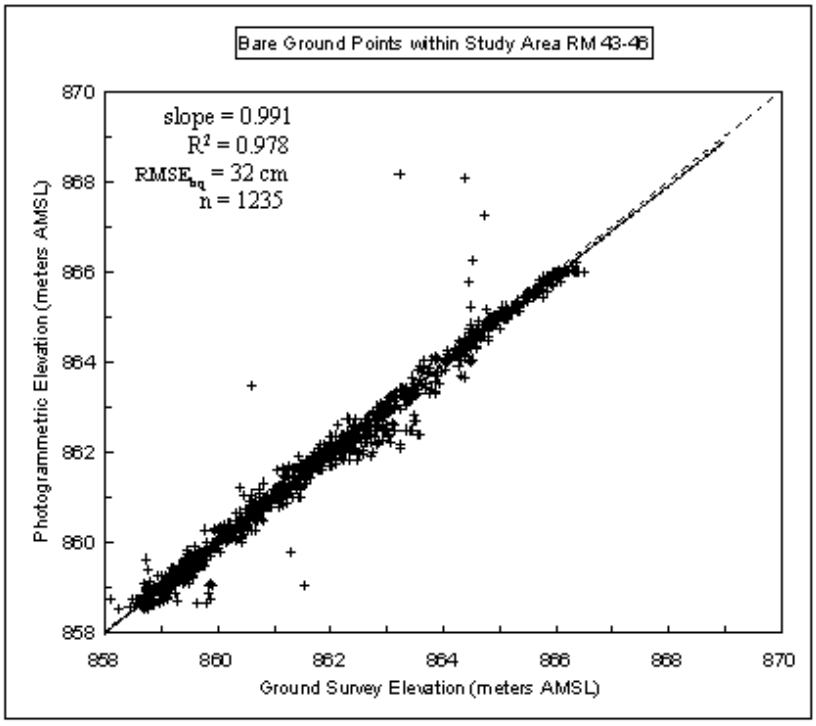

Figure 35. Scatter plots of September 2000 photogrammetric elevations and ground survey elevations on bare ground for study area RM 43-46. Solid lines are least-squares regression lines; dashed lines represent perfect agreement between LIDAR and ground-survey elevations.

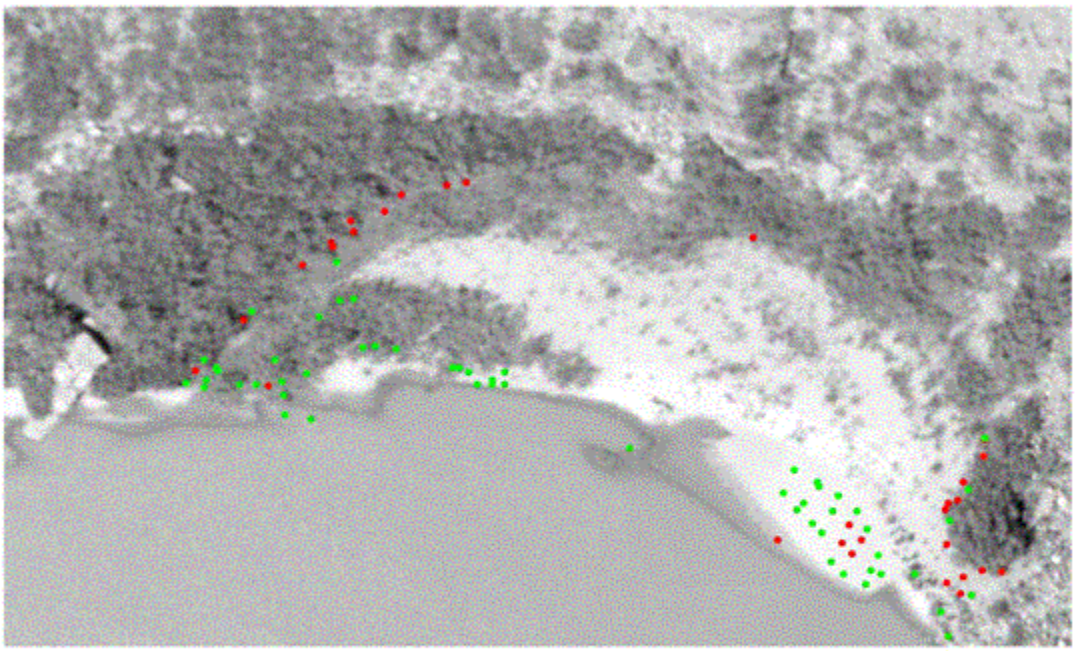

Figure 36. Panchromatic image of RM 43-46 study area showing locations of elevation errors equal to or greater than 1 m (in red) and errors between 0.5 and 0.99 m (in green) derived from photogrammetric analysis by PWT Corporation of 6-cm true-color image data.

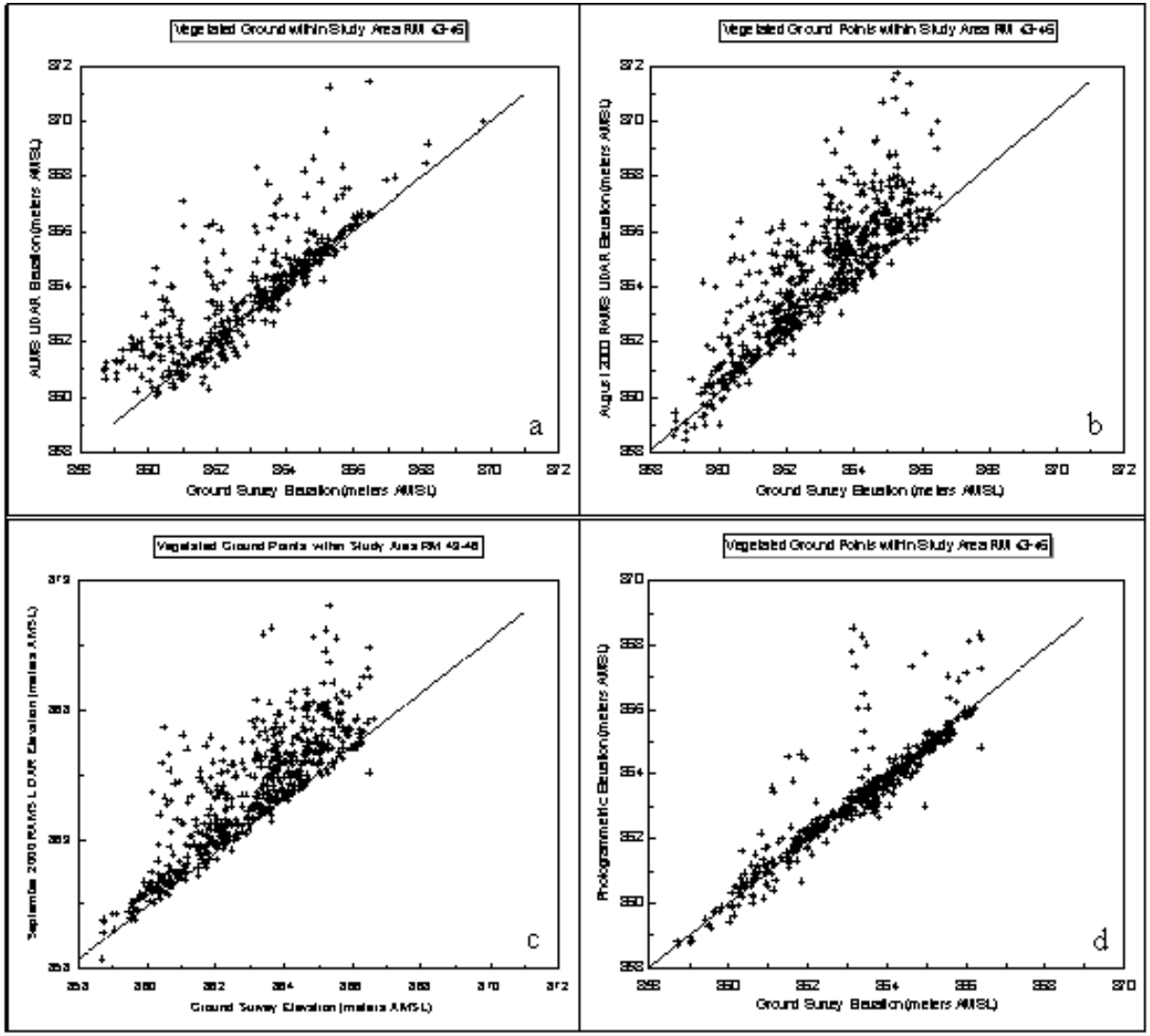

Figure 37. Scatter plots of airborne elevations and surveyed ground elevations on vegetated surfaces within study area RM 43-46. Solid lines are the least-squares regression lines from the bare-ground evaluations shown in Figures 31-34.

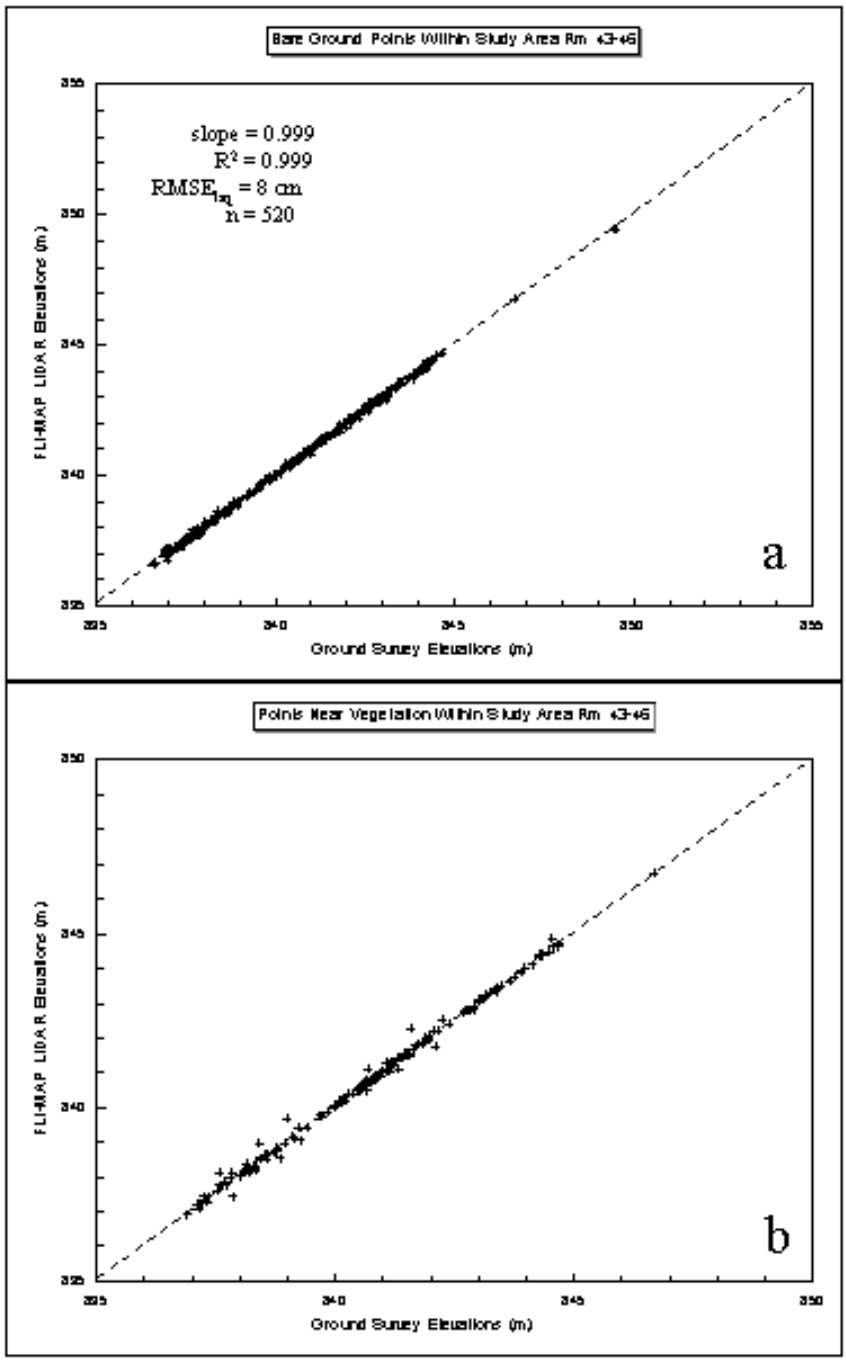

Figure 38. Scatter plots of May 2003 high-resolution FLI-MAP LIDAR elevations and ground survey elevations for points (a) on bare ground, (b) near vegetation, and (c) within dense vegetation for study area RM 43-46. Dashed line represents both the regression line and perfect agreement between LIDAR and ground-survey elevations on bare ground, which is duplicated in (b) and (c).

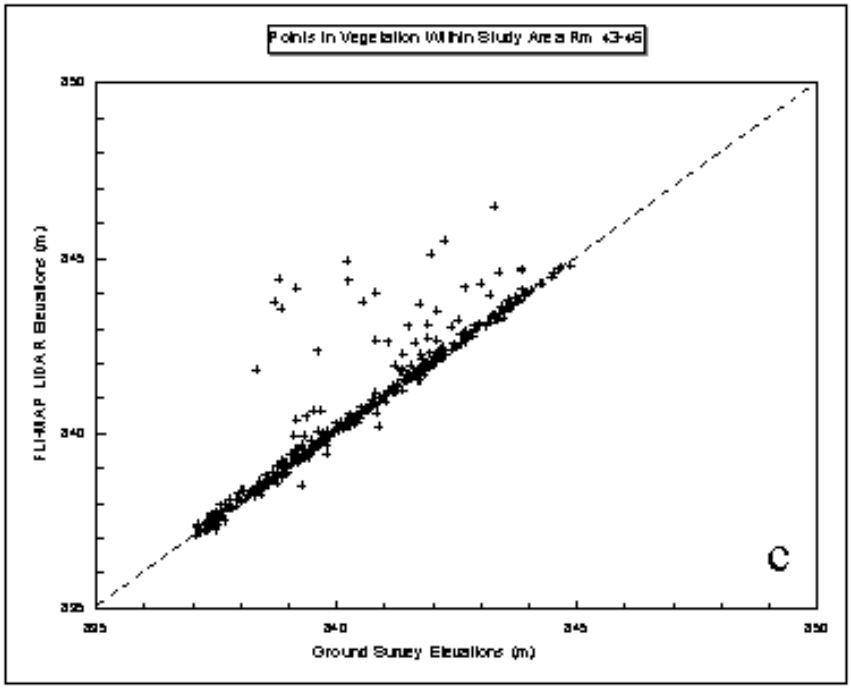

Figure 38. Scatter plots of May 2003 high-resolution FLI-MAP LIDAR elevations and ground survey elevations for points (a) on bare ground, (b) near vegetation, and (c) within dense vegetation for study area RM 43-46. Dashed line represents both the regression line and perfect agreement between LIDAR and ground-survey elevations on bare ground, which is duplicated in (b) and (c).

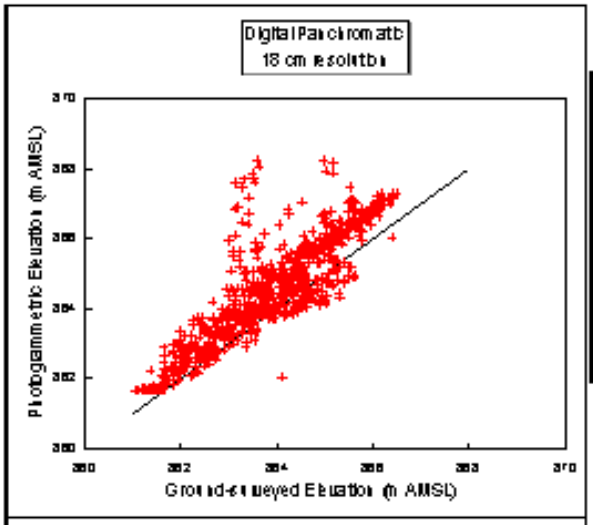

Figure 39. Comparison of photogrammetric ground elevations derived from 18-cm digital panchromatic image data with surveyed ground elevations. Line represents perfect agreement. Adjusted RMSE values derived from photogrammetric elevations have been adjusted downward for an observed average vertical offset from ground-survey elevation data.

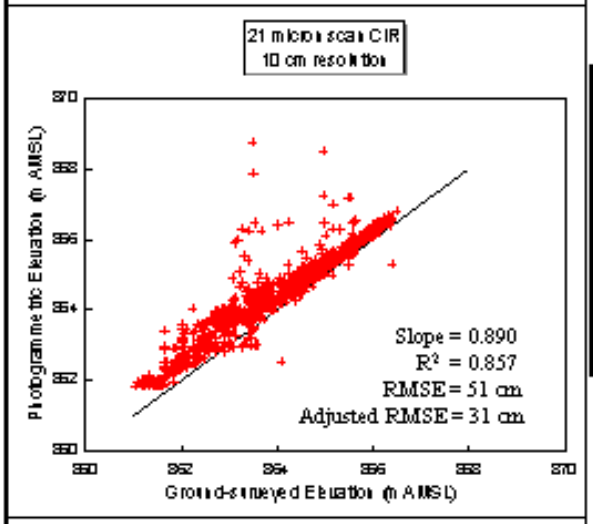

Figure 40. Comparison of photogrammetric ground elevations derived from 10-cm scanned CIR film image data with surveyed ground elevations. Line represents perfect agreement. Adjusted RMSE values derived from photogrammetric elevations have been adjusted downward for an observed average vertical offset from ground-survey elevation data.

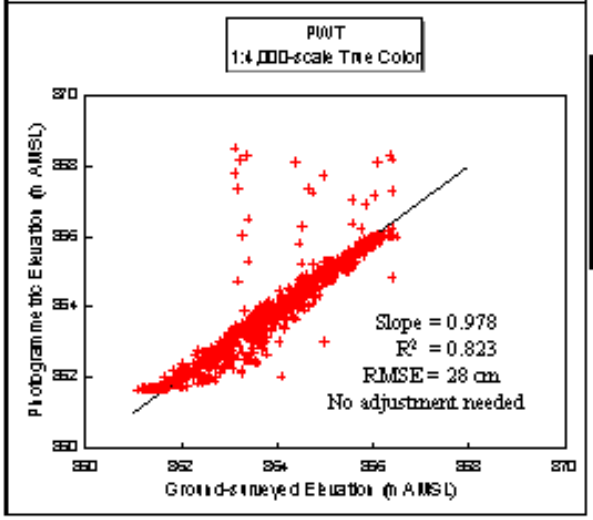

Figure 41. Comparison of photogrammetric ground elevations derived by Pacific Western Technologies (PWT) using 1:4,000-scale true-color film with surveyed ground elevations. Line represents perfect agreement.